Charles University
Faculty of Science
Department of Analytical Chemistry
Ph.D. study program: Analytical Chemistry

Ph.D. Thesis

Mgr. Štěpánka Skalová

Development of Novel Electrochemical Methods Using Various Membrane Materials for Monitoring of Selected Anticancer Drugs and Phytochelatins

Vývoj nových elektrochemických metod s využitím různých membránových materiálů pro sledování vybraných protinádorových léčiv a fytochelatinů

Supervisor: prof. RNDr. Jiří Barek, CSc.

Supervisors-consultants: doc. RNDr. Vlastimil Vyskočil, Ph.D.
doc. Ing. Tomáš Navrátil, Ph.D.

Prohlášení

Prohlašuji, že jsem tuto závěrečnou práci zpracovala samostatně a že jsem uvedla všechny použité informační zdroje a literaturu. Tato práce ani její podstatná část nebyla předložena k získání jiného nebo stejného akademického titulu.

V Praze 28. 07. 2019 Mgr. Štěpánka Skalová

This Ph.D. thesis was elaborated in the period from 2015 to 2020 at the Charles University, Faculty of Science, Department of Analytical Chemistry, UNESCO Laboratory of Environmental Electrochemistry. Substantial parts of experimental work were carried out during the long-term internships in laboratory of prof. José António Rodrigues, Department of Chemistry and Biochemistry, Faculty of Science University of Porto, Portugal. Some experiments were also carried out in cooperation with doc. Ing. Tomáš Navrátil, Ph.D. from the J. Heyrovský Institute of Physical Chemistry of the Czech Academy of Sciences.

Acknowledgement

I would like to express acknowledgements to all who have supported my research efforts during my graduate studies. Especially, let me thank my supervisor **prof. RNDr. Jiří Barek, CSc.**, the Head of the UNESCO Laboratory of Environmental Electrochemistry at the Department of Analytical Chemistry, Faculty of Science, Charles University; my first consultant **doc. RNDr. Vlastimil Vyskočil, Ph.D.**, Department of Analytical Chemistry, Faculty of Science, Charles University; my second consultant **doc. Ing. Tomáš Navrátil, Ph.D.**, J. Heyrovský Institute of Physical Chemistry of the Czech Academy of Sciences; and all colleagues from our research group, especially Mgr. Simona Baluchová and Mgr. Vojtěch Hrdlička, and other colleagues from the Department of Analytical Chemistry for their extensive help and support. Further, I acknowledge the cooperation with **prof. José António Rodrigues**, Department of Chemistry and Biochemistry, Faculty of Science University of Porto, Portugal, for providing me with theoretical and practical support in their laboratory.

Last but not least, I thank my family and all my friends for their support during my graduate studies.

Financial support of my research was ensured by: the Grant Agency of the Charles University, Prague (Project No. 368218), the Specific University Research (SVV), Foundation "Nadání Josefa, Marie a Zdeňky Hlávkových" for support of my Erasmus+ Internship and the National Agency for European Educational Programmes, Erasmus+ (Application 2512186), and the Czech Science Foundation (Projects No. 17-05387S and 17-03868S).

CONTENT

Key Words:

Biologically Active Compounds

Membrane

Miniaturized System

Electrochemical Impedance Spectroscopy

Differential Pulse Voltammetry

Amperometric Detection

Silver Solid Amalgam Electrode

Glassy Carbon Electrode

Flow System

Klíčová slova:

Biologicky aktivní sloučeniny

Membrána

Miniaturizovaný systém

Elektrochemická impedanční spektroskopie

Diferenční pulzní voltametrie

Ampérometrická detekce

Stříbrná tuhá amalgámová elektroda

Elektroda ze skelného uhlíku

Průtokový systém

List of Symbols and Abbreviations:

After(D)	solution after dialysis
AgSAE	silver solid amalgam electrode
AQ	anthraquinone
AQS	sodium anthraquinone-2-sulphonate
BRB	Britton-Robinson buffer
c	molar concentration
CPE	carbon paste electrode
CV	cyclic voltammetry
D	dialysate
DPCSV	differential pulse cathodic stripping voltammetry
DPV	differential pulse voltammetry
DualGCE	dual glassy carbon electrode
DX	doxorubicin
E	potential
EEC	electrical equivalent circuit
EIS	electrochemical impedance spectroscopy
E_p	peak potential
FIA	flow injection analysis
GCE	glassy carbon electrode
HMDE	hanging mercury drop electrode
HPLC	high-performance liquid chromatography
I	current
I_p	peak current

LOD	limit of detection
LSV	linear-sweep voltammetry
LVC	large volume compartment
m-AgSAE	mercury meniscus modified silver solid amalgam electrode
MVC	micro-volume compartment
MVVC	micro-volume voltammetric cell
n	number of measurements
p-AgSAE	polished silver solid amalgam electrode
PC	phytochelatin
PC_2	phytochelatin 2
PLM	planar lipid membrane
PS	physiological saline
PSA	potentiometric stripping analysis
Q	quinone moiety
R^2	coefficient of determination
s-PLM	supported planar lipid membrane
UV-VIS	ultraviolet and visible spectrophotometry
α	significance level (95 %)

Abstract

Present Ph.D. Thesis is focused on the development of electrochemical methods for determination of anticancer drugs using various types of membranes for their preliminary separation. Furthermore, this Thesis reports the study of transport mechanisms of heavy metals in the presence of phytochelatins across biological membranes.

Sodium anthraquinone-2-sulphonate (AQS) was used as a model compound for its similar structure with anthraquinone-based (AQ-based) anticancer drugs (doxo/daunorubicin) and also due to its better availability. All these compounds can be easily electrochemically oxidized and/or reduced.

Redox behaviour of AQS was investigated by cyclic voltammetry (CV) and differential pulse voltammetry (DPV) in a cathodic region on mercury meniscus modified (m-AgSAE) and polished silver solid amalgam (p-AgSAE) electrodes, Obtained results were used for the development of a micro-volume voltammetric cell (MVVC). Its applicability for voltammetric determination of anticancer drugs was verified by using doxorubicin (DX) as a model substance.

The second part of this Thesis deals with therapeutic monitoring of anticancer drugs in the blood circulation of the patients. For pilot experiments, a liquid-flow system with dialysis catheter and amperometric detection was used. The flow rate of carrier solution (0.9% NaCl solution – corresponding to the sodium chloride physiological saline (PS)) was 5 and 500 μL min^{-1}. Various working electrodes and arrangements have been tested and a dual glassy carbon electrode (dualGCE) was proved as the best option. Reduction potentials of −1200 mV and −900 mV were applied on the first and the second electrode, respectively. In this arrangement, the oxygen in the analysed solution was removed by reduction at the first electrode of dualGCE, on which also reduction of AQS occurred due to the applied highly negative potential of −1200 mV. Therefore, on the second electrode, AQS was oxidized/reduced in dependence on used liquid flow rate and the obtained signal of AQS was not influenced by the presence of oxygen.

The last part is devoted to monitoring of phytochelatins and to investigation of their transport across a model phospholipid membrane (PLM). The model PLM was

prepared on a polycarbonate carrier placed between two Teflon cups and two glass tubes (containing 0.1 mol L^{-1} KCl and the investigated compounds), which mimicked extracellular and intracellular space. Constant potential of −100 mV was applied on the model membrane and the dependence of the imaginary part of impedance on the real part of impedance has been measured (Nyquist plot). Concentrations of phytochelatin, Pb^{2+} ions, and Pb-phytochelatin complex have been monitored and determined by DPV and by chronopotenciometry on a hanging mercury drop electrode (HMDE) and by CV on a carbon paste electrode (CPE) modified by silica gel.

Abstrakt

Předložená disertační práce je zaměřena na vývoj elektrochemických metod pro sledování vybraných protinádorových léčiv s použitím různých typů membrán pro jejich předběžnou separaci a studiu transportu těžkých kovů za přítomnosti fytochelatinů přes biologickou membránu.

Jako modelová látka z oblasti protinádorových léčiv byla použita dobře dostupná sodná sůl kyseliny anthrachinon-2-sulfonové (AQS), neboť je strukturně podobná protinádorovým léčivům odvozeným od anthrachinonu (doxo/daunorubicin), která jsou snadno elektrochemicky oxidovatelná i redukovatelná.

Voltametrické chování AQS bylo studováno v katodické oblasti pomocí cyklické voltametrie (CV) a diferenční pulzní voltametrie (DPV) na rtuťovým meniskem modifikované (m-AgSAE) a na leštěné stříbrné amalgámové (p-AgSAE) elektrodě, Získané výsledky byly použity k vývoji mikroobjemové voltametrické cely (MVVC). Vhodnost MVVC k voltametrickému stanovení protinádorových léčiv byla následně potvrzena použitím doxorubicinu (DX) jako další modelové látky.

Druhá část práce se zabývá terapeutickým sledováním protinádorových léčiv v krevním oběhu pacienta. K pilotním experimentům byl použit průtokový systém s dialyzačním katetrem a ampérometrickou detekcí. Bylo pracováno při rychlosti průtoku mobilní fáze (fyziologického roztoku (0.9% roztok NaCl)) 5 a 500 μL min^{-1}. Byla testována řada pracovních elektrod a uspořádání, přičemž jako optimální se ukázala duální pracovní elektroda ze skelného uhlíku (dualGCE), kdy na první elektrodu byl aplikován potenciál −1200 mV a na druhou −900 mV. V tomto uspořádání pak bylo možné stanovovat AQS tak, že na první elektrodě dualGCE došlo díky vysokému vkládanému potenciálu (−1200 mV) k redukci kyslíku a AQS. Na druhé elektrodě dualGCE byl pak redukován/oxidován AQS v závislosti na rychlosti průtoku mobilní fáze. Roztok v okolí této elektrody byl bez přítomnosti kyslíku, a signál AQS jím tak nebyl ovlivněn.

Poslední část práce je zaměřena na sledování fytochelatinu a studium jeho přenosu přes modelovou fosfolipidovou membránu (PLM). Tato membrána byla vytvořena na polykarbonátovém nosiči umístěném mezi dvěma Teflonovými kloboučky a oddělovala roztoky v dvou skelněných trubičkách, které obsahovaly 0.1mol L^{-1} KCl a

studované látky, a představovaly extracelulární a intracelulární prostor. Na PLM byl vložen konstantní potenciál a byla sledována závislost imaginární části elektrochemické impedance na reálné (Nyquist graf). Obsah fytochelatinu, Pb^{2+} iontů a komplexů Pb-fytochelatin byl sledován a stanovován pomocí DPV a chronopotenciometrie na visící rtuťové kapkové elektrodě a CV na uhlíkové pastové elektrodě modifikované silikagelem.

1. **Introduction**

This Ph.D. Thesis is focused on monitoring anticancer drugs and on the study of transport mechanisms of phytochelatins across a model phospholipid membrane (PLM) by voltammetric and amperometric methods. This work has a potential to contribute to the improvement of anticancer treatment as well as to better understanding of transport mechanisms through cell membranes, which can provide another tool for a target treatment in future. This research has been carried out within the framework of a long-term research at the UNESCO Laboratory of Environmental Electrochemistry, Faculty of Science, Charles University, Prague, and at the Department of Electrochemistry at the Nanoscale at the J. Heyrovský Institute of Physical Chemistry of the Czech Academy of Sciences, Prague.

The presented Ph.D. Thesis is based on the following five scientific papers **[1-5]** attached as Appendix parts I – V (Chapters 7 – 11). To distinguish the references related to these publications in the entire text of this Thesis, corresponding references (numbers in square brackets) are in bold.

1. **Skalova S**, Langmaier J, Barek J, Vyskocil V, Navratil T: Doxorubicin Determination Using Two Voltammetric Techniques - a Comparative Study, *submitted to Electrochimica Acta (2019)*

2. **Skalova S**, Gonçalves LM, Navratil T, Barek J, Rodrigues JA, Vyskocil V: Miniaturized Voltammetric Cell for Cathodic Voltammetry Making Use of an Agar Membrane, *Journal of Electroanalytical Chemistry 821*, 47-52 (2018)
3. Sestakova I, **Skalova S**, Navratil T: Labile Lead Phytochelatin Complex Could Enhance Transport of Lead Ions Across Biological Membrane, *Journal of Electroanalytical Chemistry 821*, 92-96 (2018)
4. **Skalova S**, Vyskocil V, Barek J, Navratil T: Model Biological Membranes and Possibilities of Application of Electrochemical Impedance Spectroscopy for their Characterization, *Electroanalysis 30*, 207-219 (2018)
5. **Skalova** S, Navratil T, Barek J, Vyskocil V: Voltammetric Determination of Sodium Anthraquinone-2-Sulfonate Using Silver Solid Amalgam Electrodes, *Monatshefte für Chemie – Chemical Monthly 14,* 577-583 (2017)

Electroanalytical chemistry represents one of the ways for investigation and determination of various compounds by sensitive, selective, fast, and low-cost methods. These characteristics can be used advantageously especially in healthcare requiring to obtain reliable results at a reasonable price and time, which can lead to improved performance of diagnostic procedures for numerous diseases.

This research has been focused on the use of voltammetric and amperometric techniques on various carbon-based and mercury-based electrodes. Voltammetric techniques have been developed after the discovery of polarography by Jaroslav Heyrovský in 1922 and until today, a wide spectrum of methods for the determination of inorganic and organic substances in various samples have been reported in the literature. Electroanalytical techniques and equipment are widely spread and present almost in every chemical laboratory and due to the advantageous features, there is an effort to employ such techniques also in clinical laboratories in hospitals. In addition, voltammetric techniques have been used in modern biochemical research of biomacromolecules (proteins, nucleic acids, etc.) and of their interactions with other compounds.

Two main goals were aimed at in the present Ph.D. Thesis. The first one being development of methods for the determination of anticancer drugs in a small volume **[1-3]**, and for therapeutic drug monitoring of anticancer drugs in a blood circulation of patients. For these measurements, sodium anthraquinone-2-sulphonate (AQS) as a model compound and doxorubicin (DX) as a representative of anticancer drugs have been used.

DX as well as daunorubicin, epirubicin, etc. belong to the group of anthracycline antibiotics, which are widely used for treatment of various types of cancer. However, effectiveness of these drugs is limited by several factors (including, e.g., drug effects, drug resistance, and fixed dosage), which can lead to patient overdose or to insufficient dosage, and ineffective treatment. For this reason, monitoring of therapeutic drugs starts to emerge in research areas as it represents a promising path for personalized cancer treatment by using individualized dosages of drugs for each patient **[4, 5]**.

The second aim of this Ph.D. Thesis is a study of cell membrane transports **[6, 7]**. In the first part, preparation of a model PLM with an ionophore was optimized. Subsequently, formation and transport of complexes of Pb cations with phytochelatin

through the formed membrane have been thoroughly investigated. Phytochelatins are cysteine rich oligomers. They play different roles in plants and, among other, they act as chelators, and are important for their heavy metal detoxification. They are important for human health, because when such plants are used to feed animals and those animals are eventually consumed by people, toxic heavy metals originally accumulated in plants can pass into the human bodies and cause serious health problems [8, 9]. Therefore, within the scope of our research, the transport of Pb cations through a membrane was examined in the presence and in the absence of a chosen phytochelatin.

2. **Analytes**

2.1 Anthracyclines

Anthracyclines are widely used anti-cancer drugs to treat various oncological diseases (such as leukaemia and solid tumours). Firstly, doxorubicin (DX) and daunorubicin (**Fig. 2.1**) were discovered, and subsequently others analogues have been developed due to the efforts to reduce their cardiotoxicity, chromosomal damage, and to increase antitumor activity. Therefore, following anthracyclines are nowadays used: idarubicin (**Fig. 2.1**), epirubicin, pirarubicin, zorubicin, and mitoxantrone [10, 11]. The above-mentioned adverse effects are generally connected with electron transfer processes in respiratory chain leading to initiation of lipid peroxidation [11].

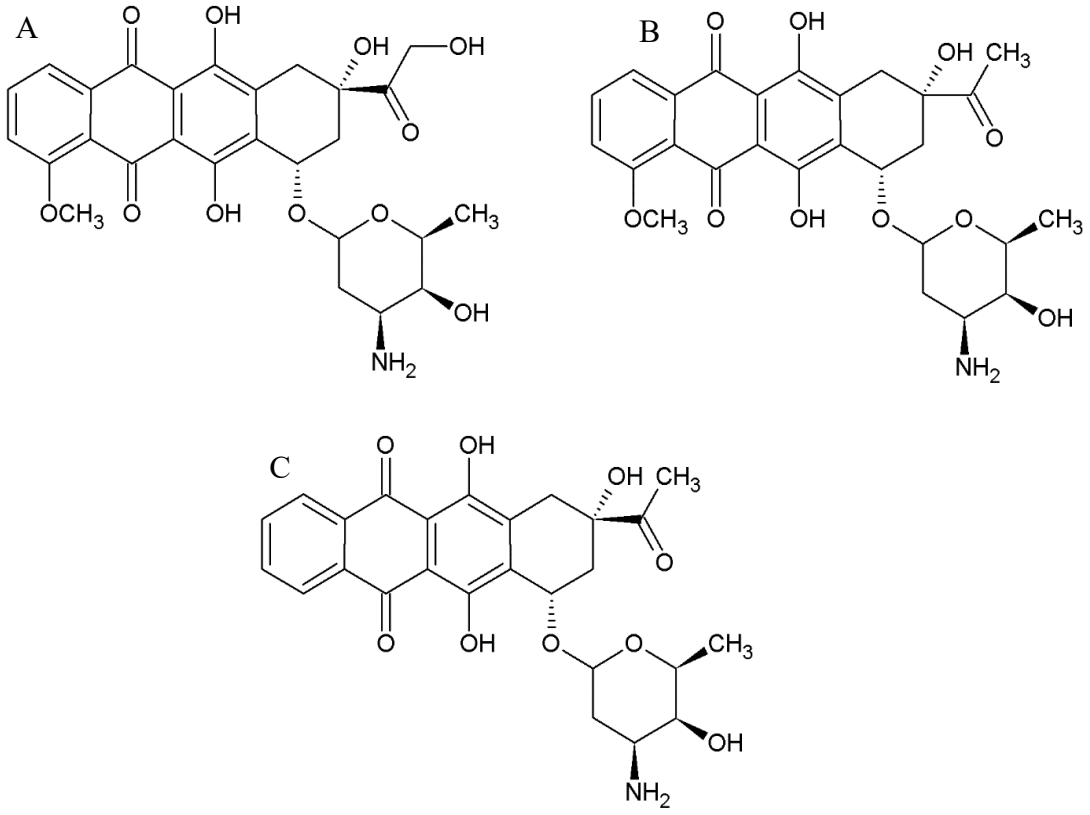

Fig. 2.1 Structures of selected anthracyclines. A: doxorubicin, B: daunorubicin, C: idarubicin.

The structure of anthracyclines includes a quinone moiety (Q, **Fig. 2.2**). In general, quinones are present in living organisms and are important for electron transfer in green plant photosystems, in bacteria (prokaryotes), and in mitochondria (of eukaryotes organisms [12]. The Q reduction proceeds via two steps, forming Q^{-} and Q^{2-}, and the cation of supporting electrolyte controls whether the reduction is accomplished in one step (in protic medium) or via an intermediate (in aprotic medium). Furthermore, the formal potentials of these reactions are dependent on the solvent polarity [13-16] and of course on pH.

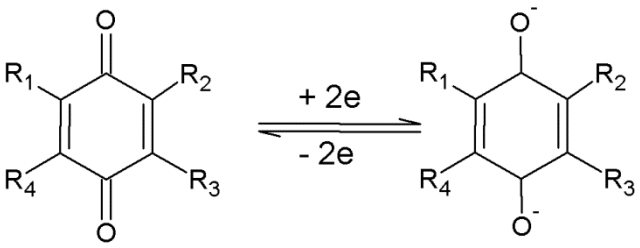

Fig. 2.2 Reduction/oxidation of quinone moiety (R – substituents).

Mechanisms of action of these molecules are mainly based on interaction with DNA, inhibition of topoisomerase II, and production of highly reactive free hydroxyl radicals. Moreover, secondary mechanisms, such as inhibition of topoisomerase I, mitochondrial oxidative phosphorylation, DNA polymerase, etc., can also play a significant role. These actions are responsible for the antitumor activity, however, also for adverse drugs effects [10, 17].

In this Ph.D. Thesis, AQS (as a model compound) and DX (as a representative of the group of anthracycline drugs) were used.

2.1.1 Sodium Anthraquinone-2-Sulphonate

Sodium anthraquinone-2-sulphonate (AQS, CAS Number: 131-08-8, **Fig. 2.3**) exists as a yellow water-soluble powder. It is a precursor of a number of dyes and is synthesized from AQS and oleum containing 25% of sulphur trioxide [18].

AQS is used also as a precursor for pharmaceuticals and pesticides. AQS has a strong effect on metabolism of microorganism by its physico-chemical and toxic properties [19] and due to them, AQS has been tested as a possible agent for efficient disinfection of wastewater with focus on its antibacterial effects [20]. Besides, it was used as a part of photoanode of reversible photocharging/discharging system of a photorechargeable air battery [21] and as an organic electrode in lithium ion batteries [22]. AQS is employed as an intermediate in the fabrication processes of dyes and analytical agents and for that reason, it occurs as a contaminant in water and soil [23].

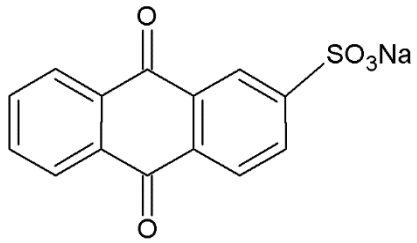

Fig. 2.3 Structure of sodium anthraquinone-2-sulphonate (AQS).

Due to the possible occurrence of AQS as a pollutant in the environment, methods for its determination have been developed. One of them has used gas chromatography-selected ion monitoring with the limit of detection (*LOD*) of 0.02 ng μL^{-1} [23]. Another method has been focused on determination of AQS in pulping liquors in which a flow analysis system with a Nafion membrane interface with UV-VIS spectrophotometry has employed. *LOD* of this method was not reported, however, dependence was found to be linear in the AQS concentration range from 0.12 to 0.48 mmol L^{-1} (λ = 520 nm) [24].

Within the scope of my Ph.D. project, I have developed various electroanalytical methods for voltammetric determinations of AQS, as a model compound of AQ-based anticancer drugs. For methods utilizing DPV technique, achieved *LODs* were 1 µmol L^{-1} on a polished silver solid amalgam electrode (p-AgSAE) and 0.6 µmol L^{-1} on a mercury meniscus modified silver solid amalgam electrode (m-AgSAE) **[2]**. Moreover, p-AgSAE was also used for measurements in micro-volume voltammetric cell (MVVC) and even lower *LOD* value of 0.2 µmol L^{-1} has been obtained **[1]**.

2.1.2 Doxorubicin hydrochloride

Doxorubicin hydrochloride (DX, CAS Number: 25316-40-9, **Fig. 2.1**) is red, crystalline, solid compound, soluble in water. DX, a 14-hydroxylated form of daunorubicin, is biosynthesized by *Streptomyces peucetius* [25]. Besides, it can be prepared by synthesis using tritium catalytic exchange or ^{14}C-labelled diazomethane [26].

As already mentioned, DX is an anthracycline chemotherapeutic drug which is metabolised in human plasma with the DX half-life of 28.3 ± 2.8 h [27] (estimated on measurements in eight patients). Its main metabolite, doxorubicinol (C-13 alcohol metabolite), is suspected to be responsible for cardiotoxicity and it is also the reason for development of several DX derivatives [28, 29]. DX derivatives can be used for treatment of other diseases, not just tumours, e.g., yellow fever or dengue fever [30].

Various methods for measuring DX concentration levels have been developed including voltammetric methods, e.g., DPV on Fe_3O_4@Pt nanoparticle and multi-walled carbon nanotube modified carbon paste electrode (CPE) (a linear calibration curve was obtained in the DX concentration range in human urine from 0.05 to 70.0 mmol L^{-1}) [31], DPV on graphene quantum dot modified glassy carbon electrode (GCE) in human plasma (*LOD* of 0.016 μmol L^{-1}) [32], and DPV on p-AgSAE in MVVC (*LOD* of 0.44 μmol L^{-1}) in urine **[3]**. Moreover, separation techniques were employed for DX determination, e.g., high performance liquid chromatography with fluorescence detection in mice plasma (*LOD* of 5.0 ng mL^{-1}) [33], capillary electrophoresis with laser-induced fluorescence detection in cell lysate (*LOD* of 4.9 ng mL^{-1}) [34], and solid-phase microextraction coupled with liquid chromatography-tandem mass spectrometry in lung tissue (*LOD* of 2.5 μg g^{-1} of tissue) [35].

2.2 Phytochelatins

Phytochelatins (**Fig. 2.4)**, are peptides with the primary structure of (γ-Glu-Cys)$_n$-Gly. Moreover, there are groups of other peptides with a similar structure to phytochelatin, but where the last amino acid is not glycine. Generally, phytochelatins are divided into five families of γ-Glu-Cys peptides and may differ in their functions and effects [36]. They are post-translationally synthetized in plants and in some fungi (but not in animals); their syntheses proceed enzymatically from glutathione [37, 38]

and such productions of phytochelatins represents one of the defence mechanisms to eliminate toxic effects of heavy metals [9]. In our research, phytochelatin 2 (PC_2, L-γ-glutamyl-L-cysteinyl-L-γ-glutamyl-L-cysteinylglycine, CAS Number N/A) was used. Various studies related to binding of PC_2 with Cd, Pb and a few other cations can be found in the literature [36, 39].

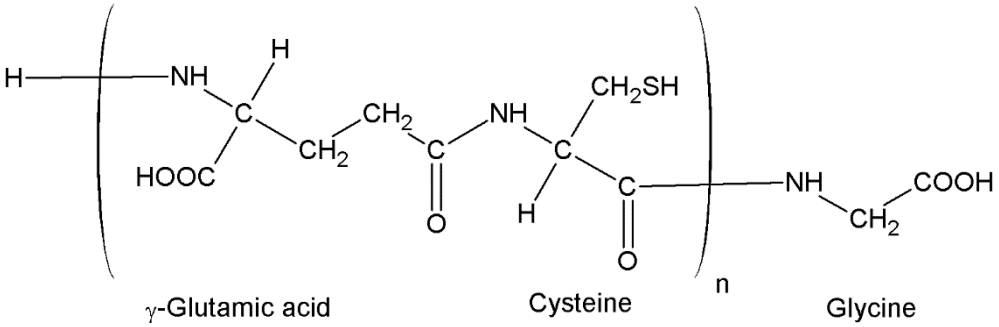

Fig. 2.4 Structure of phytochelatins.

As already mentioned, synthesis of PCs starts after the exposure of plants (or fungi) to heavy metals as they can bind to these metals which lead to the formation of complexes, and for that reason, they are also called metal-binding proteins [9]. Evidently, PCs play an important role for detoxification of plants from heavy metals [38]. However, the ability of plants to produce PCs considerably differs and plants with more intensive PC production, which can uptake extremely high amounts of contaminants (so called hyperaccumulators), may present - after heavy metals accumulation - a significant risk for a health of people (e.g., *Pistia stratiotes*, component of animal feed [8]).

PC_2 has been determined by various methods, some of them are listed here (along with the achieved *LOD* values): high-performance liquid chromatography coupled with electrochemical detection (*LOD* of 0.5 μmol L^{-1}) [40], direct current voltammetry on a copper solid amalgam electrode (*LOD* of 2.1 – 2.6 nmol L^{-1}) [41], pneumatically assisted electrospray ionisation tandem mass spectrometry (*LOD* of 9 μg L^{-1}) [42] or high-performance liquid chromatography with fluorescence detection (*LOD* of 9 nmol L^{-1}) [43].

3. Working Electrodes and Techniques

3.1 Mercury Based Working Electrodes

3.1.1 Hanging Mercury Drop Working Electrode

A hanging mercury drop electrode (HMDE) is used in the cathodic potential region and provides a wide range of possible applications in pharmacy and medicine [44-46], in environmental field [47-49], or in study of macromolecules [50-52]. HMDE possesses many advantageous characteristics, including simple cleaning process (measurements are performed on a renewed surface of a freshly created new drop), relatively wide working potential window in the cathodic region (from +400 to −2500 mV depending on the used supporting electrolyte), possibility of modification, adsorption of various important compounds on the surface of HMDE [53]. Low *LOD*s in order of 10 pmol L^{-1} or even of 1 pmol L^{-1} can be achieved in the case of application of the pulse voltammetric techniques [54].

In this Ph.D. Thesis, HDME was used for monitoring of complexes of PC_2 with Pb^{2+} ions as the part of transport study of heavy metals across tested PLMs with ionophore calcimycin. DPV and differential potentiometric stripping analysis (PSA, chronopotentiometry) were used as the most suitable techniques for performing such experiments. Measurements were carried out by using an Eco-Tribo polarograph controlled by PolarPro 5.1 software (both Polaro-Sensors, Czech Republic). HDME was employed as a working electrode in a conventional three-electrode set up in which an Ag/AgCl/KCl (sat.) electrode (Elektrochemické Detektory, Czech Republic) and a platinum wire (Ø 1 mm, Monokrystaly, Czech Republic) **[6]** were used as a reference and an auxiliary electrode, respectively.

3.1.2 Silver Solid Amalgam Working Electrodes

Solid amalgam electrodes belong to a relatively new generation of mercury-based electrodes with a potential to successfully replace liquid mercury electrodes and to provide a tool to avoid unsubstantiated fears of working with metallic mercury [54, 55]. Naturally, the electrode properties are dependent on the type of metal used for their preparation as these metals may exhibit either better (Cu, Bi, Cd, etc.) or worse (Pt, Au, Ag, etc.) electrochemical activity in comparison with mercury [56]. Based on their

surface and consistence, amalgam electrodes can be divided into several groups as follows: polished solid amalgam electrodes, film modified solid amalgam electrodes, meniscus modified solid amalgam electrodes, composite solid amalgam electrodes, paste solid amalgam electrodes with pasting liquid, single crystal silver amalgam electrodes, etc. [55]. Besides batch arrangements, amalgam electrodes can be also employed, e.g., in amperometric detection in liquid-flow systems such as HPLC [57, 58] and FIA [59, 60].

In this Ph.D. Thesis, m-AgSAE and p-AgSAE were used to develop novel electroanalytical methods for AQS and DX determination by employing following voltammetric techniques: DPV, linear-sweep voltammetry (LSV), differential pulse cathodic stripping voltammetry (DPCSV), and cyclic voltammetry (CV). Measurements were carried out either by above-mentioned Eco-Tribo polarograph controlled by PolarPro 3.1 software (lab-developed in J. Heyrovský Institute of Physical Chemistry of the Czech Academy of Sciences) or by PalmSens potentiostat/galvanostat equipped with a PSTrace software 4.2.2 (both Electrochemical Sensor Interface, Palm Instruments, The Netherlands). Again, a three-electrode arrangement was used: p-AgSAE and m-AgSAE served as working electrodes, Ag/AgCl/KCl (sat.) electrode (Elektrochemické Detektory, Czech Republic) as a reference electrode, and a platinum wire (Ø 1 mm, Monokrystaly, Czech Republic) as an auxiliary electrode **[1-3]**.

3. 2 Carbon Working Electrodes

3.2.1 Glassy Carbon Working Electrode

GCEs are highly chemically resistant, gas-impermeable, and electrically conductive electrodes usable in the potential range from approximately +1200 mV to −800 mV vs. saturated calomel electrode in acidic medium [61]. GCEs can be used in different arrangements such as rotating disk GCE [62] or dual GCE (dualGCE) (**Fig. 3.1)** [63]. Nowadays, GCEs are widely spread in various areas of electroanalytical chemistry due to the above-mentioned favourable features and also due to the possibility to easily modify their surface [64-66].

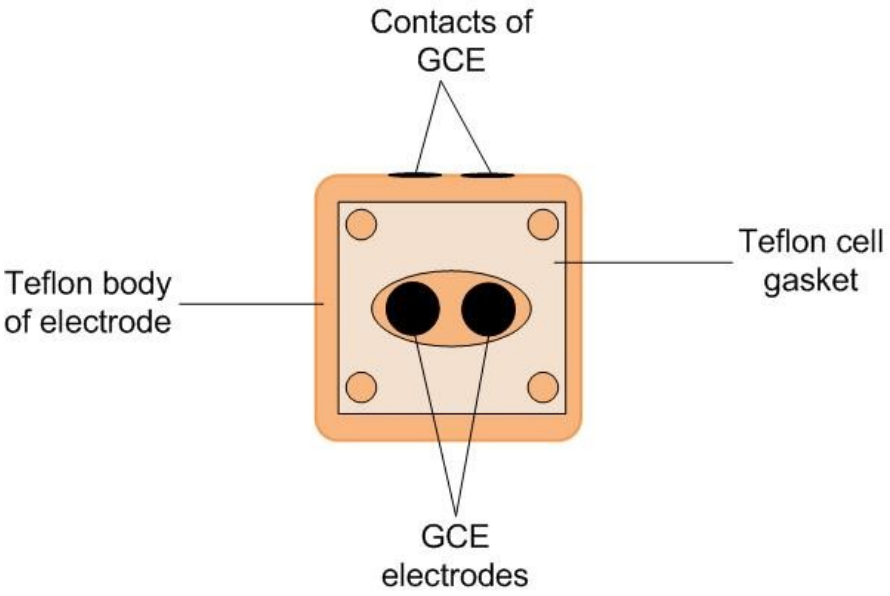

Fig. 3.1 Dual glassy carbon electrode (dualGCE).

In this work, dualGCE was used for the determination of AQS in physiological saline (PS) by flow injection system with amperometric detection. DualGCE was employed as a working electrode in the electrochemical cell (BASI, USA), consisting of two independent GCEs (Ø 3 mm), of an Ag/AgCl/KCl (sat.) reference electrode (BASI, USA), and a stainless capillary at the end of the cell which served as an auxiliary electrode. Thickness of the Teflon cell gasket was 0.127 mm (0.005 inch) (BASI, USA). Measurements were carried out by PalmSens potentiostat/galvanostat equipped with a PSTrace software v. 4.2.2 (both Electrochemical Sensor Interface, Palm Instruments, The Netherlands).

3.2.2 Carbon Paste Working Electrode

First CPE was developed as a by-product of the search for a dropping carbon electrode due to its extended potential window in the region of anodic potentials in contrast to mercury-based electrodes [67]. One of the biggest advantages of CPEs consists in a very simple way of surface treatment/renewal in order to remove possibly adsorbed compounds or formed passivating film. Thus, measurements are performed on a renewed carbon paste surface providing signals with a relatively good reproducibility. Carbon pastes are usually prepared by mixing a carbon powder with an organic liquid; peak currents usually decrease with an increasing amount of organic liquid [68]. Non-

modified as well as modified CPEs have been applied in various fields of analytical chemistry [69].

In our research, to exclude an influence of mercury compounds during measurements with HDME, a silica gel-modified CPE was used as an alternative working electrode to study transport of Pb-PC_2 complexes across a PLM. CV with accumulation potential −100 mV at different accumulation times was used as a suitable technique. Measurements were carried out by Eco-Tribo polarograph controlled by PolarPro 5.1 software (both Polaro-Sensors, Czech Republic). Such a modified CPE was employed as a working electrode in a three-electrode set up (a reference electrode: Ag/AgCl/KCl (sat.) electrode (Elektrochemické Detektory, Czech Republic), an auxiliary electrode: a platinum wire (Ø 1 mm, Monokrystaly, Czech Republic) **[6].**

3.3 Electrochemical Techniques Used

In general, various analytical techniques have been commonly employed in the process of development of novel compounds, of drugs or for study of behaviour of molecules in various environments and under different conditions. Electrochemistry in combination with radiometric, spectrophotometric, and chromatographic analysis represents a base of instrumental methods used in pharmaceutical laboratories [70].

Voltammetric methods, based on electrochemical redox reactions or on other charge transfer phenomena, are widely used [71-75]. In this Ph.D. Thesis, CV, LSV, DPV, DPCSV, amperometric detection and electrochemical impedance spectroscopy (EIS) were employed to accomplish its goals.

CV is usually performed in the beginning of a study as it can provide useful information about the state of the electrode surface, biological material, and behaviour of investigated compounds or biological materials. In contrast to CV, DPV is usually much more sensitive technique due to its ability to suppress the influence of the background currents, which results in achievement of significantly lower *LOD* values. Therefore, DPV has been advantageously employed for sensitive determination of trace amounts of analytes (in some cases even in biological fluids). Next, DPCSV is a modern highly sensitive technique used for the determination of a wide range of

compounds as it is considered being fast and simple. Moreover, DPCSV possesses lower susceptibility to matrix effects than DPV [76].

Amperometric detection is suitable for the determination of electroactive compounds in flow-liquid systems [77-79]. To obtain repeatable results in the case of amperometric detection, it is important to control pH, temperature, and flow rate of the eluent [80]. Amperometry is used for the determination of various compounds in batch systems as well as in electrochemical detectors coupled to ion chromatography [80], flow injection analysis (FIA) [79], liquid chromatography [81], and capillary electrophoresis [82].

EIS is another electrochemical technique which exhibits a wide range of applications, e.g., in microbiological analysis [83], in screening of body fluids [84], in investigation of corrosion mechanism [85], in study of transport processes across biological membranes **[6, 7]**, etc.. This technique gives a thorough insight into general description of the electrochemical behaviour of the investigated system and provides description of faradaic and non-faradaic processes. Besides, EIS may be also applied in solutions possessing small conductivity [86].

4. Results and Discussion

4.1 Micro-Volume Voltammetric Cell with Agar Membrane for Determination of Anticancer Drugs

4.1.1 Determination of Sodium Anthraquinone-2-Suplphonate by Voltammetric Techniques

Firstly, electrochemical behaviour of sodium AQS in a batch arrangement (volume of analysed solution amounted to 10 mL) was studied by cyclic voltammetry (CV), linear-sweep voltammetry (LSV) and differential pulse voltammetry (DPV) on two types of AgSAEs, namely m-AgSAE and p-AgSAE (inner Ø of both electrodes 5 mm). Recorded cyclic voltammograms showed one anodic and one cathodic peak in the whole tested range of pH (Britton-Robinsons buffers (BRB) of pH 2 − 12). The peaks indicated a reversible/quasireverisble behaviour and since the highest reversibility of examined system was observed in weakly alkaline media, i.e. pH 9 and 10 were chosen for AQS determination on both used amalgam electrodes. In further experiments, only the reduction process of AQS was investigated as AQS is more common form in contrast to its reduction product, dihydroAQS **[2]**.

By LSV, the dependence of cathodic peak potential of AQS on pH was investigated **[2]** and it was concluded that the reduction of AQS differs considerably in alkaline from that in acidic solutions. Moreover, this technique was used to confirm that AQS reduction is controlled solely by diffusion without any contribution from adsorption processes **[2]**.

Regarding DPV technique, optimization of parameters (pH, electrode surface pre-treatment, pulse width, and pulse height) was firstly performed and subsequently, such optimized method was used for the determination of AQS and for the construction of concentration dependences; achieved *LOD*s were 1.0 μmol L^{-1} on p-AgSAE and 0.4 μmol L^{-1} on m-AgSAE. Subsequently, this method was applied on model solutions of deionized water, river water, and human urine, all of them spiked by AQS **[2]**. The obtained results confirmed the possibility of using this novel method as a suitable method for the development of the MVVC **[1]**.

4.1.2 Development of Micro-Volume Voltammetric Cell

Further, a novel MVVC **(Fig. 4.1)** has been developed. It is composed from two compartments: micro-volume compartment (MVC) and large volume compartment (LVC). They are separated by an agar membrane, formed in the bottom of the MVC (i.e., of a glass tube) and it represents a conductive connection between a sample (20 − 50 µL, placed on the MVC bottom) and a supporting electrolyte (BRB) in the LVC. As can be seen in Fig. 4.1, the LVC is formed by a large volume voltammetric vessel (10 − 20 mL) with incorporated auxiliary and reference electrodes immersed in the supporting electrolyte. The working electrode is immersed into a sample in the MVC **[1]**.

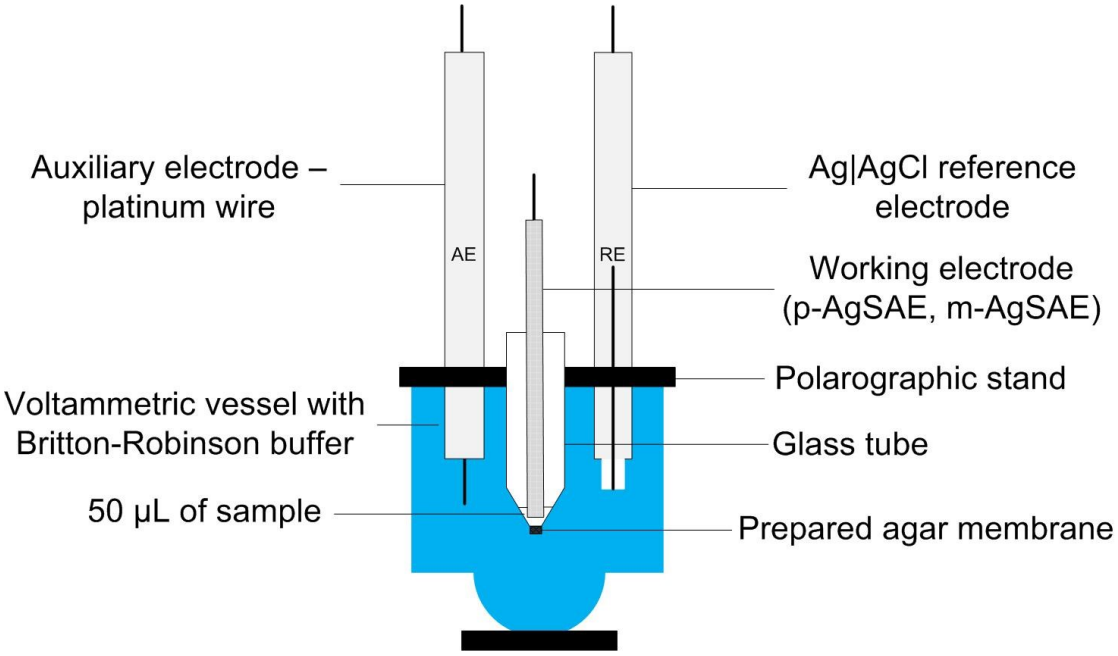

Fig. 4.1 Scheme of the newly developed micro-volume voltammetric cell (MVVC) **[1]**.

In the first step, preparation of agar membrane has been carefully optimized. Different solvents for agar membrane preparation were examined and 0.1 mol L^{-1} NaCl media was chosen as it provided the highest repeatability of recorded voltammetric signals. Subsequently, solutions with different agar concentrations have been tested. Concentration of agar of 30 g L^{-1} exhibited a good adhesion of agar to the glass tube and acceptable repeatability of the current signals. In addition, preparation of such concentrated solution was repeatable and the hardening process took approximately

10 min (however, in some cases it was even more than 30 min). The last investigated parameter was the thickness of the prepared membrane. Considering time stability, repeatability of agar membrane preparation and of measured current signals, thickness of 2.3 mm was used in all following measurements. A simple preparation procedure of a novel agar membrane is schematically depicted in **Fig. 4.2**. Prepared agar membrane may be used for a set of measurements for at least 7 days, if the MVC is stored in a humidity chamber **[1]**.

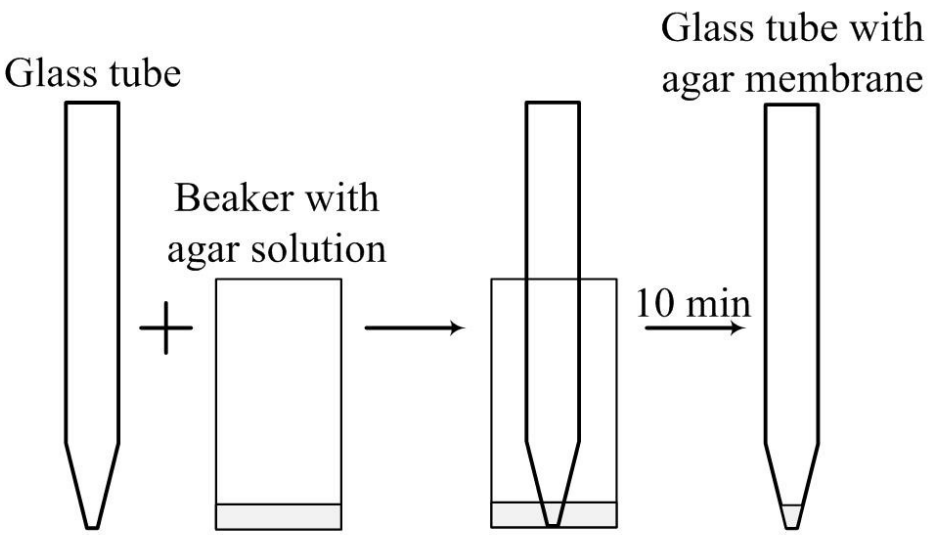

Fig. 4.2 Preparation of agar membrane at the end of the micro-volume compartment (MVC).

4.1.3 Determination of AQS and of Doxorubicin in the Micro-Volume Voltammetric Cell

MVVC was tested for the determination of AQ-based drugs in a small volume. Pilot experiments were performed with AQS due to its low price and availability by using previously optimized DPV method (see Chapter 4.1.1, **[2]**). To remove oxygen from measured solutions, addition of Na_2SO_3 was chosen as a better way than bubbling with nitrogen due to its more difficult access to the glass tube. The results of these measurements showed slightly lower *LOD*s in comparison with batch volume ones (for p-AgSAE in batch and in MVVC *LOD*s are 1 μmol L^{-1} and 0.15 μmol L^{-1}, respectively) and confirmed applicability of this MVVC for these determinations. Furthermore, MVVC was tested for analysis of spiked model samples of drinking water

(at the concentrations of DX from 1 to 100 μmol L^{-1}) and urine (at the concentrations of DX from 2 to 200 μmol L^{-1}) with high recoveries (for urine better than 97 ± 13 %) and small relative standard deviations (for urine better than 2.9 %) **[1]**.

Moreover, MVVC was used for the development of a novel method for DX determination. Due to of DX ability to be adsorbed on the electrode surface, differential pulse cathodic stripping voltammetry (DPCSV) on p-AgSAE was tested and subsequently used. Oxygen could not be removed by addition of Na_2SO_3 as BRB of more acidic pH was used as a supporting electrolyte. By this method, *LOD* 0.2 μmol L^{-1} was obtained and spiked human urine was tested with a recovery of 100.7 ± 6.6 % at concentration levels from 1 to 10 μmol L^{-1} **[3]**.

4.2 Application of Dialysis Catheter for Monitoring of Anticancer drugs

4.2.1 Pilot Experiments with Dialysis Catheter

The main aim was to determine the concentration of AQS as a readily available derivate of AQ-based anticancer drugs in spiked PS (154 mmol L^{-1} of NaCl, p.a., Lach-Ner, Czech Republic). PS was chosen as the AQS solvent and also as a carrier solution, because PS is the most frequently used in clinical practice for dialysis of substances from blood circulation.

Firstly, determination of AQS in PS was tested by DPV on p-AgSAE (geometric surface area 0.39 mm^2) in the cathodic region within the potential range from 0 mV to −850 mV. Used DPV parameters were as follows: scan rate (v) of 20 mV s^{-1}; pulse height (E_p) of −50 mV, and pulse width (t_p) of 100 ms, current values were recorded in the last 20 ms before the pulse start and in the lass 20 ms of the pulse duration. Measurements were carried out in a batch arrangement (sample volume of 3 mL) by employing a three-electrode set-up with a reference electrode Ag/AgCl/3 mol L^{-1} KCl electrode (BVT Technologies, Czech Republic) and an auxiliary electrode a platinum wire (Ø 1 mm, BVT Technologies, Czech Republic) by using PalmSens potentiostat/galvanostat cotrolled by the PSTrace software v. 4.2.2 (both Electrochemical Sensor Interface, Palm Instruments, The Netherlands).

Dependence of peak currents (I_p) on concentrations (c) of AQS in PS was measured and the corresponding graphs were constructed (**Fig. 4.3**). Dependence was proved to be linear within the concentration range from 2 to 1000 µmol L^{-1} (the equation of the linear dependence: I_p (nA) = –1370 (nA L $mmol^{-1}$) × c (µmol L^{-1}) + (–24.5) (nA). *LOD* 1.0 µmol L^{-1} was achieved. By these experiments, the applicability of p-AgSAE for voltammetric determination of AQS in PS was successfully verified.

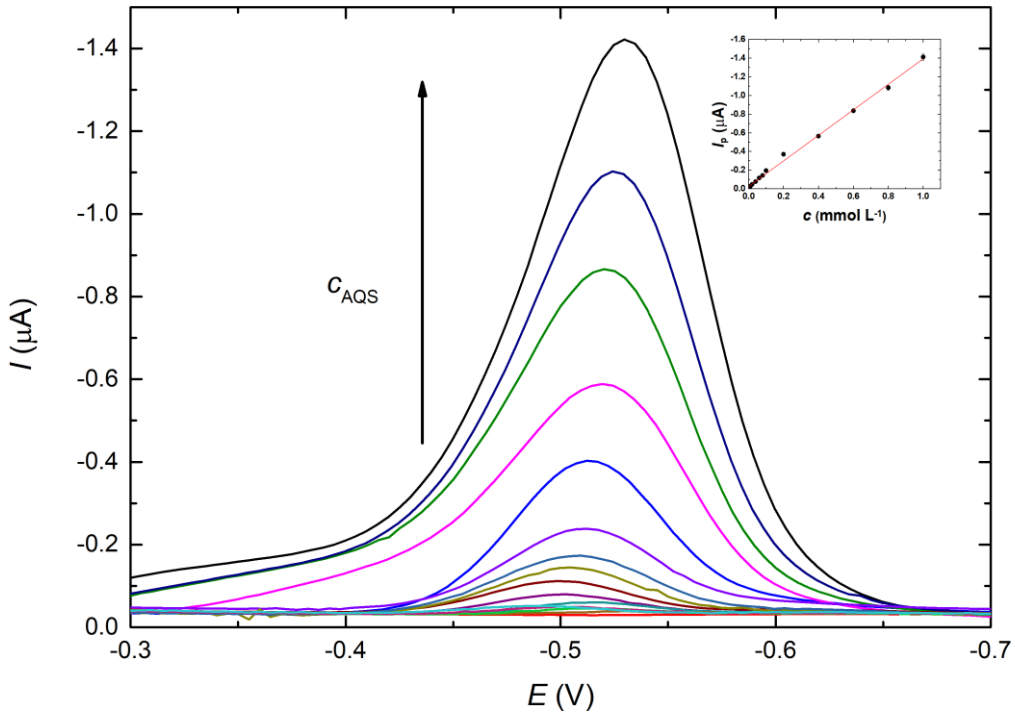

Fig. 4.3 DP voltammograms of AQS (c from 2 to 1000 µ mol L^{-1}) on p-AgSAE in PS after oxygen removal by bubbling with N_2. Parameters of DPV: v of 20 mV s^{-1}; E_{pulse} of −50 mV; t_{pulse} of 100 ms; E_{range} from 0 mV to −850 mV. A red line represents the supporting electrolyte (PS). Inset: Corresponding concentration dependence.

Further, UV-VIS spectrophotometry (UV/VIS) was employed as a comparative method. Measurements were performed by Agilent 8453 UV-Vis Spectrophotometer (USA) controlled by software UV-Visible ChemStation v. A0901[76], 1 mm quartz cuvette was used for the measurements and PS served as a blank solution. Concentration dependence of AQS was linear within the concentration range from 1 to 100 µmol L^{-1} with achieved *LOD* of 0.33 µmol L^{-1} (**Fig. 4.4**).

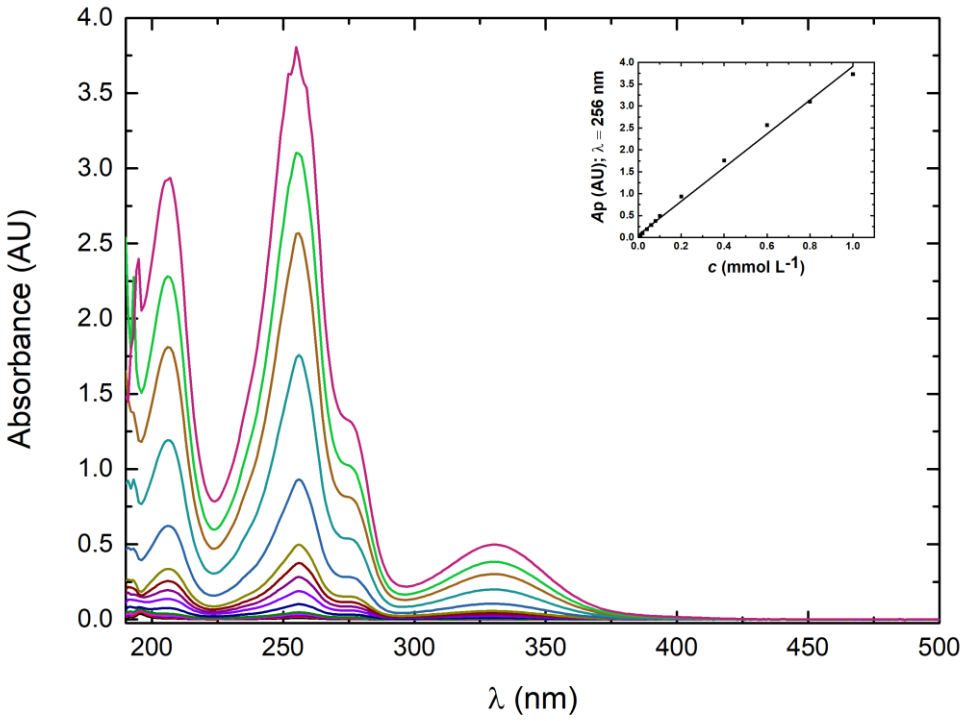

Fig. 4.4 Absorption spectra of AQS (*c* from 2 to 1000 μmol L^{-1}) in PS. Measured by UV-VIS spectrophotometry in 1 mm quartz cuvette with PS as a blank. Inset: Corresponding concentration dependence.

Transport (penetration) of AQS through the dialysis membrane in dialysis catheter was monitored in the following step. Dialysis apparatus (**Fig. 4.5**) consisted of syringe pump (SyringePump NO. NE-510L, USA) controlled by software New Era WinPumpTerm v. 0.6, syringe with PS, catheter with dialysis membrane inserted in a glass tube with 5 mL of AQS solution in PS, and a vial for collecting of dialysate. Dialysate was collected at two flow rates of 1 μL min^{-1} and 5 μL min^{-1}. These two values were chosen and tested because with increasing rates of liquid flow, firstly, a probability of dialysis membrane damage increases, and secondly, recovery exponentially decreases as it has been previously reported in ref. [87].

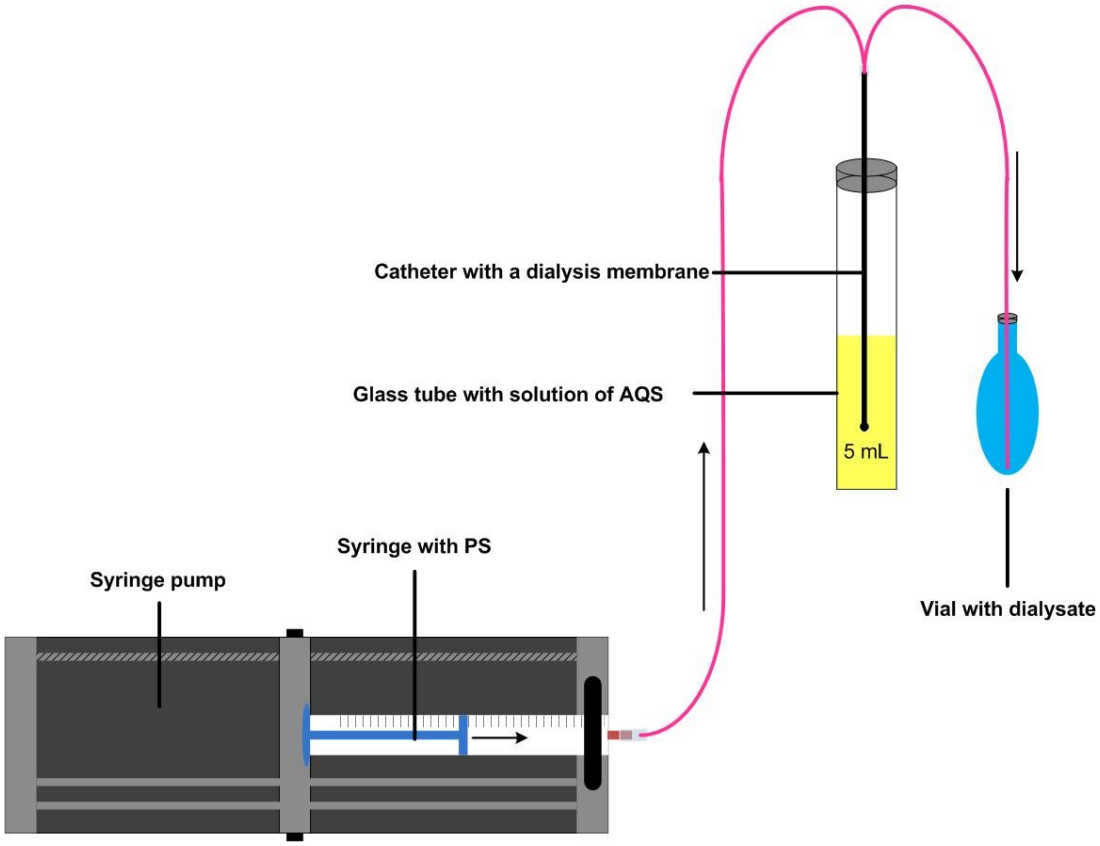

Fig. 4.5 Scheme of dialysis apparatus.

Next, recovery of dialysis procedure (**Table 1**) was evaluated by DPV as well as by UV/VIS spectrophotometry as already mentioned, and subsequently evaluated by using a standard addition method (DPV) and previously constructed calibration dependences (DPV; UV/VIS). The recovery values were assessed as a ratio of amount of AQS in dialysate (D) and amount of AQS in D plus in solution after dialysis (a solution after the dialysis in the glass tube) (After(D), **Equation 4.1**).

Equation 4.1 Assessment of dialysis recovery.

$$\text{recovery (\%)} = \frac{\mathbf{D}}{\mathbf{D+After(D)}} \times 100$$

Table 4.1 Evaluation of recovery of dialysis procedures. Reported recoveries are based on DPV measurements (on p-AgSAE in PS after oxygen removal by bubbling with N_2; applied DPV parameters: v of 20 mV s^{-1}; E_{pulse} of −50 mV; t_{pulse} of 100 ms; E_{range} from 0 mV to −850 mV) and by using UV-VIS spectrophotometric measurements (in 1 mm quartz cuvette, blank – PS). Two flow rates of 1 and 5 mL min^{-1} were tested.

c_{AQS} before dialysis (μmol L^{-1})	Flow rate (mL min^{-1})	Recovery		
		DPV: standard addition	DPV: calibration dependence	UV-VIS: calibration dependence
1000	1	-	42.60 %	42.40 %
	5	-	17.20 %	13.90 %
100	1	65.50 %	64.60 %	63.50 %
	5	24.10 %	22.70 %	22.00 %
10	1	52.30 %	51.40 %	51.90 %
	5	20.10 %	15.70 %	26.80 %

Second part of this research was focused on amperometric determination of AQS using dualGCE. For this purpose, a flow-cell (MF-1093, BASI, USA), a dualGCE (2× Ø 3 mm, MF-1000, BASI, USA), a syringe pump (SyringePump NO. NE-510L, USA) controlled by software New Era WinPumpTerm v. 0.6, and a six-way valve (V-451, Labicom, Czech Republic) were used. The scheme of the apparatus is depicted in **Fig. 4.6**.

Naturally, amperometric detection of AQS had to be optimized. Firstly, the effect of different detection potentials applied on dualGCE were tested. The best results /(the highest I_p of AQS on GCE 2) were achieved at a potential E_{GCE1} of −1200 mV and at E_{GCE2} −900 mV (conditions: c_{AQS} of 10 μmol L^{-1}, flow rate of 500 μL min^{-1}, thickness of Teflon gasket of 127 μm, syringe volume of 25 mL). Moreover, other parameters such as syringe volume, different types of arrangements, and thickness of Teflon cell gaskets were optimized in order to suppress the noise and increase the sensitivity of the measurements. Tested syringe volumes were 1 mL, 5 mL, and 25 mL. The found optimum conditions were as follow: PS without AQS, flow rate of 5 μL min^{-1}, thickness of Teflon gasket of 127 μm, E_{GCE1} of −1200 mV, E_{GCE2} of −900 mV, and the lowest noise was recorded when a syringe volume of 5 mL was used.

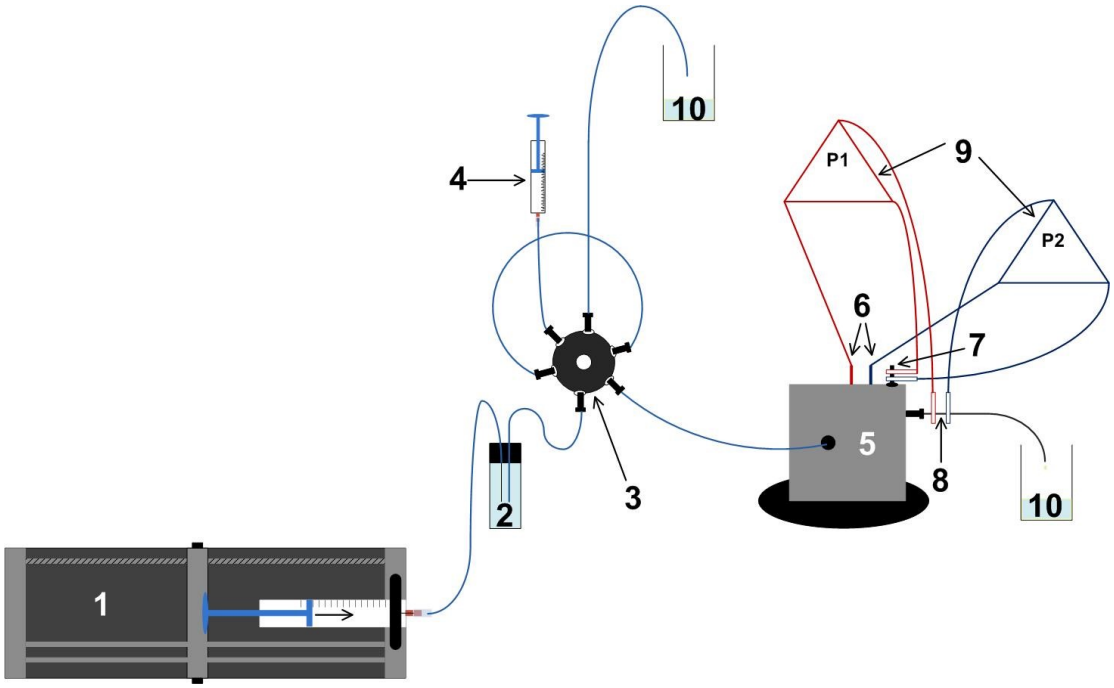

Fig. 4.6 Scheme of apparatus for amperometric detection in a liquid-flow system consisting of an injection pump with a carrier solution (PS) (1), a vial with PS (2), a 6/2-way valve (3), syringe with a sample (4), electrochemical cell (5), connections of the working electrodes (dualGCE) (6), connection of the reference electrode (7), connection of the auxiliary electrode (8), potentiostats P1 and P2 (9), and waste beakers (10).

Further, different types of connections were examined: (1) with/without a vial (with PS) placed in a flow system between a syringe and a 6-way valve, (2) three-electrode system/two-electrode system, and (3) with original auxiliary electrode (body of the electrochemical cell), with a stainless steel capillary auxiliary electrode, and with a stainless steel capillary auxiliary electrode terminated with a rubber tube. The found optimum conditions as follow: PS without AQS (for comparison of two electrode and three electrode arrangements, 100 µmol L^{-1} AQS) was used, flow rate of 5 µL min^{-1}, thickness of Teflon gasket of 127 µm, E_{GCE1} of −1200 mV, E_{GCE2} of −900 mV, syringe volume of 5 mL. The lowest noise and enhanced sensitivity was obtained with the three-electrode set-up with vial with PS, and with the stainless steel capillary auxiliary electrode terminated with a rubber tube. The last optimized parameter was the thickness of the Teflon cell gasket. Three different values of 380 µm, 127 µm, and 51 µm have been tested. The best results in the terms of the lowest noise, improved sensitivity, and repeatability were obtained with the thickness of Teflon cell gasket of 127 µm (**Fig. 4.7**).

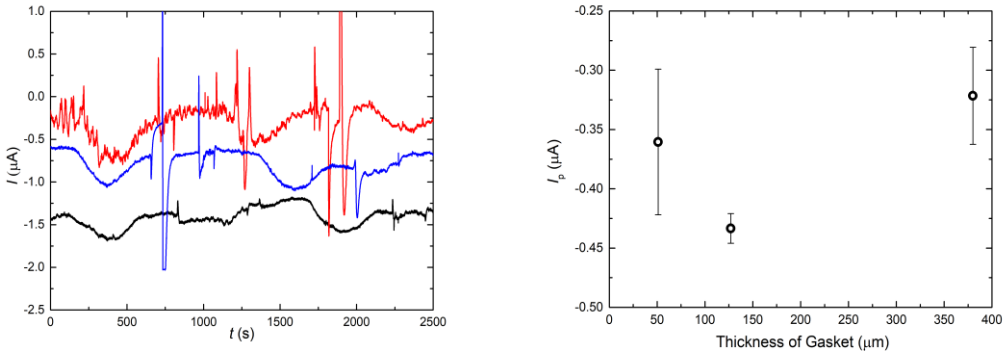

Fig. 4.7 Left: Time dependences of amperometric signals of PS with AQS (c_{AQS} of 100 μmol L^{-1}) on dualGCE with employed **51 μm Teflon cell gasket**, **127 μm Teflon cell gasket**, and **380 μm Teflon cell gasket thickness**. Right: Dependence of I_p of AQS on thickness of Teflon cell gasket measured by amperometry. For each measured value of Teflon cell gasket thickness, the confidence interval for the significance level of $\alpha = 0.05$ is displayed (for $n = 6$); Flow rate of 5 μL min^{-1}, E_{GCE1} of −1200 mV, E_{GCE2} of −900 mV, syringe volume of 5 mL, volume of sample loop of 10 μL.

Finally, the dependence of recorded peak currents on AQS concentration was investigated in the AQS concentration range from 0.1 to 1.0 mmol L^{-1} (**Fig. 4.8**) and from 10 to 100 μmol L^{-1} (**Fig. 4.9**). Regrettably, due to the slow flow rate, the whole calibration dependence was not constructed at once. However, it presented no problem. Usually, three concentration levels were measured in one day, and on the beginning of the next working day it was verified that sensitivity of employed electrode towards AQS remained constant by repeating the measurements with the last measured concentration of previous day and comparing both values. The dependences were linear in the whole concentration ranges as shown in **Fig. 4.8** and **Fig. 4.9**. The equation of linear dependence in the concentration range from 0.10 to 1.0 mmol L^{-1} was I_p (μA) = –4.64 (μA L mol^{-1}) × c (mmol L^{-1}) – 0.07 (μA). For the range from 0.01 to 0.1 mmol L^{-1}, it was I_p (μA) = –5.04 (μA L mol^{-1}) × c (mmol L^{-1}) – 0.01 (μA). The reached *LOD* was 15 μmol L^{-1}. It is possible to conclude that the applicability of p-AgSAE for voltammetric determination of AQS in PS was successfully verified by these experiments.

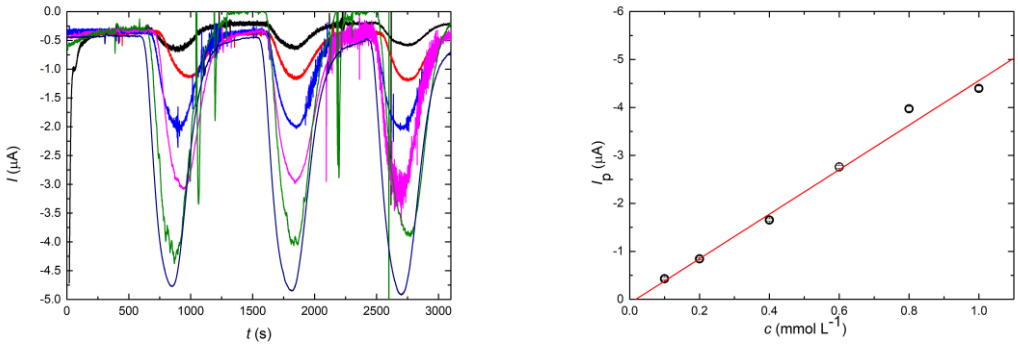

Fig. 4.8 Left: Time dependences of amperometric signals of AQS with varying c_{AQS} from from 10 to 100 µmol L^{-1} recorded on dualGCE. Right: Corresponding concentration dependence. Flow rate of 5 µL min^{-1}, E_{GCE1} of −1200 mV, E_{GCE2} of −900 mV, syringe volume of 5 mL, 127 µm Teflon cell gasket thickness, volume of sample loop of 10 µL.

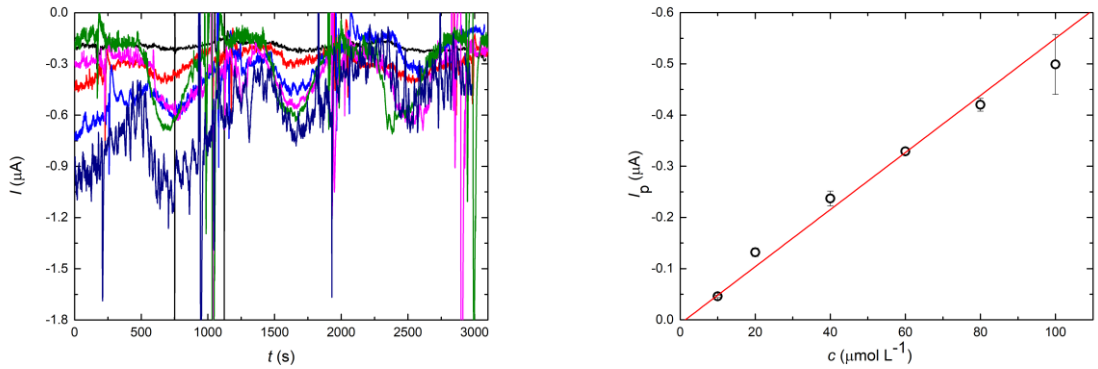

Fig. 4.9 Left: Time dependences of amperometric signals of AQS with varying c_{AQS} from 10 to 100 µmol L^{-1}) recorded on dualGCE. Right: Corresponding concentration dependence. Flow rate of 5 µL min^{-1}, E_{GCE1} of −1200 mV, E_{GCE2} of −900 mV, syringe volume of 5 mL, 127 µm Teflon cell gasket thickness, volume of sample loop of 10 µL.

4.3 Using of Model Biological Membrane

4.3.1 Model Supported Phospholipid Membrane

In general, model supported PLMs (s-PLMs) have been used for studying properties of real biological membranes. Development of research concerning real biological membranes and information regarding different types and the development of model biological membranes are summarized in a review **[7]**. Basically, biological membranes consist of two phospholipid monolayers which have hydrophobic tail and hydrophilic head parts. Hydrophobic parts are oriented towards each other and hydrophilic parts are oriented to aqueous solutions (to intracellular and extracellular, respectively) **[7]**. For our measurements, a model membrane – planar s-PLM – was used **[6]**. Planar s-PLM represents the simplest PLM model because of the accessibility of its both sides (representing extracellular and intracellular spaces), its stability, simple preparation, and its thickness (similar to a real membrane) [88].

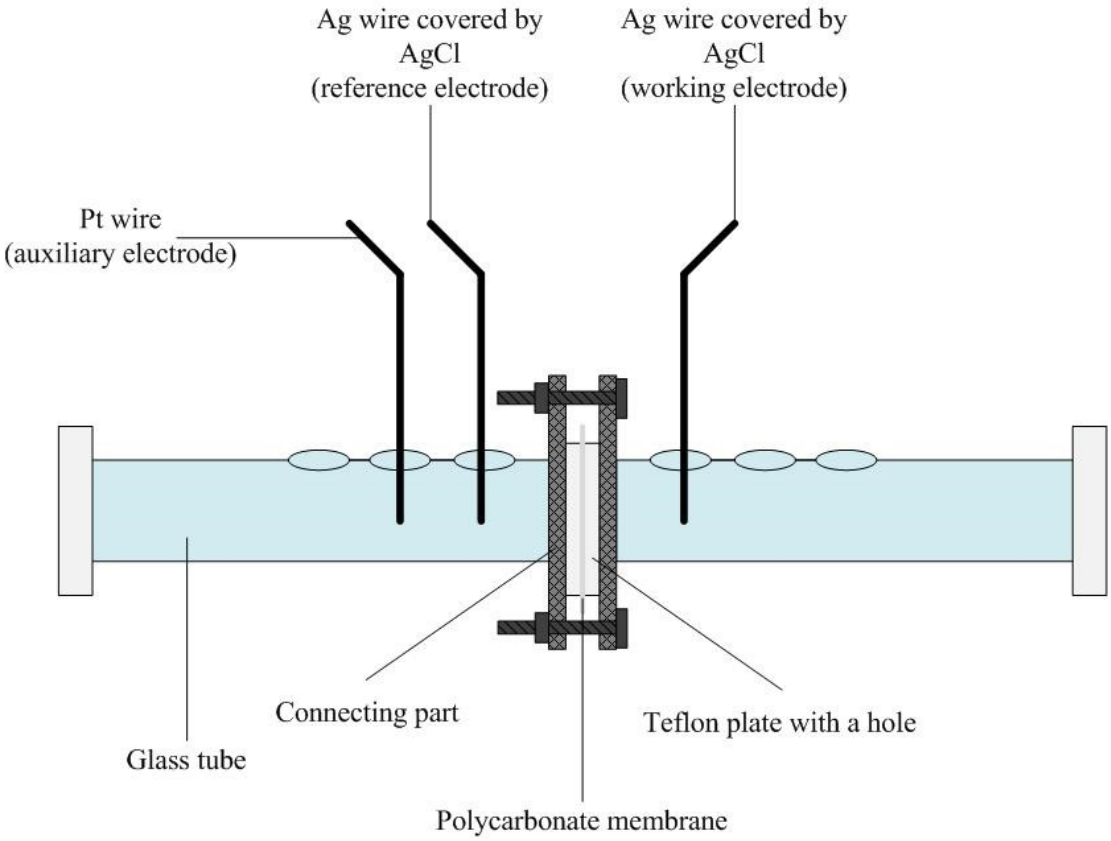

Fig. 4.10 Scheme of electrochemical glass cell for creating and studying cell membranes.

For our research, the s-PLM was prepared in "electrochemical glass cell" (**Fig. 4.10**) where porous polycarbonate membrane was used as a carrier of the s-PLM and placed between two glassy compartments with holes for electrodes and also for manipulation with a solution inside the cell. Its properties have been investigated by using EIS which is a non-invasive technique suitable for PLM studies in detail (particularly, structural and functional properties). Electrical impedance of a PLM depends on various factors such as membrane potential, temperature, presence of pores in membranes, and membrane composition **[7]**.

Various electrical equivalent circuits (EECs) have been tested to electrically describe and to model investigated PLMs and realized transporting processes across them. EEC depicted in **Fig. 4.11** was created from two simple EECs applied for characterisation of non-covered electrodes and biological membranes [88]. This EEC is useful for characterization of PLM formed in pores of a polycarbonate carrier by resistors and capacitors in the circuit. Serial resistance (R_s) corresponds to resistance of the connectors and of the electrolyte (0.1 mol L^{-1} KCl). Parallel capacitor (C_{p1}) corresponds to parasitic capacitance of the carrier membrane and parallel resistor (R_{p1}) to its parallel resistance. R_{p2} and C_{p2} correspond to electrical properties of formed PLM in the carrier membrane pores [89].

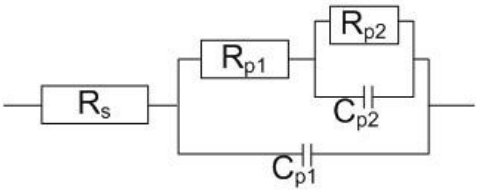

Fig. 4.11 Electrical equivalent circuit used for EIS characterization of s-PLM (adapted from **[7]**) (R_s – Serial resistor, R_p – Parallel resistors, C_p – Parallel capacitors).

4.3.2 Study of Transport of Complexes of Lead with Phytochelatin across Biological Membrane

In the beginning, s-PLM was prepared by application of solution of 1,2-dipalmitoyl-sn-glycero-3-phosphocholine and calcimycin (divalent cation ionophore used for simulation of ion channels for cadmium and lead ions) in ethanol and *n*-heptane on a polycarbonate carrier placed in electrochemical glass cell (**Fig. 4.10**).

After solvent evaporation from the applied solution on a polycarbonate carrier (45 min in total), 3 mL of 0.1 mol L^{-1} KCl were pipetted into each of glass tubes. s-PLM stabilisation, which took approximately 60 min, was monitored by EIS with applied voltage of −100 mV, which is a value close to the real cell membrane potential **[6]**.

After the stabilisation of the s-PLM, Pb ions were added to one of solutions in the glass tubes of electrochemical glass cell (one part of the experiment) or 2 mL of electrolyte in one of glass tubes were replaced by 2 mL of KCl solution containing Pb-phytochelatin complex (second part of the experiment). Then, transport of Pb ions/Pb-phytochelatin complex across s-PLM to the second glass tube was monitored by EIS for exactly 60 min. Subsequently, the solution from the second glass tube was transferred to a voltammetric vessel for the determination of Pb ions/Pb complexes by anodic stripping voltammetry on HMDE **[6]**.

Voltammetric measurements performed after the transport of Pb ions/Pb-phytochelatine complex across s-PLM showed that only 0.25 % of Pb^{2+} of initial amount was transported when phytochelatin was absent. However, when solution contained both Pb^{2+} and PC_2 (pH of medium was 6.8), 6.66 % of initial amount of Pb ions was transported through the s-PLM **[6]**.

5. Conclusion

This Ph.D. Thesis represents a step for finding suitable analytical methods for monitoring anticancer drugs in urine or blood circulation in order to improve cancer treatment by individualized dosages. Furthermore, for this purpose, new arrangements of electroanalytical methods have been successfully constructed and tested. These arrangements provide low-cost, easy to fabricate, and user-friendly electroanalytical methods with a high level of precision and selectivity.

It describes development and application of MVVC with agar membrane, which represents a semi-permeable barrier between a sample and a working electrode in MVC, and a supporting electrolyte and a reference electrode and an auxiliary electrode in LVC. By employing such cell, samples with a volume of 20 μL could be analysed. The applicability of the developed MVVC was consequently tested with determination of sodium AQS as a model compound, and of doxorubicin, which is a representative of the AQ-based anticancer group of drugs. Moreover, both of studied analytes were successfully determined in drinking water and in human urine spiked samples.

Second part of this Thesis is focused on the development of a liquid flow injection system for monitoring anticancer drugs in the blood circulation. The usage of a dialysis catheter for separation of a model compound, AQS in PS, which was connected with a syringe pump at two different flow rates (1 and 5 μL min^{-1}), was successfully tested. Furthermore, dependence of amperometric signals of AQS on its concentration on a dualGCE by using a low flow rate of 5 μL min^{-1} was investigated.

Third part of this Thesis investigates transport of Pb ions through a model biological membrane in presence and in absence, respectively, of phytochelatins. As it was shown, higher concentration of Pb ions was transported through a model biological membrane in the form of Pb-phytochelatin complexes Thus, plants with higher concentration of phytochelatins can presumably accumulate heavy metals, they can enter the food chain (e.g., via animal feed), and subsequently intoxicate animal and even human bodies. The presented research focused on transport mechanisms across biological membranes may be used advantageously for the description of more complicated transport mechanisms, e.g., for the transport of anticancer drugs which can potentially lead to the improvement of targeted treatments.

The results obtained within the framework of this Ph.D. Thesis can be summarised as follows:

- Successful development of a DPV method employing a p-AgSAE and a m-AgSAE for the determination of AQS in a batch arrangement.
- LOD_{AQS} of the developed DPV method amounted to 1.0 μmol L^{-1} (on p-AgASE) and 0.4 μmol L^{-1} (on m-AgSAE).
- Determination of AQS in river water and human urine performed by using the developed DPV method.
- Development of MVVC with a semi-permeable agar membrane for a minimum volume of 20 μL; optimization of an agar membrane preparation.
- MVVC testing in combination with DPV determination of AQS in model samples (*LOD* of 0.2 μmol L^{-1} on p-AgASE).
- Verification of MVVC application by the AQS determination in tap water and human urine.
- Determination of DX in MVVC by optimized DPCSV. *LOD* of 0.2 μmol L^{-1} on p-AgSAE.
- DX determined in tap water and human urine (recovery 100.7 ± 6.6 % (c_{DX} of 1.0 μmol L^{-1}) by using MVVC.
- Separation of AQS in PS by a dialysis catheter. Reached recovery measured by DPV on p-AgSAE: 51.4 % for a flow rate of 1 μL min^{-1} and 15.7 % for a flow rate of 5 μL min^{-1}.
- Optimized amperometric detection of AQS in liquid flow system with a flow rate of 5 μL min^{-1}. Achieved *LOD* of 15 μmol L^{-1} on dualGCE.
- Preparation of a model biological PLM for elucidation of transport mechanism of Pb cations in the presence of phytochelatins.
- Toxic Pb cations were transported to the cells 26-times more effectively in the presence of phytochelatins. 6.6 % of Pb cations transported across a model PLM in the presence of phytochelatins due to the formation of Pb-phytochelatin complexes, and only 0.25 % of Pb cations transported when phytochelatins were absent.

6. **References**

[1] **Š. Skalová**, L. M. Gonçalves, T. Navrátil, J. Barek, J. A. Rodrigues, V. Vyskočil: Miniaturized Voltammetric Cell for Cathodic Voltammetry Making Use of an Agar Membrane, *Journal of Electroanalytical Chemistry* **2018**, *821*, 47.

[2] **Š. Skalová**, T. Navrátil, J. Barek, V. Vyskočil: Voltammetric Determination of Sodium Anthraquinone-2-Sulfonate using Silver Solid Amalgam Electrodes, *Monatshefte für Chemie – Chemical Monthly* **2017**, *148*, 577.

[3] **S. Skalova**, J. Langmaier, J. Barek, V. Vyskocil, T. Navratil: Doxorubicin determination using two voltammetric techniques - a comparative study, ***submitted to Electrochemical Acta***.

[4] L. A. Decosterd, N. Widmer, K. Zaman, E. Cardoso, T. Buclin, C. Csajka: Therapeutic Drug Monitoring of Targeted Anticancer Therapy, *Biomarkers in Medicine* **2015**, *9*, 887.

[5] P. Herviou, E. Thivat, D. Richard, L. Roche, J. Dohou, M. Pouget, A. Eschalier, X. Durando, N. Authier: Therapeutic Drug Monitoring and Tyrosine Kinase Inhibitors, *Oncology letters* **2016**, *12*, 1223.

[6] I. Šestáková, **Š. Skalová**, T. Navrátil: Labile Lead Phytochelatin Complex Could Enhance Transport of Lead Ions across Biological Membrane, *Journal of Electroanalytical Chemistry* **2018**, *821*, 92.

[7] **Š. Skalová**, V. Vyskočil, J. Barek, T. Navrátil: Model Biological Membranes and Possibilities of Application of Electrochemical Impedance Spectroscopy for their Characterization, *Electroanalysis* **2018**, *30*, 207.

[8] Z. Čadková, J. Száková, D. Miholová, B. Horáková, O. Kopecký, D. Křivská, I. Langrová, P. Tlustoš: Bioaccessibility versus Bioavailability of Essential (Cu, Fe, Mn, and Zn) and Toxic (Pb) Elements from Phyto Hyperaccumulator Pistia stratiotes: Potential Risk of Dietary Intake, *Journal of Agricultural and Food Chemistry* **2015**, *63*, 2344.

[9] C. S. Cobbett: Phytochelatins and Their Roles in Heavy Metal Detoxification, *Plant Physiology* **2000**, *123*, 825.

[10] G. N. Hortobágyi: Anthracyclines in the Treatment of Cancer, *Drugs* **1997**, *54*, 1.

[11] P. S. Guin, S. Das, P. C. Mandal: Electrochemical Reduction of Sodium 1,4-Dihydroxy-9,10-Anthraquinone-2-Sulphonate in Aqueous and Aqueous Dimethyl Formamide Mixed Solvent: A Cyclic Voltammetric Study, *International Journal of Electrochemical Science* **2008**, *3*, 1016.

[12] A. E. Alegria, A. Ferrer, E. Sepulveda: Photochemistry of Water-soluble Quinones. Production of a Water-derived Spin Adduct, *Photochemistry and Photobiology* **1997**, *66*, 436.

[13] J. H. Wilford, M. D. Archer: Solvent Effects on the Redox Potentials of Benzoquinone, *Journal of Electroanalytical Chemistry and Interfacial Electrochemistry* **1985**, *190*, 271.

[14] B. Paduszek, M. K. Kalinowski: Redox Behaviour of Phenothiazine and Phenazine in Organic Solvents, *Electrochimica Acta* **1983**, *28*, 639.

[15] B. R. Eggins: Interpretation of Electrochemical Reduction and Oxidation Waves of Quinone–hydroquinone System in Acetonitrile, *Journal of the Chemical Society D: Chemical Communications* **1969**, *21*, 1267.

[16] T. Fujinaga, K. Izutsu, T. Nomura: Effect of Metal Ions on the Polarographic Reduction of Organic Compounds in Dipolar Arrotic Solvents, *Journal of Electroanalytical Chemistry and Interfacial Electrochemistry* **1971**, *29*, 203.
[17] D. J. Booser, G. N. Hortobagyi: Anthracycline Antibiotics in Cancer Therapy, *Drugs* **1994**, *47*, 223.
[18] W. M. Cumming, I. V. Hopper, T. Wheeler, *Systematic Organic Chemistry : Modern Methods of Preparation and Estimation*, Constable, London **1937**.
[19] M. Bokhamy, N. Adler, C. Pulgarin, M. Deront, C. Seignez, P. Péringer: Degradation of Sodium Anthraquinone Sulphonate by Free and Immobilized Bacterial Cultures, *Applied Microbiology and Biotechnology* **1994**, *41*, 110.
[20] M. Singh, K. Pakshirajan, V. Trivedi: Photo-Inactivation of Escherichia Coli and Enterococcus Hirae Using Methylene Blue and Sodium Anthraquinone-2-Sulphonate: Effect of Process Parameters, *3 Biotech* **2016**, *6*, 176.
[21] K. Oyaizu, Y. Niibori, A. Takahashi, H. Nishide: BODIPY-Sensitized Photocharging of Anthraquinone-Populated Polymer Layers for Organic Photorechargeable Air Battery, *Journal of Inorganic and Organometallic Polymers and Materials* **2013**, *23*, 243.
[22] C. M. Zhang, Z. Huang, Y. Yang, D. Wang, D. N. He: Preparation of Polypyrrole/Anthraquinone-2-Sulfonate Nanocomposite and Application in Li-Ion Battery, *Chinese Journal of Organic Chemistry* **2014**, *34*, 1347.
[23] T. Tsukioka, H. Ozawa, T. Murakami: Gas Chromatographic-Mass Spectrometric Determination of Anthraquinonesulfonates in Environmental Samples, *Analytical Sciences* **1991**, *7*, 897.
[24] X. T. Yang, X. S. Chai, Q. X. Hou, J. Y. Zhu, L. G. Danielsson: Determination of Anthraquinone-2-Sulfonate in Alkaline Pulping Liquor by Spectrophotometry Using a Nafion Membrane Interface, *Analytica Chimica Acta* **2002**, *474*, 69.
[25] N. Lomovskaya, S. L. Otten, Y. Doi-Katayama, L. Fonstein, X. C. Liu, T. Takatsu, A. Inventi-Solari, S. Filippini, F. Torti, A. L. Colombo, C. R. Hutchinson: Doxorubicin Overproduction in Streptomyces Peucetius: Cloning and Characterization of the dnrU Ketoreductase and dnrV Genes and the doxA Cytochrome P-450 Hydroxylase Gene, *Journal of bacteriology* **1999**, *181*, 305.
[26] S. Penco, G. Vicario, F. Angelucci, F. Arcamone: Synthesis of 14-C-14 Daunorubicin and Doxorubicin, *Journal of Antibiotics* **1977**, *30*, 773.
[27] K. Mross, P. Maessen, W. J. v. d. Vijgh, H. Gall, E. Boven, H. M. Pinedo: Pharmacokinetics and Metabolism of Epidoxorubicin and Doxorubicin in Humans, *Journal of Clinical Oncology* **1988**, *6*, 517.
[28] R. D. Olson, P. S. Mushlin, D. E. Brenner, S. Fleischer, B. J. Cusack, B. K. Chang, R. J. Boucek: Doxorubicin Cardiotoxicity May Be Caused By Its Metabolite, Doxorubicinol, *Proceedings of the National Academy of Sciences of the United States of America* **1988**, *85*, 3585.
[29] E. Salvatorelli, P. Menna, S. Cascegna, G. Liberi, A. M. Calafiore, L. Gianni, G. Minotti: Paclitaxel and Docetaxel Stimulation of Doxorubicinol Formation in the Human Heart: Implications for Cardiotoxicity of Doxorubicin-taxane Chemotherapies, *Journal of Pharmacology and Experimental Therapeutics* **2006**, *318*, 424.
[30] S. J. F. Kaptein, T. De Burghgraeve, M. Froeyen, B. Pastorino, M. M. F. Alen, J. A. Mondotte, P. Herdewijn, M. Jacobs, X. de Lamballerie, D. Schols, A. V. Gamarnik, F. Sztaricskai, J. Neyts: A Derivate of the Antibiotic Doxorubicin Is a Selective Inhibitor of Dengue and Yellow Fever Virus Replication *In Vitro*, *Antimicrobial Agents and Chemotherapy* **2010**, *54*, 5269.

[31] T. Madrakian, K. D. Asl, M. Ahmadi, A. Afkhami: Fe_3O_4@Pt/MWCNT/Carbon Paste Electrode for Determination of a Doxorubicin Anticancer Drug in a Human Urine Sample, *Rsc Advances* **2016**, *6*, 72803.
[32] N. Hashemzadeh, M. Hasanzadeh, N. Shadjou, J. Eivazi-Ziaei, M. Khoubnasabjafari, A. Jouyban: Graphene Quantum Dot Modified Glassy Carbon Electrode for the Determination of Doxorubicin Hydrochloride in Human Plasma, *Journal of Pharmaceutical Analysis* **2016**, *6*, 235.
[33] J. Han, J. Zhang, H. Y. Zhao, Y. Li, Z. L. Chen: Simultaneous Determination of Doxorubicin and Its Dipeptide Prodrug in Mice Plasma by HPLC with Fluorescence Detection, *Journal of Pharmaceutical Analysis* **2016**, *6*, 199.
[34] J. Mbuna, T. Kaneta: Capillary Electrophoresis with Laser-Induced Fluorescence Detection for Application in Intracellular Investigation of Anthracyclines and Multidrug Resistance Proteins, *Analytical Sciences* **2015**, *31*, 1121.
[35] A. Roszkowska, M. Tascon, B. Bojko, K. Goryński, P. R. dos Santos, M. Cypel, J. Pawliszyn: Equilibrium Ex Vivo Calibration of Homogenized Tissue for *In Vivo* SPME Quantitation of Doxorubicin in Lung Tissue, *Talanta* **2018**, *183*, 304.
[36] W. E. Rauser: Phytochelatins and Related Peptides. Structure, Biosynthesis, and Function, *Plant Physiology* **1995**, *109*, 1141.
[37] O. K. Vatamaniuk, E. A. Bucher, J. T. Ward, P. A. Rea: A New Pathway for Heavy Metal Detoxification in Animals: Phytochelatin Synthase Is Required for Cadmium Tolerance Incaenorhabditis Elegans, *Journal of Biological Chemistry* **2001**, *276*, 20817.
[38] S.-B. Ha, A. P. Smith, R. Howden, W. M. Dietrich, S. Bugg, M. J. O'Connell, P. B. Goldsbrough, C. S. Cobbett: Phytochelatin Synthase Genes from Arabidopsis and the Yeast Schizosaccharomyces Pombe, *The Plant Cell* **1999**, *11*, 1153.
[39] D. K. Gupta, H. G. Huang, F. J. Corpas: Lead Tolerance in Plants: Strategies for Phytoremediation, *Environmental Science and Pollution Research* **2013**, *20*, 2150.
[40] D. Potesil, J. Petrlova, V. Adam, J. Vacek, B. Klejdus, J. Zehnalek, L. Trnkova, L. Havel, R. Kizek: Simultaneous Femtomole Determination of Cysteine, Reduced and Oxidized Glutathione, and Phytochelatin in Maize (Zea Mays L.) Kernels Using High-Performance Liquid Chromatography with Electrochemical Detection, *Journal of Chromatography A* **2005**, *1084*, 134.
[41] B. Yosypchuk, I. Sestakova, L. Novotny: Voltammetric Determination of Phytochelatins Using Copper Solid Amalgam Electrode, *Talanta* **2003**, *59*, 1253.
[42] V. Vacchina, H. Chassaigne, M. Oven, M. H. Zenk, R. Lobinski: Characterisation and Determination of Phytochelatins in Plant Extracts by Electrospray Tandem Mass Spectrometry, *Analyst* **1999**, *124*, 1425.
[43] S. K. Kawakami, M. Gledhill, E. P. Achterberg: Determination of Phytochelatins and Glutathione in Phytoplankton from Natural Waters Using HPLC with Fluorescence Detection, *Trac-Trends in Analytical Chemistry* **2006**, *25*, 133.
[44] R. Jain, V. K. Gupta, N. Jadon, K. Radhapyari: Voltammetric Determination of Cefixime in Pharmaceuticals and Biological Fluids, *Analytical Biochemistry* **2010**, *407*, 79.

[45] L. O. Dubenska, M. Y. Blazhejevskyj, S. I. Plotycya, M. Y. Pylypets, O. M. Sarahman: Voltammetric Methods for the Determination of Prarmaceuticals, *Methods and Objects of Chemical Analysis* **2017**, *12*, 61.
[46] P. D. Stivaktakis, E. Giannakopoulos, D. Vlastos, D. P. Matthopoulos: Determination of Genotoxic Effects of Methidathion Alkaline Hydrolysis in Human Lymphocytes Using the Micronucleus Assay and Square-Wave Voltammetry, *Bioelectrochemistry* **2017**, *113*, 9.
[47] C. N. Nunes, V. E. dos Anjos, S. P. Quinaia: Determination of Diazepam and Clonazepam in Natural Water – A Voltammetric Study, *Electroanalysis* **2018**, *30*, 109.
[48] Deswati, H. Pardi, H. Suyani, Y. Yusuf, T. W. Edelwis: Application of Calcon as Complexing Agent for the Simultaneous Determination of Lead and Cadmium in Sea Water with Adsorptive Cathodic Stripping Voltammetry, *Analytical and Bioanalytical Electrochemistry* **2018**, *10*, 541.
[49] L. C. Melo, M. S. S. Juliao, M. A. L. Milhome, R. F. do Nascimento, D. De Souza, P. de Lima-Neto, A. N. Correia: Square Wave Adsorptive Stripping Voltammetry Determination of Chlorpyriphos in Irrigation Agricultural Water, *Journal of Analytical Chemistry* **2018**, *73*, 695.
[50] J. Slavik, L. Trnkova, J. Hubalek: Interaction of Selenite with Metallothionein Studied by Brdika Reaction, *Monatshefte für Chemie – Chemical Monthly* **2019**, *150*, 469.
[51] A. Danhel, Z. Trosanova, J. Balintova, A. Simonova, L. Pospisil, J. Cvacka, M. Hocek, M. Fojta: Electrochemical Reduction of Azidophenyl-Deoxynucleoside Conjugates at Mercury Surface, *Electrochimica Acta* **2018**, *259*, 377.
[52] H. Cernocka, E. Palecek: Voltammetric and Chronopotentiometric Protein Structure-sensitive Analysis, *Electrochimica Acta* **2017**, *224*, 211.
[53] J. Barek, A. G. Fogg, A. Muck, J. Zima: Polarography and Voltammetry at Mercury Electrodes, *Critical Reviews in Analytical Chemistry* **2010**, *31*, 291.
[54] B. Yosypchuk, L. Novotny: Nontoxic Electrodes of Solid Amalgams, *Critical Reviews in Analytical Chemistry* **2002**, *32*, 141.
[55] B. Yosypchuk, J. Barek: Analytical Applications of Solid and Paste Amalgam Electrodes, *Critical Reviews in Analytical Chemistry* **2009**, *39*, 189.
[56] A. Danhel, J. Barek: Amalgam Electrodes in Organic Electrochemistry, *Current Organic Chemistry* **2011**, *15*, 2957.
[57] A. Danhel, K. K. Shiu, B. Yosypchuk, J. Barek, K. Peckova, V. Vyskocil: The Use of Silver Solid Amalgam Working Electrode for Determination of Nitrophenols by HPLC with Electrochemical Detection, *Electroanalysis* **2009**, *21*, 303.
[58] J. Tvrdikova, A. Danhel, J. Barek, V. Vyskocil: Voltammetric and Amperometric Determination of Selected Dinitronaphthalenes Using Single Crystal Silver Amalgam Based Sensors, *Electrochimica Acta* **2012**, *73*, 23.
[59] O. Yosypchuk, J. Barek, B. Yosypchuk: Tubular Detector of Silver Solid Amalgam for Electrochemical Measurements in Flow Systems, *Electroanalysis* **2012**, *24*, 2230.
[60] O. Josypcuk, J. Barek, B. Josypcuk: Construction and Application of Flow Enzymatic Biosensor Based of Silver Solid Amalgam Electrode for Determination of Sarcosine, *Electroanalysis* **2015**, *27*, 2559.
[61] H. E. Zittel, F. J. Miller: A Glassy-Carbon Electrode for Voltammetry, *Analytical Chemistry* **1965**, *37*, 200.

[62] T. J. Schmidt, H. A. Gasteiger, G. D. Stab, P. M. Urban, D. M. Kolb, R. J. Behm: Characterization of High-Surface Area Electrocatalysts Using a Rotating Disk Electrode Configuration, *Journal of the Electrochemical Society* **1998**, *145*, 2354.
[63] E. Majid, S. Hrapovic, Y. Liu, K. B. Male, J. H. T. Luong: Electrochemical Determination of Arsenite Using a Gold Nanoparticle Modified Glassy Carbon Electrode and Flow Analysis, *Analytical Chemistry* **2006**, *78*, 762.
[64] J. X. Wang, M. X. Li, Z. J. Shi, N. Q. Li, Z. N. Gu: Direct Electrochemistry of Cytochrome C at a Glassy Carbon Electrode Modified with Single-wall Carbon Nanotubes, *Analytical Chemistry* **2002**, *74*, 1993.
[65] S. Tajik, H. Beitollahi: A Sensitive Chlorpromazine Voltammetric Sensor Based on Graphene Oxide Modified Glassy Carbon Electrode, *Analytical and Bioanalytical Chemistry Research* **2019**, *6*, 171.
[66] P. Ranganathan, B. Mutharani, S. M. Ghen, P. Sireesha: Biocompatible Chitosan-Pectin Polyelectrolyte Complex for Simultaneous Electrochemical Determination of Metronidazole and Metribuzin, *Carbohydrate Polymers* **2019**, *214*, 317.
[67] R. N. Adams: Carbon Paste Electrodes, *Analytical Chemistry* **1958**, *30*, 1576.
[68] C. Olson, R. N. Adams: Carbon Paste Electrodes Application to Anodic Voltammetry, *Analytica Chimica Acta* **1960**, *22*, 582.
[69] I. Svancara, K. Vytras, J. Barek, J. Zima: Carbon Paste Electrodes in Modern Electroanalysis, *Critical Reviews in Analytical Chemistry* **2001**, *31*, 311.
[70] D. J. Chesney: Laboratory Techniques in Electroanalytical Chemistry, 2nd Edition Edited, *Journal of the American Chemical Society* **1996**, *118*, 10946.
[71] J. P. Du, A. Wilting, I. Siewert: Are Two Metal Ions Better than One? Mono- and Binuclear α-Diimine-Re(CO)$_3$ Complexes with Proton-Responsive Ligands in CO2 Reduction Catalysis, *Chemistry – A European Journal* **2019**, *25*, 5555.
[72] J. Klouda, J. Barek, K. Nesmerak, K. Schwarzova-Peckova: Non-Enzymatic Electrochemistry in Characterization and Analysis of Steroid Compounds, *Critical Reviews in Analytical Chemistry* **2017**, *47*, 384.
[73] M. Brycht, A. Leniart, J. Zavasnik, A. Nosal-Wiercinska, K. Wasinski, P. Polrolniczak, S. Skrzypek, K. Kalcher: Synthesis and Characterization of the Thermally Reduced Graphene Oxide in Argon Atmosphere, and Its Application to Construct Graphene Paste Electrode as a Naptalam Electrochemical Sensor, *Analytica Chimica Acta* **2018**, *1035*, 22.
[74] M. Hermanova, P. Orsag, J. Balintova, M. Hocek, M. Fojta: Dual Redox Labeling of DNA as a Tool for Electrochemical Detection of p53 Protein-DNA Interactions, *Analytica Chimica Acta* **2019**, *1050*, 123.
[75] N. Cibiček, J. Vacek, a. kol., *Principy a Využití Vybraných Analytických Metod v Laboratorní Medicíně*, Univerzita Palackého v Olomouci **2014**.
[76] V. K. Gupta, R. Jain, K. Radhapyari, N. Jadon, S. Agarwal: Voltammetric Techniques for the Assay of Pharmaceuticals – A Review, *Analytical Biochemistry* **2011**, *408*, 179.
[77] M. A. Islam, S. C. Lam, Y. Li, M. A. Atia, P. Mahbub, P. N. Nesterenko, B. Paull, M. Macka: Capillary Gap Flow Cell as Capillary-End Electrochemical Detector in Flow-Based Analysis, *Electrochimica Acta* **2019**, *303*, 85.
[78] C. S. Pundir, P. Kumar, R. Jaiwal: Biosensing Methods for Determination of Creatinine: A Review, *Biosensors and Bioelectronics* **2019**, *126*, 707.
[79] R. Ciriello, F. De Gennaro, S. Frascaro, A. Guerrieri: A Novel Approach for the Selective Analysis of L-Lysine in Untreated Human Serum by a Co-Crosslinked

L-Lysine-α-Oxidase/Overoxidized Polypyrrole Bilayer Based Amperometric Biosensor, *Bioelectrochemistry* **2018**, *124*, 47.

[80] B. Paull, P. N. Nesterenko, in *Liquid Chromatography* (Eds: S. Fanali, P. R. Haddad, C. F. Poole, P. Schoenmakers, and D. Lloyd), *Elsevier*, Amsterdam **2013**, pp. 157.

[81] M. C. Granger, J. S. Xu, J. W. Strojek, G. M. Swain: Polycrystalline Diamond Electrodes: Basic Properties and Applications as Amperometric Detectors in Flow Injection Analysis and Liquid Chromatography, *Analytica Chimica Acta* **1999**, *397*, 145.

[82] S. Hoffstetterkuhn, A. Paulus, E. Gassmann, H. M. Widmer: Influence Of Borate Complexation on the Electrophoretic Behavior of Carbohydrates in Capillary Electrophoresi, *Analytical Chemistry* **1991**, *63*, 1541.

[83] A. Bockisch, E. Kielhorn, P. Neubauer, S. Junne: Process Analytical Technologies to Monitor the Liquid Phase of Anaerobic Cultures, *Process Biochemistry* **2019**, *76*, 1.

[84] G. C. Han, X. R. Su, J. T. Hou, A. Ferranco, X. Z. Feng, R. S. Zeng, Z. C. Chen, H. B. Kraatz: Disposable Electrochemical Sensors for Hemoglobin Detection Based on Ferrocenoyl Cysteine Conjugates Modified Electrode, *Sensors and Actuators B-Chemical* **2019**, *282*, 130.

[85] A. Singh, K. R. Ansari, J. Haque, P. Dohare, H. Lgaz, R. Salghi, M. A. Quraishi: Effect of Electron Donating Functional Groups on Corrosion Inhibition of Mild Steel in Hydrochloric Acid: Experimental and Quantum Chemical Study, *Journal of the Taiwan Institute of Chemical Engineers* **2018**, *82*, 233.

[86] M. Tatarkovic, G. Broncova, M. Krondak: Electrochemical Impedance Spectroscopy and Its Application in Chemical Analysis, *Chemicke Listy* **2012**, *106*, 1067.

[87] E. Krauzová, P. Tůma, I. de Glisezinski, V. Štich, M. Šiklová: Metformin Does Not Inhibit Exercise-Induced Lipolysis in Adipose Tissue in Young Healthy Lean Men, *Frontiers in Physiology* **2018**, *9*.

[88] K. Novakova, T. Navratil, I. Sestakova, V. Marecek, J. Chylkova: Utilization of Electrochemical Impedance Spectroscopy for Elucidation of Electrochemical Properties of Lecithin – Cholesterol Mixtures in Model Phospholipid Membranes, *Chemicke Listy* **2014**, *108*, 219.

[89] K. Nováková, T. Navrátil, I. Šestáková, M. P. Le, H. Vodičková, B. Zámečníková, R. Sokolová, J. Bulíčková, M. Gál: Characterization of Cadmium Ion Transport Across Model and Real Biomembranes and Indication of Induced Damage of Plant Tissues, *Monatshefte für Chemie - Chemical Monthly* **2015**, *146*, 819.

7. Appendix I

Voltammetric Determination of Sodium Anthraquinone-2-Sulfonate Using Silver Solid Amalgam Electrodes

Skalová Štěpánka, Navrátil Tomáš, Barek Jiří, Vyskočil Vlastimil

Monatshefte für Chemie – Chemical Monthly

Volume 148, Pages 577-583, Year 2017

Monatsh Chem (2017) 148:577–583
DOI 10.1007/s00706-017-1926-8

ORIGINAL PAPER

Voltammetric determination of sodium anthraquinone-2-sulfonate using silver solid amalgam electrodes

Štěpánka Skalová[1,2] · Tomáš Navrátil[1] · Jiří Barek[2] · Vlastimil Vyskočil[2]

Received: 1 December 2016 / Accepted: 25 January 2017 / Published online: 9 February 2017

Abstract Voltammetric determination of sodium anthraquinone-2-sulfonate (AQ) was investigated at a polished silver solid amalgam electrode (p-AgSAE) and at a mercury meniscus modified silver solid amalgam electrode (m-AgSAE) (inner diameter of both 0.5 mm). The reaction mechanisms of AQ at p-AgSAE and at m-AgSAE were studied by cyclic voltammetry, direct current voltammetry, and by elimination voltammetry with linear scan. Limits of detection obtained by differential pulse voltammetry were 1×10^{-6} mol dm^{-3} for p-AgSAE and 4×10^{-7} mol dm^{-3} for m-AgSAE. Both electrodes were successfully applied for differential pulse voltammetry of AQ in model samples of deionized water, river water, and human urine.

Graphical abstract

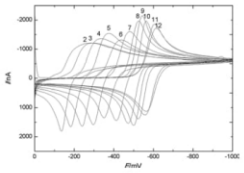

✉ Tomáš Navrátil
Tomas.Navratil@jh-inst.cas.cz

[1] J. Heyrovský Institute of Physical Chemistry of the CAS, v.v.i., Dolejškova 3, 182 23 Prague 8, Czech Republic

[2] Charles University, Faculty of Science, Department of Analytical Chemistry, UNESCO Laboratory of Environmental Electrochemistry, Hlavova 2030/8, 128 43 Prague 2, Czech Republic

Keywords Anthraquinone · Silver solid amalgam electrode · Voltammetry · Drugs

Introduction

Sodium anthraquinone-2-sulfonate (AQ, Fig. 1) is a water-soluble derivative of anthraquinone which is a precursor of anticancer drugs (e.g., of epirubicin, daunorubicin, doxorubicin, nemorubicin, and idarubicin). These drugs react with DNA of cancer cells (as inhibitors of synthesis of nucleic acids and of mitosis, intercalators, etc.), thus preventing their division [1–4].

The anthraquinones are aromatic organic compounds which contain quinone moiety (Q) (Fig. 1). Quinone–hydroquinone organic redox systems have an important function in living systems, for example as electron-proton carrier in respiratory chain. Mechanism of Q reduction depends on pH of the solution: single step two-electron and two-proton exchange at acidic pH; two-electron and one-proton exchange, or two-electron exchange only at neutral pH; and two-electron exchange at alkaline pH were suggested [5–8].

Electrochemical methods represent a relatively inexpensive, fast, and simple way of determination of biologically active compounds [9–15]. Many research teams have been recently focused on the construction of sensors and development of determination procedures of drugs in urine and in other body fluids using electrochemical techniques. Figures of merits of these methods are usually sufficient for their sensitive, specific, and repeatable determination with sufficiently low limits of detection (LODs). The developed methods and (first of all

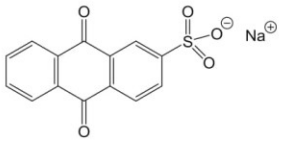

Fig. 1 Structural formula of sodium anthraquinone-2-sulfonate (AQ)

disposable) sensors could find application in common medical laboratories in future [16–20].

In the research described in this paper, we have used two types of a silver solid amalgam electrode (AgSAE), which are denoted according to modifications of their surface: polished (p-AgSAE) and mercury meniscus modified (m-AgSAE) [21]. These electrodes were introduced by Yosypchuk [21, 22] in 2000 and similar electrodes were introduced by Mikkelsen [23] in the same year. The used electrodes present a compromise between liquid mercury electrodes and solid electrodes (wide range of working potential, high hydrogen overvoltage, mechanical stability, and easy manipulation) [22, 24, 25]. AgSAEs can be applied for the determination of both organic [9, 15, 26–31] and inorganic compounds [32–34].

This work is focused on the development of a simple, fast, and inexpensive method for voltammetric determination of AQ. The newly developed method was verified on model samples of deionized water, river water, and human urine.

Results and discussion

Influence of pH on electrochemical behavior of AQ

Cyclic voltammetry (CV), direct current voltammetry (DCV), and differential pulse voltammetry (DPV) were used to study electrochemical behavior of AQ at m-AgSAE and p-AgSAE at different pH. At first, pH dependence of CV signals of AQ was investigated at pH from 2 to 12. The concentration of AQ was 1×10^{-3} mol dm^{-3} for both tested electrodes (p-AgSAE, m-AgSAE). Before each measurement, the electrodes were regenerated as described further in the paragraph "Regeneration of amalgam electrodes" (see below).

One cathodic peak and one anodic peak were observed. This pair of peaks corresponds to a reversible or a quasireversible process. The highest reversibility (according to the difference between anodic and cathodic peak potentials and the ratio of peak heights) was observed at pH 9–10.

The CV as well as DPV peak potentials (data not shown for DPV) of both peaks (i.e., of the reduction and of the oxidation peaks) shifted to more negative potentials with increasing pH (see Figs. 2 and 3). However, due to the fact that AQ form is the prevailing form of the investigated system AQ/dihydroAQ in the solution, it was decided to investigate the reduction process, i.e., the cathodic signal only.

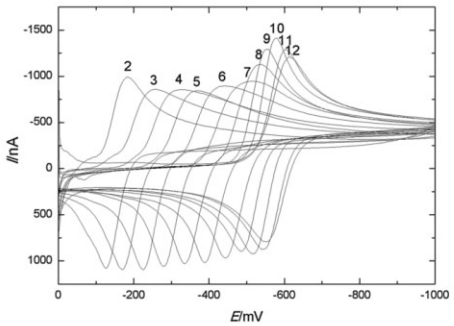

Fig. 2 Cyclic voltammograms of 1×10^{-3} mol dm^{-3} AQ in Britton-Robinson buffer (BRB) pH 2–12 at p-AgSAE; initial potential (E_{in}): 0 mV, final potential (E_{fin}): −1000 mV, scan rate (v): 100 mV s^{-1}, negative regeneration potential (E_{reg1}): −1050 mV, positive regeneration potential (E_{reg2}): 80 mV, number of cycles (N): 200; numbers (*2–12*) above voltammograms correspond to pH of the BRB used

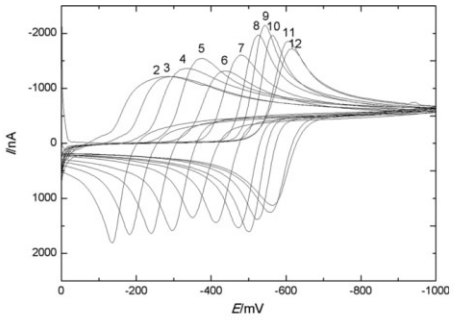

Fig. 3 Cyclic voltammograms of 1×10^{-3} mol dm^{-3} AQ in Britton-Robinson buffer (BRB) pH 2–12 at m-AgSAE; initial potential (E_{in}): 0 mV, final potential (E_{fin}): −1000 mV, scan rate (v): 100 mV s^{-1}, negative regeneration potential (E_{reg1}): −1050 mV, positive regeneration potential (E_{reg2}): 80 mV, number of cycles (N): 400. Numbers (*2–12*) above voltammograms correspond to pH of the BRB used

The linear dependences of AQ cathodic DCV peak potentials on pH are described by [Eqs. (1)–(4)]. All these equations are characterized by very high correlation coefficients (r) (the confidence intervals were calculated on the level of significance (α) = 0.05).

$$E_p/\mathrm{mV} = (-63.4 \pm 3.5)\mathrm{pH} + (-62 \pm 17) \quad (r = -0.999)\ (\mathrm{pH}\ 3-7,\ \text{p-AgSAE}) \tag{1}$$

$$E_p/\mathrm{mV} = (-22.3 \pm 2.2)\mathrm{pH} + (-354 \pm 21) \quad (r = -0.998)\ (\mathrm{pH}\ 7-12,\ \text{p-AgSAE}) \tag{2}$$

$$E_p/\mathrm{mV} = (-50.2 \pm 3.1)\mathrm{pH} + (-128 \pm 18) \quad (r = -0.999)\ (\mathrm{pH}\ 3-8,\ \text{m-AgSAE}) \tag{3}$$

$$E_p/\mathrm{mV} = (-24.4 \pm 8.1)\mathrm{pH} + (-329 \pm 82) \quad (r = -0.984)\ (\mathrm{pH}\ 8-12,\ \text{m-AgSAE}). \tag{4}$$

From the slopes of these dependences, it can be concluded that AQ is reduced by different reduction mechanism in acidic and in alkaline media resulting in different number of exchanged electrons and protons and thus in different slopes of straight-lines described by Eqs. (1)–(4) in agreement with analogous compounds described in papers [5–8]. The highest and the most repeatable current responses were obtained at pH 10 at p-AgSAE and at pH 9 at m-AgSAE (see Figs. 2 and 3).

Regeneration of amalgam electrodes

To clean electrode surfaces, to prevent their passivation, to remove undesired adsorbed compounds from electrode surfaces, etc., electrochemical regeneration was applied. It consisted of periodical switching of applied potentials (positive regeneration potential (E_{reg2}) and negative regeneration potential (E_{reg1}) applied for chosen time interval N times). At first, their values had to be optimized. The influence of the application of regeneration potentials on recorded DCV signals was investigated at p-AgSAE and m-AgSAE, respectively. Regeneration potentials were investigated in BRB solutions at optimum pH values (pH 10 at p-AgSAE and pH 9 at m-AgSAE, respectively) with concentration of AQ 1×10^{-3} mol dm^{-3}.

The best evaluable, the highest, and the best repeatable peaks were obtained using regeneration potentials $E_{reg1} = -1050$ mV and $E_{reg2} = 80$ mV (see Table 1). Each of these potentials was applied for 0.1 s with 200 (p-AgSAE) and 400 (m-AgSAE) cleaning cycles. The repeatability of 15 measurements of peak heights for the highest evaluated concentration (1×10^{-3} mol dm^{-3}) expressed as RSD was 3.6% for p-AgSAE and 1.6% for m-AgSAE, respectively. Similarly, the repeatability of 15 measurements for the lowest evaluated concentration expressed as RSD was 6.5% for p-AgSAE (1×10^{-6} mol dm^{-3} AQ) and 3.0% for m-AgSAE (4×10^{-7} mol dm^{-3} AQ).

Table 1 Optimized parameters for working electrode pre-treatment

Working electrode	E_{reg1}/mV	E_{reg2}/mV	N	pH
p-AgSAE	−1050	80	200	10
m-AgSAE	−1050	80	400	9

Dependence of DCV peak heights on the scan rate

The dependences of AQ current signals (DCV peaks) on scan rates (v) were evaluated at p-AgSAE and m-AgSAE in BRB solution of optimum pH with concentration of AQ 1×10^{-3} mol dm^{-3}. Tested scan rates were from 10 to 1280 mV s^{-1}. The dependence of peak current (I_p) on $v^{1/2}$ was linear in the whole range of tested v for both electrodes (see Table 2). These results have suggested a diffusion controlled process of reduction of AQ at both p-AgSAE and m-AgSAE.

The obtained data were further evaluated using log (I_p)–log (v) analysis. Slope of these dependences (see Table 3) amounted to 0.470 for p-AgSAE and 0.426 for m-AgSAE, respectively. These results confirm the above mentioned conclusion that the AQ reduction processes at both electrodes are diffusion controlled without any influence of adsorption.

Even though the values 0.5 are not inside calculated confidence intervals of the slopes in Table 3, no influence of a kinetically controlled process has been confirmed neither experimentally nor using elimination voltammetry with linear scan (EVLS) (see the following paragraph).

Elimination voltammetry with linear scan

The electrode processes were further studied and elucidated using EVLS [35–37]. Both cathodic and anodic peaks of cyclic voltammograms recorded with scan rate from 10 to 1280 mV s^{-1} were evaluated. They were divided into 5 groups: 10, 20, 40, and 80 mV s^{-1}; 20, 40, 80, and 160 mV s^{-1}; 40, 80, 160, and 320 mV s^{-1}; 80, 160, 320, and 640 mV s^{-1}; and 160, 320, 640, and 1280 mV s^{-1}. In these groups, the second highest scan rate was denoted as reference scan rate and the elimination curves were calculated.

The evaluations were realized using equations published in [38]. The shapes of calculated elimination curves corresponded to a diffusion controlled processes, the signals of which were conserved; and the others, corresponding to capacity or kinetically controlled processes, were almost eliminated [35, 36, 38]. No counter-peak, corresponding to a "combined process" [37, 38], was observed. Therefore, it can be concluded that no such more complicated process (i.e., reduction in adsorbed state, reduction proceeded by a kinetically controlled

Table 2 Parameters of the dependence of the DCV peak current (I_p) on $v^{1/2}$ for the solution of AQ (1×10^{-3} mol dm^{-3}) in BRB (pH 10) at p-AgSAE and in BRB (pH 9) at m-AgSAE

Working electrode	Slope[a] /nA mV$^{-1/2}$ s$^{1/2}$	Intercept[a] /nA	R
p-AgSAE	−99.5 ± 7.0	12 ± 15[b]	-0.998
m-AgSAE	−53.7 ± 3.3	131 ± 60	-0.998

[a] Expressed as confidence interval on level of significance $\alpha = 0.05$

[b] This value is not statistically significantly different from zero on level of significance $\alpha = 0.05$

Table 3 Parameters of the dependence of log I_p (nA) on log v (mV s^{-1}) for the solution of AQ (1×10^{-3} mol dm^{-3}) in BRB (pH 10) at p-AgSAE and in BRB (pH 9) at m-AgSAE measured by DCV

Working electrode	Slope[a]	Intercept[a]	R
p-AgSAE	0.470 ± 0.014	2.109 ± 0.030	1.000
m-AgSAE	0.426 ± 0.012	1.984 ± 0.025	1.000

[a] Expressed as confidence interval on level of significance $\alpha = 0.05$

process, etc.) is involved in the investigated processes and that both the cathodic and the anodic peak correspond to the simple diffusion controlled process without any influence of adsorption.

Concentration dependences

The concentration dependences of AQ were measured in the concentration range from 1×10^{-7} to 1×10^{-3} mol dm^{-3} using DPV under optimum conditions (see Table 4). The concentration dependences were linear in the whole mentioned concentration range for both electrodes. However, the signals at the lowest concentration levels were below the LOD calculated using direct signal method according to IUPAC [39] (see Table 4). Corresponding voltammograms are depicted in Figs. 4 and 5; voltammograms corresponding to concentrations below calculated LOD are not depicted in Figs. 4 and 5.

Determination of AQ in model solutions

Determinations of AQ in model solutions (deionized water, river water, and human urine spiked by AQ) were carried out using optimized DPV parameters (see Table 1). The determinations were repeated five times within one day. The samples were analyzed one week later again. Results of both determinations are summarized in Table 5.

Conclusions

The new voltammetric determination of AQ, as an important precursor of drugs used in cancer chemotherapy, was developed using m-AgSAE and p-AgSAE. It was confirmed that this fast, simple, and reliable method can be used for its determination in various matrices, namely in drinking and river water and in human urine.

It was found that AQ is reduced at both electrodes in a wide range of pH values. The best repeatable cathodic peak of AQ was found at pH 10 at p-AgSAE and at pH 9 at m-AgSAE, respectively. LODs 1×10^{-6} mol dm^{-3} at p-AgSAE and 4×10^{-7} mol dm^{-3} at m-AgSAE were achieved using DPV under the found optimum working conditions. Statistical treatment of obtained data confirmed good reproducibility of the newly developed method with both tested amalgam electrodes. In all investigated matrices, the LODs were lower and repeatability better in the case of m-AgSAE than in the case of p-AgSAE.

Experimental

Chemicals

Stock solution of AQ ($c = 1 \times 10^{-2}$ mol dm^{-3}) was prepared by dissolving 0.3103 g of AQ (Merck, Germany) in 100 cm^3 of deionized water. BRBs with pH from 2 to 12 were prepared by mixing of appropriate volumes of acidic (0.04 mol dm^{-3}) and basic (0.2 mol dm^{-3}) BRB

Table 4 Parameters of AQ concentration dependences measured by DPV (p-AgSAE: in BRB with pH 10; initial potential (E_{in}): 0 mV, final potential (E_{fin}): −850 mV, scan rate (v): 20 mV s^{-1}, negative regeneration potential (E_{reg1}): −1050 mV, positive regeneration potential (E_{reg2}): 80 mV, number of cycles (N): 200; pulse height −100 mV, pulse width 40 ms with the sampling interval 20 ms; m-AgSAE: in BRB with pH 9; E_{in}: 0 mV, E_{fin}: −850 mV, v: 20 mV s^{-1}, E_{reg1}: −1050 mV, E_{reg2}: 80 mV, N: 400; pulse height −100 mV, pulse width 40 ms with the sampling interval 20 ms) in concentration ranges from 1×10^{-6} to 1×10^{-3} mol dm^{-3} at p-AgSAE and from 4×10^{-7} to 1×10^{-3} mol dm^{-3} at m-AgSAE

Working electrode	Slope[a]/μA dm^3 mol^{-1}	Intercept[a]/μA	R	LOD/mol dm^{-3}
p-AgSAE	−3.621 ± 0.060	30 ± 24	−0.998	1×10^{-6}
m-AgSAE	−7.72 ± 0.11	23 ± 38[b]	−0.999	0.4×10^{-6}

[a] Expressed as confidence interval on level of significance $\alpha = 0.05$

[b] This value is not statistically significantly different from zero on level of significance $\alpha = 0.05$

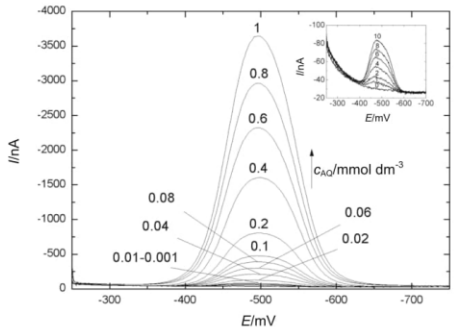

Fig. 4 DP voltammograms of AQ (from 1×10^{-6} to 1×10^{-3} mol dm^{-3}) in BRB pH 10 at p-AgSAE; initial potential (E_{in}): 0 mV, final potential (E_{fin}): −850 mV, scan rate (v): 20 mV s^{-1}, negative regeneration potential (E_{reg1}): −1050 mV, positive regeneration potential (E_{reg2}): 80 mV, number of cycles (N): 200; pulse height −100 mV, pulse width 40 ms with the sampling interval 20 ms. Corresponding concentration in mmol dm^{-3} is displayed above the curves. Inset DP voltammograms of AQ from 1 to 10 μmol dm^{-3} in BRB pH 10 at p-AgSAE. Corresponding concentrations in μmol dm^{-3} are displayed above the curves

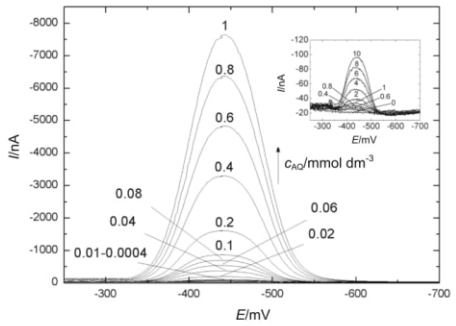

Fig. 5 DP voltammograms of AQ (from 4×10^{-7} to 1×10^{-3} mol dm^{-3}) in BRB pH 9 at m-AgSAE; initial potential (E_{in}): 0 mV, final potential (E_{fin}): −850 mV, scan rate (v): 20 mV s^{-1}, negative regeneration potential (E_{reg1}): −1050 mV, positive regeneration potential (E_{reg2}): 80 mV, number of cycles (N): 400; pulse height −100 mV, pulse width 40 ms with the sampling interval 20 ms. Corresponding concentration in mmol dm^{-3} is displayed above the curves. Inset DP voltammograms of AQ from 0.4 to 10 μmol dm^{-3} in BRB pH 9 at m-AgSAE. Corresponding concentrations in μmol dm^{-3} are displayed above the curves

components. 1 dm^3 of the acidic component was prepared from 2.47 g H_3BO_3, 2.3 cm^3 98% CH_3COOH, and 2.5 cm^3 85% H_3PO_4 (all Merck, Germany); the basic component was prepared by dissolving 8.00 g NaOH (Merck, Germany) in 1 dm^3 of deionized water. The solution of 0.2 mol dm^{-3} KCl was prepared by dissolving 7.46 g KCl in 500 cm^3 of deionized water. Deionized water, prepared by AQUA 35-300 system (GORO, Czech Republic) was used. All solutions were stored in glass bottles in dark at laboratory temperature.

Table 5 Determination of AQ by DPV at p-AgSAE and m-AgSAE in model sample solutions (deionized water, river water, human urine) containing known added amount of AQ

	Added/ 10^{-6} mol dm^{-3}	Found[a]/ 10^{-6} mol dm^{-3}	Recovery/ %	RSD/ %
Deionized water				
1st day				
p-AgSAE	1.1	1.141 ± 0.080	96–111	5.6
	11	11.47 ± 0.62	99–110	4.4
m-AgSAE	1.1	1.130 ± 0.061	97–108	4.3
	11	11.13 ± 0.33	98–104	2.4
7th day				
p-AgSAE	1.1	1.119 ± 0.072	95–108	5.2
	11	11.42 ± 0.67	98–110	4.7
m-AgSAE	1.1	1.092 ± 0.054	94–104	4.0
	11	11.45 ± 0.51	99–109	3.6
River water				
1st day				
p-AgSAE	1.1	1.120 ± 0.081	94–109	5.8
	11	11.43 ± 0.67	98–110	4.7
m-AgSAE	1.1	1.139 ± 0.060	98–109	4.2
	11	11.32 ± 0.52	98–108	3.7
7th day				
p-AgSAE	1.1	1.091 ± 0.070	93–106	5.2
	11	11.15 ± 0.32	98–105	2.3
m-AgSAE	1.1	1.070 ± 0.050	93–102	3.8
	11	11.24 ± 0.30	99–105	2.1
Human urine				
1st day				
p-AgSAE	1.6	1.578 ± 0.061	95–102	3.1
	16	16.53 ± 0.64	99–107	3.1
m-AgSAE	1.6	1.652 ± 0.070	99–108	3.4
	16	16.69 ± 0.79	99–109	3.8
7th day				
p-AgSAE	1.6	1.620 ± 0.083	96–106	4.1
	16	16.50 ± 0.64	97–107	3.1
m-AgSAE	1.6	1.630 ± 0.041	99–104	2.0
	16	16.27 ± 0.31	100–104	1.5

Declared concentrations (both added and found) correspond to calculated concentrations in spiked model samples. Therefore, the real concentrations in voltammetric vessel are lower (90% in the case of water samples and 45% in the case of urine samples)

The confidence intervals were calculated on level of significance $\alpha = 0.05$

[a] Expressed as confidence interval on level of significance $\alpha = 0.05$

Apparatus

The CV, DCV, and DPV measurements were realized by Eco-Tribo-Polarograph (ETP) (Polaro-Sensors, Czech Republic). This device was controlled by a desktop computer with operating system Microsoft Windows 7 (64-bit, Microsoft, USA) and electrochemical software MultiElChem (version 3.1, J. Heyrovský Institute of Physical Chemistry of the CAS, v.v.i., Czech Republic).

Measurements were carried out in a three-electrode system with AgSAEs as working electrodes. The surface areas of the electrodes were calculated as follows: the geometric parameters (i.e., electrode diameter and meniscus height) were measured using an optical microscope. It was supposed that meniscus is a segment of a sphere and the surface of the p-AgSAE is a flat circle. Then, the surface areas were calculated by simple geometric formulas. Two types of surface modifications of these electrodes were used: p-AgSAE (surface area 0.28 mm^2) and m-AgSAE (surface area 0.39 mm^2). Ag|AgCl (saturated KCl) was used as the reference electrode (Monokrystaly, Czech Republic), and a platinum wire (diameter 1 mm) as the auxiliary electrode (Elektrochemické Detektory, Czech Republic).

The pH of solution was measured with a pH meter Jenway 3505 (Jenway, United Kingdom) with a combined glass electrode.

Procedures

CV and DCV were applied for studies of electrochemical behavior of AQ at p-AgSAE and m-AgSAE. The influence of pH on voltammetric behavior of AQ was investigated by CV and by DPV. Similarly, the influence of scan rate was investigated by DCV and CV. Parameters of CV were as follows: potential range (E) from 0 to −1000 mV, regeneration potentials (E_{reg1}) −1050 mV and (E_{reg2}) 80 mV were applied for 0.1 s, number of regeneration cycles (N) was 200 for p-AgSAE and 400 for m-AgSAE, scan rate (v) 100 mV s^{-1}. Initial parameters of DPV during pH optimization were as follows: potential scan from 0 to −1000 mV, regeneration potentials −1050 mV and 80 mV were applied for 0.1 s, polarization rate 20 mV s^{-1}, N 200 for p-AgSAE and 400 for m-AgSAE, pulse width 80 ms with the sampling interval 20 ms was used for investigation of the influence of pH on DP voltammograms, pulse height −50 mV. Afterwards, parameters of pulse width and pulse height were optimized after optimization of pH solution. The optimized pulse width 40 ms with the sampling interval 20 ms and pulse height −100 mV were used in all further measurements.

All voltammetric measurements were carried out in a total volume of 10 cm^3 and at laboratory temperature. Oxygen was removed by bubbling with nitrogen for 5 min (purity class 4.0, Linde, Czech Republic) before each measurement. Each measurement of the current signal was repeated at least three times under the same conditions. The minimum number of standard additions in the case of evaluations of model sample concentrations was 5.

Preparation of silver amalgam electrodes

AgSAE (diameter 0.55 mm) was made from a drawn-out glass tube. Firstly, the drawn-out glass tube was filled by silver powder and platinum wire was inserted. Then, it was inserted into bottle with mercury for two hours. Finally, support of electric current was secured to the upper end of the wire. Detailed preparation AgSAE is described in papers [21, 40]. The electrode consisted of a drawn-out glass tube, the bore of which near the tip was filled with a fine silver powder, amalgamated by liquid mercury and connected to an electric contact [21, 40]. p-AgSAE was polished at first by fine emery paper and then by the polishing kit consisting of polishing polyurethane pad, Al_2O_3 suspension (particle size 1.1 μm), and fine polishing Al_2O_3 powder (particle size 0.3 μm; Elektrochemické Detektory, Czech Republic). m-AgSAE was prepared from p-AgSAE by its immersing into approximately 15 cm^3 of liquid mercury for 15 s. During this time, the meniscus on the surface of p-AgSAE was formed [21, 40].

If time interval between measurements was longer than one hour, the electrode surfaces of both AgSAEs were activated in stirred solution of 0.2 mol dm^{-3} KCl by applying the potential of −2200 mV for 300 s in the presence of oxygen.

Elimination voltammetry with linear scan

EVLS is a one of methods used for elucidation of reaction process at various electrodes [35–38, 41, 42]. A prerequisite for EVLS is the idea that the registered current is the sum of particular current contributions (charging (capacity) current I_c, diffusion current I_d, kinetic current I_k, and irreversible current I_{ir}); Eq. (5) [35, 43, 44].

$$I = \sum I_j = I_k + I_c + I_d + I_{ir} + \cdots \quad (5)$$

Each particular current in Eq. (5) must be expressible in the form Eq. (6):

$$I_j = W_j(v) \cdot Y_j(E) = v^x Y_j(E). \quad (6)$$

(I_j a particular current, W_j (v) a function of the scan rate, v a scan rate, $Y_j(E)$ a function of the potential).

Preparation and analysis of spiked model sample solutions

Deionized water, river water (sampled from river Vltava, Prague), and human urine were used as model sample solutions. River water and human urine were stored in plastic bottles and placed in a fridge (4 °C) until analysis (not longer than 12 h after sampling). Human urine model sample was diluted by deionized water 1:1 (to decrease the concentration of interfering compounds); the water model samples were not diluted. Then, 1 cm^3 of BRB was added to 9 cm^3 of water model samples or to diluted human urine model sample, oxygen was removed by bubbling with nitrogen for 5 min, and the DP voltammograms under optimized conditions were recorded.

Acknowledgements This research was carried out within the framework of the Specific University Research Charles University (SVV). TN and ŠS are grateful for the financial support from J. Heyrovský Institute of Physical Chemistry of the CAS, v.v.i., JB and VV would like to thank the Grant Agency of the Czech Republic (Project P206/12/G151).

References

1. Golunski G, Borowik A, Lipinska A, Romanik M, Derewonko N, Woziwodzka A, Piosik J (2016) Bioorg Chem 65:118
2. Scaglioni L, Mondelli R, Artali R, Sirtori FR, Mazzini S (2016) Biochim Biophys Acta, Gen Subj 1860:1129
3. Ribeiro JA, Pereira CM, Silva F (2015) Electrochim Acta 180:687
4. Charak S, Jangir DK, Tyagi G, Mehrotra R (2011) J Mol Struct 1000:150
5. Guin PS, Das S, Mandal PC (2011) Int J Electrochem 2011:816202
6. Plambeck JA, Lown JW (1984) J Electrochem Soc 131:2556
7. Guin PS, Das S, Mandal PC (2008) Int J Electrochem Sci 3:1016
8. Kalaivani A, Narayanan SS (2015) J Nanosci Nanotechnol 15:4697
9. Navratil T, Novakova K, Barek J, Vyskocil V, Chylkova J (2016) Anal Lett 49:37
10. Shishkanova TV, Fitl P, Kral V, Barek J (2016) J Electroanal Chem 761:106
11. Danhel A, Trosanova Z, Balintova J, Havran L, Hocek M, Barek J, Fojta M (2016) Electrochim Acta 215:72
12. Bavol D, Zima J, Barek J, Dejmkova H (2016) Electroanalysis 28:1029
13. Selesovska R, Bandzuchova L, Navratil T (2011) Electroanalysis 23:177
14. Selesovska R, Bandzuchova L, Navratil T, Chylkova J (2012) Electrochim Acta 60:375
15. Selesovska-Fadrna R, Fojta M, Navratil T, Chylkova J (2007) Anal Chim Acta 582:344
16. Peckova K, Vrzalova L, Bencko V, Barek J (2009) Collect Czech Chem Commun 74:1697
17. Sadok I, Tyszczuk-Rotko K, Nosal-Wiercinska A (2016) Sensor Actuat B-Chem 235:263
18. Karimi-Maleh H, Shojaei AF, Tabatabaeian K, Karimi F, Shakeri S, Moradi R (2016) Biosens Bioelectron 86:879
19. Libansky M, Zima J, Barek J, Dejmkova H (2016) Monatsh Chem 147:89
20. Peckova K, Navratil T, Yosypchuk B, Moreira JC, Leandro KC, Barek J (2009) Electroanalysis 21:1750
21. Novotny L, Yosypchuk B (2000) Chem Listy 94:1118
22. Yosypchuk B, Novotny L (2002) Crit Rev Anal Chem 32:141
23. Mikkelsen O, Schroder K (2000) Anal Lett 33:3253
24. Barek J, Fischer J, Navratil T, Peckova K, Yosypchuk B, Zima J (2007) Electroanalysis 19:2003
25. Navratil T, Yosypchuk B, Barek J (2009) Chem Anal (Warsaw) 54:3
26. Bandzuchova L, Selesovska R, Navratil T, Chylkova J, Novotny L (2012) Electrochim Acta 75:316
27. Deylova D, Vyskocil V, Barek J (2014) J Electroanal Chem 717–718:237
28. Fadrna R, Yosypchuk B, Fojta M, Navratil T, Novotny L (2004) Anal Lett 37:399
29. Barek J, Dodova E, Navratil T, Yosypchuk B, Novotny L, Zima J (2003) Electroanalysis 15:1778
30. Barek J, Fischer J, Navratil T, Peckova K, Yosypchuk B (2006) Sensors-Basel 6:445
31. Fischer J, Vanourkova L, Danhel A, Vyskocil V, Cizek K, Barek J, Peckova K, Yosypchuk B, Navratil T (2007) Int J Electrochem Sci 2:226
32. Yosypchuk B, Novotny L (2002) Chem Listy 96:756
33. Cizkova P, Navratil T, Sestakova I, Yosypchuk B (2007) Electroanalysis 19:161
34. Jaklova Dytrtova J, Sestakova I, Jakl M, Navratil T (2009) Electroanalysis 21:573
35. Dracka O (1996) J Electroanal Chem 402:19
36. Trnkova L, Dracka O (1996) J Electroanal Chem 413:123
37. Trnkova L, Kizek R, Dracka O (2000) Electroanalysis 12:905
38. Skopalova J, Navratil T (2007) Chem Anal (Warsaw) 52:961
39. Miller JN, Miller JC (2005) Statistics and chemometrics for analytical chemistry, 2nd edn. Pearson Education, Harlow
40. Yosypchuk B, Novotny L (2002) Electroanalysis 14:1138
41. Trnkova L, Jelen F, Petrlova J, Adam V, Potesil D, Kizek R (2005) Sensors-Basel 5:448
42. Trnkova L, Serrano N, Klosova K (2010) Electroanalysis 22:2071
43. Trnkova L (2005) J Electroanal Chem 582:258
44. Sander S, Navratil T, Basova P, Novotny L (2002) Electroanalysis 14:1133

8. **Appendix II**

Labile Lead Phytochelatin Complex Could Enhance Transport of Lead Ions across Biological Membrane

Šestáková Ivana, **Skalová Štěpánka**, Navrátil Tomáš

Journal of Electroanalytical Chemistry

Volume 821, Pages 92-96, Year 2018

Journal of Electroanalytical Chemistry 821 (2018) 92–96

Contents lists available at ScienceDirect

Journal of Electroanalytical Chemistry

journal homepage: www.elsevier.com/locate/jelechem

Labile lead phytochelatin complex could enhance transport of lead ions across biological membrane

Ivana Šestáková[a], Štěpánka Skalová[a,b], Tomáš Navrátil[a,*]

[a] J. Heyrovský Institute of Physical Chemistry of the Czech Academy of Sciences, Dolejškova 3, 182 23 Prague 8, Czech Republic
[b] Charles University, Faculty of Science, Department of Analytical Chemistry, UNESCO Laboratory of Environmental Electrochemistry, Albertov 6, 128 43 Prague 2, Czech Republic

ARTICLE INFO

Keywords:
Phytochelatin PC_2
Lead
Complex
Voltammetry
Differential potentiometric stripping analysis (PSA, Chronopotentiometry)
Electrochemical impedance spectroscopy (EIS)

ABSTRACT

In connection with studies of transport of hazardous metals across model phospholipid membranes (PLMs), behavior of complexes of lead with phytochelatin PC_2 has been examined. Using differential potentiometric stripping analysis (PSA, Chronopotentiometry) with different values of constant negative current, the release of free lead ions confirmed their labile behavior. Similar conclusion resulted from voltammetry on silica gel modified carbon paste electrode. Diffusion controlled transport across a PLMs containing ionophore calcimycin (A23187) revealed 26 times more lead ions transported in case of Pb-phytochelatin complexes than in case of free lead ions. For labile behavior, complex with two Pb atoms at phytochelatin molecule is responsible.

1. Introduction

Lead is a toxic metal occurring naturally in relatively small extent, but due to huge men activities, it represents one of main contaminants of the environment, mainly of soil, of groundwater, and of surface waters. Pb^{2+} is the most common and reactive form of lead, forming mononuclear and polynuclear oxides and hydroxides. Entering of lead into plants, as the beginning of food chain, poses danger of toxicity for animal and human population [1].

Each plant cell and some of its sub-organelles are surrounded by phospholipid (PL) membranes (PLMs), composed mainly from different fatty acids, glycerol, and ethanolamine, choline, inositol, cholesterol and of some other basic molecules. Such PL membranes are created of a thin layer of amphiphatic molecules of PLs. They are organized spontaneously so that their hydrophobic tails are separated from surrounding polar liquids by hydrophilic heads [2].

Cholesterol represents other substantial and important part of plasma membrane and in low concentrations of the membranes of intracellular organelles [3]. This biomolecule does not form bilayer by itself, however, it is nonhomogeneously distributed in PL membranes [4]. Cholesterol positively effects on stability of biomembranes [2]. Moreover, various polysaccharides and partly or fully built-in peptides are incorporated into these relatively flat membranes.

Only very small and simple molecules (e.g., oxygen, water) can be transported spontaneously across such very thin membranes. Transport of most of other molecules and species must be realized via various ion channels, which are formed by pore-forming membrane proteins. They are responsible for establishing of membrane potentials and similar electrical signals, which enable the flow of species across membranes and regulate cell or compartment volumes. In some cases, it is necessary to supply some energy (e.g., in the form of adenosine triphosphate (ATP)) required for transport. Via such ion channels, most of ions are moved, e.g., biologically important Na^+, K^+, Ca^{2+} cations, transport mechanisms and composition of which have been elucidated in detail, and on the other hand, toxic Cd^{2+}, Pb^{2+} cations, transports of which have been studied, nevertheless, remained unelucidated up to now [5–9].

As it has been confirmed, transport process of various ions can be affected by presence of complexes of low molecular weight organic acids (e.g., oxalic, citric, malic) [10–13] or phytochelatins [14].

Plants have developed variety of mechanisms of defense against toxic influence of heavy metals - adsorption at cell walls, production of low molecular weight organic acids (e.g., oxalic, citric), and of sulfur containing ligands, especially phytochelatins [15–18]. Phytochelatins – polypeptides of structure $[(\gamma\text{-Glu-Cys})_n\text{-Gly}]$ (where "γ-Glu" means γ-glutamic acid, "Cys" means cysteine, and "Gly" means glycine) - PC_n - were studied mainly with the influence of cadmium ions on different types of plants. Although lead ions are in the list of activators of phytochelatins synthesis, only few cases of Pb phytochelatins occurrence were described lately [1,19,20].

Properties of various types of phytochelatins (PC_2, PC_3, PC_4) [21] and metallothioneins [22] have been investigated in last decades

* Corresponding author.
E-mail address: navratil@jh-inst.cas.cz (T. Navrátil).

https://doi.org/10.1016/j.jelechem.2017.11.052
Received 27 September 2017; Received in revised form 16 November 2017; Accepted 20 November 2017
Available online 21 November 2017
1572-6657/

intensively using different methods, e.g., NMR, UV–vis spectroscopy [23], electrospray ionization tandem mass spectrometry (ESI MS-MS) [21]. Different electrochemical methods have been relatively frequently used for these purposes, often in combination with other analytical techniques [24–31]. First of all, Voltammetry and potentiometric stripping analysis (PSA, chronopotentiometry) can yield us very valuable data in this research too [24,25,27].

To elucidate transport processes across biological membranes, synthetically prepared phospholipid membranes have been utilized, e.g., in the form of black membranes, vesicles, or supported membranes with incorporated ion channels [32,33] and characterized by electrochemical impedance spectroscopy (EIS) [5,27,28,34].

In previous studies of cadmium ion transport across model PL membrane containing ionophore A23187 (calcimycin) [5,14], we found enhanced transport of cadmium ions when a labile complex Cd-malic acid was present. Such influence of labile complexes in diffusion-controlled transport was studied also with diffusion gradient technique (DGT) and documented with higher levels of cadmium in concerned plants [35].

Pistia stratiotes is one of plants where intense synthesis of phytochelatins was described [36]. Moreover, in some countries, this plant is used as a component of animal feed. In this connection, lead levels in rats were analyzed and its high levels were found in all samples from the experimental group, which feed contained *pistia* [37]. Therefore, the behavior of lead phytochelatin complexes and transport of lead across PLMs is next question to study. The ionophore calcimycin is effective also for transport of lead ions [32] and voltammetric study with the application of multivariate curve resolution suggested formation of two Pb-phytochelatin complexes, reduced at hanging mercury drop electrode (HMDE). The peak potential difference of these two complexes higher than 200 mV [38] witnesses their different stabilities.

2. Experimental

2.1. Reagents and materials

The 0.1 M KCl supporting electrolyte solutions were prepared from KCl Suprapur, purchased from Merck, Czech Republic. The p.a. solvents were obtained from Ing. Petr Švec - PENTA, Czech Republic. All other chemicals used were of analytical purity grade. Borate buffer pH 8.2 was prepared from Suprapur sodium tetraborate acidified by HNO_3, suprapur (Merck, Czech Republic). The AAS standard solution of Pb^{2+} (1000 mg L^{-1} in 2% HNO_3) was purchased from Analytica, Czech Republic. The solution pH was adjusted to desired value using NaOH, suprapur (Merck, Czech Republic). For the preparation of supported PLMs (s-PLMs) 1,2-dipalmitoyl-sn-glycero-3-phosphocholine (DPPC) (Avanti Polar Lipids, USA) was used.

Phytochelatin PC_2 [(γ-Glu-Cys)$_2$-Gly] was obtained from Genosphere Biotechnologies, France.

The used ionophore A23187 (Calcimycin, Calcium Ionophore, Antibiotic A23187, Calcium Ionophore A23187) was purchased from Sigma-Aldrich, Czech Republic.

For all measurements, deionized water from Milli-Q-Gradient, Millipore, Czech Republic (conductivity < 0.05 μS cm^{-1}) was used.

2.2. Instrumentation and procedures

2.2.1. Voltammetry a potentiometric stripping analysis (chronopotentiometry)

Voltammetric and differential PSA measurements were carried out by the PC-controlled voltammetric analyzer *ECO-TRIBO polarograph* (Polaro-Sensors, Czech Republic), equipped with *POLAR.PRO* software v. 5.1 (Polaro-Sensors, Czech Republic) and with *MultiElchem* v. 3.1 software (J. Heyrovský Institute of Physical Chemistry of CAS, v.v.i., Czech Republic). *Pen-type hanging mercury drop electrode* (Polaro-Sensors, Czech Republic) and SiO_2-modified carbon paste electrode were used as the working electrodes. $Ag/AgCl/KCl_{sat}$ electrode (Elektrochemické Detektory, Czech Republic) was a reference electrode and the platinum wire (diameter 1 mm) wire served as a counter electrode. The measurements were performed at laboratory temperature (25 ± 2 °C).

The values of pH were measured using pH-meter Jenway 3505 (Bibby Scientific Ltd., UK).

Silica gel-modified carbon paste electrode, which offers possibility to accumulate electroactive analytes [39] was prepared by hand mixing of graphite powder with paraffin oil and 10% w.w. of silica gel.

The paste was packed into a Teflon electrode body with a stainless steel piston, serving for renewing of the paste surface as well as for an electric contact [40,41]. The area of this used electrode amounted to 7.1 mm^2. The new surface was smoothed on a card paper.

2.2.2. Electrochemical impedance spectroscopy

The EIS measurements were realized using potentiostat PGSTAT302N + FRA2 module, equipped with software Nova 1.11 (both Metrohm, Czech Republic). The electrochemical impedances were determined using Ag/AgCl electrodes (silver wire, diameter 1 mm, electroplated by silver chloride), which have been used as a working and a reference electrodes. Platinum wire, diameter 1 mm, served as the auxiliary electrode. The Nyquist plots (the dependence of the imaginary part (Z″) on the real part (Z′) of impedance) recorded in 0.1 M KCl with applied amplitude 0.005 V provided satisfactory results in the frequency range of 0.1–1000 Hz.

2.3. Transport of lead ions across model membrane

Because ionophore calcimycin acts as a divalent cation ionophore, it has been used for simulation of real ion channels and model transporter of dications. This ionophore was described as effective transporter of cadmium ions across PLMs as well as of lead ions [32,33,42,43]. Therefore, the same electrochemical cell developed earlier for experiments with transport of cadmium ions across the PLMs [44] was used. Such cell consists from two glass columns, separated by two Teflon parts with holes (0.07 cm^2), between which the polycarbonate membrane is inserted. Two separated compartments represent then extracellular (*Electrolyte 1*) and intracellular (*Electrolyte 2*) milieu, each of them containing 3 mL of 0.1 M KCl solution. The electrodes were placed into the holes in the top of glass compartments (one silver wire coated with silver chloride as working electrode was immersed into the *Electrolyte 1*, the other silver wire coated with silver chloride as reference electrode and platinum wire as auxiliary electrode were immersed into the *Electrolyte 2*) [44].

2.4. Model supported phospholipid membrane

The s-PLMs were formed by self-assembling of PLs in the holes of the IsoporeS Membrane Filters (Millipore, USA) polycarbonate, hydrophilic 8.0 μm, and the supporting membrane thickness amounted to 7–22 μm. For PLM preparation, 2 mg of DPPC, 20 μL of $1 \cdot 10^{-6}$ M calcimycin solution in ethanol (p.a. ethanol 99.88%) and 100 μL of n-heptane were dissolved at a hot water bath. Then a volume of 15 μL of such prepared DPPC solution was applied to one side of the polycarbonate support, the solvent was let to evaporate, and then another volume of 15 μL was applied to the other side of the support. After 30 min., both sides were simultaneously exposed to aqueous electrolyte (0.1 M KCl).

Formation of PLM was monitored by EIS measurement. After steady state has been reached (approximately 1 h), changes of *Electrolyte 1* were realized (addition of Pb ions or the exchange of 2 mL of KCl solution for that containing Pb-phytochelatin complexes) and transport across PLM, monitored by EIS measurement, was allowed for exactly1 hour. Subsequently, transported Pb ions were determined in *Electrolyte 2* (after its acidification with HNO_3) using anodic stripping voltammetry on HMDE.

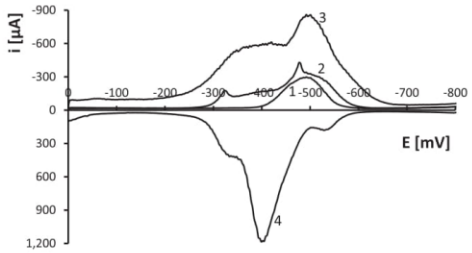

Fig. 1. DP voltammetry on HMDE, borate buffer pH 8.2, scan rate 20 mV s^{-1}, pulse width 100 ms. Curves (1), (2), (3): E_{in} = 0 mV, pulse height: − 50 mV; Curve 4: E_{in} = − 800 mV, pulse height: + 50 mV. Curve (1): 6×10^{-6} M PC_2, Curve (2): addition of 1.7×10^{-6} M Pb^{2+}; Curve (3): 60 s accumulation at 0 mV, Curve (4): 5 s accumulation at − 800 mV

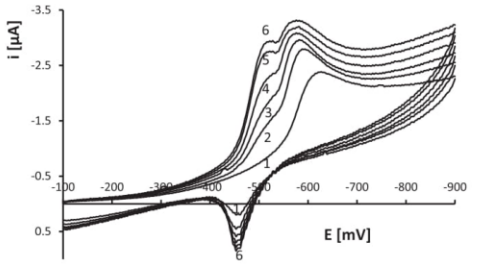

Fig. 3. Cyclic voltammetry on silica gel modified carbon paste electrode. Borate buffer pH 6.8, 6×10^{-6} M PC_2 and 1.7×10^{-6} M Pb^{2+}. Scan rate 100 mV s^{-1}, E_{in} = − 100 mV, E_{fin} = − 900 mV. Accumulation potential − 100 mV, accumulation time (1) 0 s, (2) 10 s, (3) 20 s, (4) 30 s, (6) 60s, (6) 120 s.

3. Results and discussion

Using HMDE, in borate buffer pH 8.2 with no metal ions present, only reduction peak of PC_2 complex with mercury is observed (Fig. 1, curve 1). The height of this peak was exploited in earlier studies of possibility of phytochelatin transport across model membranes [27] (PC_2 is not transported using ionophore calcimycin, transmembrane proteins had to be used [27]). When Pb^{2+} ions are added, new peaks corresponding to Pb complexes appear at potentials less or more negative than original peak. Moreover, another new peak corresponding to dissolution of mercury in presence of Pb−S compounds appears (Fig. 1, curve 4).

However, at pH close to the physiological value, peaks are overlapping and multivariate curve resolution method with alternating least squares (MCR-ALS) has to be applied for establishing stoichiometry of complexes [38]. At pH 6.8, two types of complexes of Pb with PC_2 are formed: 1:1 complex (1 Pb bound by 2 S atoms) – its reduction peak is at about − 0.620 mV, about 100 mV more negative than that of free PC_2. Second complex gives reduction peak at about − 450 mV and involves two Pb atoms for one PC molecule (each Pb bound by one S atom). Whereas 1:1 complex (PbPC) appears from this study as stable, complex with Pb atom on each sulfur (Pb_2PC) is formed at the excess of Pb ions and is weaker. As established by MCR-ALS study [38], both types of complexes are at pH 6.8 present at close to equimolar concentration of Pb^{2+} and PC_2. Using voltammetry only, no separation of reduction peaks is possible. Therefore, we performed differential PSA after accumulation at − 300 mV (to avoid formation of a mercury compound). As it is demonstrated on Fig. 2, the peak at about − 600 mV (which should correspond to PbPC complex) is increasing with decreasing value of stripping current.

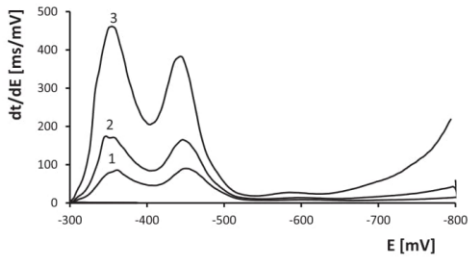

Fig. 2. Differential potentiometric stripping analysis (PSA, chronopotentiometry) on HMDE. Borate buffer pH 6.8, 6×10^{-6} M PC_2 and 1.7×10^{-6} M Pb^{2+}. Accumulation 5 s, − 300 mV, stripping currents: (1) − 100 nA, (2) − 75 nA, (3) − 50 nA.

The second peak situated at about − 450 mV (complex Pb_2PC) is with lower stripping current increasing only slightly and a new peak at about − 350 mV (corresponding to free Pb ions) is increasing strongly.

In order to exclude the influence of mercury compounds, we analyzed the same solution using silica gel modified carbon paste working electrode. On this electrode, PC_2 gives signal due to the oxidation of -SH group at region above + 600 mV, so there is no interference with reduction peaks [22]. As it is documented on Fig. 3, in dependence on accumulation time at potential − 100 mV using constant scan rate, the height of peak corresponding to unresolved Pb-phytochelatin complexes reduction (at about − 600 mV) decreases, whereas peak corresponding to Pb^{2+} reduction (at about − 500 mV) is increasing.

The measurement described on Fig. 2 and Fig. 3 confirmed labile behavior of one from Pb phytochelatin complexes. For similar cases the exception from free-ion-activity model (FIAM) were described in case of different complexes with cadmium ions [35]. In our experiments with transport across PLM containing calcimycin ionophore, comparing transport of free cadmium ions with that of Cd complexes of malic acid and citric acid, the highest amount of ions was transported in case of labile complex Cd-malic acid (at pH 6.5) [14]. Therefore, comparison of transport across PLM of free Pb^{2+} ions and of Pb ions complexed by phytochelatin seems necessary.

3.1. Transport across phospholipid membrane with ionophore calcimycin

First, the transport of 40 μg of Pb^{2+} in 0.1 M KCl (final concentration of Pb^{2+} amounted to 6.4×10^{-5} mol L^{-1}) was examined: 0.25% of initial amount was transported.

Then *Electrolyte 1* containing 40 μg of Pb^{2+} (final concentration of Pb^{2+} amounted to 6.4×10^{-5} mol L^{-1}) and 8.2×10^{-4} mol L^{-1} of PC_2 was prepared and pH adjusted to 6.8, where both Pb- phytochelatin complexes are present. After transport into *Electrolyte 2*, transported portion of Pb^{2+} was 6.66% of the initial amount – that is more than 26 times more than in the case of free ions. Fig. 4 shows records of EIS measurement: a) formation of s-PLB,reaching steady state b)- records after the addition of Pb-PC_2 complexes into *Electrolyte 1,* where huge diffusion process is visible.

After transport experiments, voltammetry of *Electrolyte 1* showed that, apart from mercury compound at about − 300 mV, only peak PC_2 with shoulder of complex PbPC remained. Complex, which is labile, is therefore Pb_2PC. This labile complex was after transport experiment not present, because his bound Pb was transported across the PLM to *Electrolyte 2*. When higher amount of Pb was available, peak of Pb_2PC again appeared (Fig. 5, Curve (3)).

When differential PSA on HMDE of *Electrolyte 1* after transport experiments was performed (its DP voltammetry is depicted on Fig. 5), behavior of observed two peaks corresponds to electrochemically inert

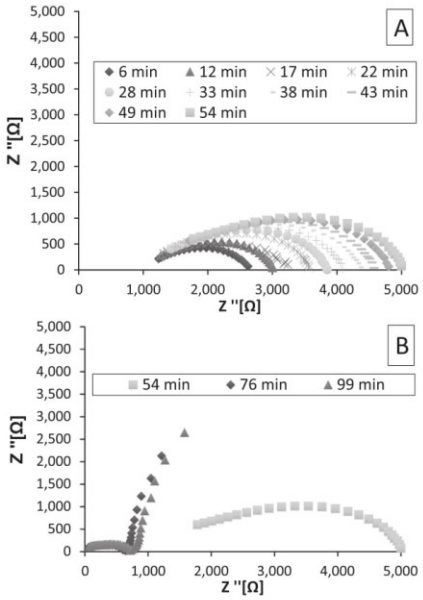

Fig. 4. A: Nyquist plots of stabilization of PL membrane in time. B: Nyquist plots of lead ions transport across the stabilized PL membrane. Times in legends correspond to the starting times of particular Nyquist curves. Lead added in t = 60 min.

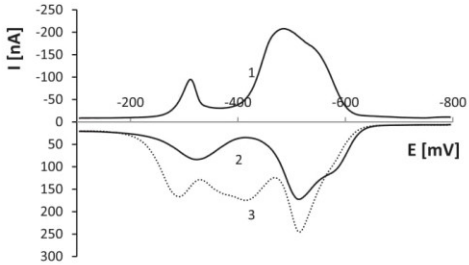

Fig. 5. DP voltammetry on HMDE of *Electrolyte 1* after transport experiment. 2 mL of *Electrolyte 1* + 8 mL of H_2O, scan rate 20 mV s^{-1}, Curve (1): E_{in} = − 100 mV, E_{fin} − 800 mV, pulse height − 50 mV. Curve (2): E_{in} − 800 mV, E_{fin} − 100 mV, pulse height + 50 mV. Curve (3): Accumulation time 5 s at accumulation potential − 800 mV, E_{in} = − 800 mV, E_{fin} = − 100 mV, pulse height = + 50 mV.

complexes [45,46]. With lowering the stripping current, the increase of the height of the peak corresponding to PbPC complex (shifting from about − 620 mV) and the increase of peak of free PC_2 (shifting from − 550 mV) was observed (Fig. 6). This confirms that labile behavior documented on Fig. 2 and on Fig. 3 was due to the presence of complex Pb_2PC.

4. Conclusion

Using differential PSA (chronopotentiometry) realized on HMDE (as working electrode) with adsorptive accumulation and different values of constant negative stripping current, the release of free lead ions

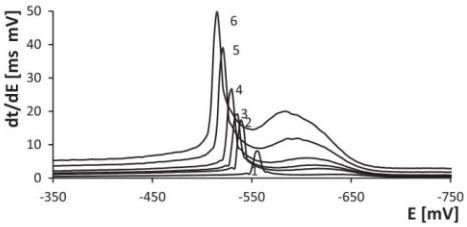

Fig. 6. Differential potentiometric stripping analysis on HMDE of *Electrolyte 1* after transport experiment. 2 mL of *Electrolyte 1* + 8 mL of H_2O, accumulation time 10 s at − 300 mV, E_{in} = − 350 mV, E_{fin} = − 750 mV, stripping currents [nA]: (1) − 500, (2) − 250, (3) − 200, (4) − 150, (5) − 100, (6) − 75.

confirms labile behavior of one from Pb-phytochelatin complexes present at pH 6.8. Similar conclusion resulted from voltammetry on silica gel modified carbon paste working electrode. Experiment with transport across PLM with ionophore calcimycin also confirmed labile behavior - in presence of Pb complexes, 26 times more Pb^{2+} ions was transported. Differential PSA performed with solution after transport experiment showed peaks of remaining electrochemically inert complexes – free PC_2 and the complex with bound one Pb atom. Observed labile behavior of second complex - Pb_2PC - is important for transport of toxic lead: instead of protecting, lead phytochelatin complex Pb_2PC formed at higher Pb concentration may increase lead transport across biological membranes.

Acknowledgements

The authors gratefully acknowledge financial support by Czech Science Foundation (project No. 17-05387S). Š.S. thanks the project Specific University Research (SVV 260440).

References

[1] D.K. Gupta, H.G. Huang, F.J. Corpas, Lead tolerance in plants: strategies for phytoremediation, Environ. Sci. Pollut. Res. 20 (4) (2013) 2150–2161.
[2] K. Novakova, T. Navratil, I. Sestakova, V. Marecek, J. Chylkova, Characterization of electrochemical behavior of lecithin-cholesterol mixture in formation of model phospholipid membranes, in: T. Navratil, M. Fojta, K. Peckova (Eds.), XXXIII Moderni Elektrochemicke Metody (Modern Electrochemical Methods XXXIII), Best servis, Jetrichovice, 2013, pp. 128–131.
[3] D. Bach, E. Wachtel, Phospholipid/cholesterol model membranes: formation of cholesterol crystallites, BBA-Biomembranes 1610 (2) (2003) 187–197.
[4] K.A. Melzak, S.A. Melzak, E. Gizeli, J.L. Toca-Herrera, Cholesterol organization in phosphatidylcholine liposomes: a surface plasmon resonance study, Dent. Mater. 5 (11) (2012) 2306–2325.
[5] T. Navratil, I. Sestakova, K. Stulik, V. Marecek, Electrochemical measurements on supported phospholipid bilayers: preparation, properties and ion transport using incorporated ionophores, Electroanalysis 22 (17–18) (2010) 2043–2050.
[6] J. Jaklova Dytrtova, T. Navratil, V. Marecek, Phospholipid layer stabilization via Yb (III) on ities and facilitated K(I) transport, Collect. Czech. Chem. Commun. 76 (12) (2011) 1917–1930.
[7] T. Navratil, I. Sestakova, V. Marecek, Transport of heavy metals across the supported phospholipid bilayers, Int. J. Energy Environ. 5 (3) (2011) 337–346.
[8] T. Navratil, I. Sestakova, V. Marecek, Supported phospholipid membranes formation at a gel electrode and transport of divalent cations across them, Int. J. Electrochem. Sci. 6 (12) (2011) 6032–6046.
[9] K. Novakova, T. Navratil, I. Sestakova, V. Marecek, J. Chylkova, Utilization of electrochemical impedance spectroscopy for elucidation of electrochemical properties of lecithin - cholesterol mixtures in model phospholipid membranes, Chem. Listy 108 (3) (2014) 219–225.
[10] J. Jaklova Dytrtova, I. Sestakova, M. Jakl, T. Navratil, Electrochemical detection of cadmium and lead complexes with low molecular weight organic acids, Electroanalysis 21 (3–5) (2009) 573–579.
[11] J. Jaklova Dytrtova, M. Jakl, I. Sestakova, E.L. Zins, D. Schroder, T. Navratil, A new approach to study cadmium complexes with oxalic acid in soil solution, Anal. Chim. Acta 693 (1–2) (2011) 100–105.
[12] J. Jaklova Dytrtova, M. Jakl, D. Schroder, T. Navratil, Electrochemical and spectrometric detection of low-molecular-weight organic acids and their complexes with metals, Curr. Org. Chem. 15 (17) (2011) 2970–2982.
[13] J. Jaklova Dytrtova, M. Jakl, K. Novakova, T. Navratil, V. Sadek, Binding abilities of

copper to phospholipids and transport of oxalate, Monatsh. Chem. 146 (5) (2015) 831–837.
[14] I. Sestakova, T. Navratil, B. Josypcuk, Employment of voltammetry in studies of transport processes across artificial phospholipid membranes, Electroanalysis 28 (11) (2016) 2754–2759.
[15] W.E. Rauser, Phytochelatins and related peptides. Structure, biosynthesis, and function, Plant Physiol. 109 (4) (1995) 1141–1149.
[16] C.S. Cobbett, Phytochelatins and their roles in heavy metal detoxification, Plant Physiol. 123 (3) (2000) 825–832.
[17] C.S. Cobbett, Phytochelatin biosynthesis and function in heavy-metal detoxification, Curr. Opin. Plant Biol. 3 (3) (2000) 211–216.
[18] M. Lao, A. Dago, N. Serrano, E. Companys, J. Puy, J. Galceran, Free Zn^{2+} determination in systems with Zn-glutathione, J. Electroanal. Chem. 756 (2015) 207–211.
[19] H. Zaier, A. Mudarra, D. Kutscher, M.R. Fernandez de la Campa, C. Abdelly, A. Sanz-Medel, Induced lead binding phytochelatins in brassica juncea and sesuvium portulacastrum investigated by orthogonal chromatography inductively coupled plasma-mass spectrometry and matrix assisted laser desorption ionization-time of flight-mass spectrometry, Anal. Chim. Acta 671 (1–2) (2010) 48–54.
[20] X.V. Nguyen, K.H. Le-Ho, J. Papenbrock, Phytochelatin 2 accumulates in roots of the seagrass enhalus acoroides collected from sediment highly contaminated with lead, Biometals 30 (2) (2017) 249–260.
[21] V. Vacchina, H. Chassaigne, M. Oven, M.H. Zenk, R. Lobinski, Characterisation and determination of phytochelatins in plant extracts by electrospray tandem mass spectrometry, Analyst 124 (10) (1999) 1425–1430.
[22] I. Sestakova, T. Navratil, Voltammetric methods in metallothionein research, Bioinorg. Chem. Appl. 3 (1–2) (2005) 43–53.
[23] V. Dorcak, A. Krezel, Correlation of acid-base chemistry of phytochelatin PC2 with its coordination properties towards the toxic metal ion Cd(II), Dalton Trans. 11 (2003) 2253–2259.
[24] B.H. Cruz, J.M. Diaz-Cruz, I. Sestakova, J. Velek, C. Arino, M. Esteban, Differential pulse voltammetric study of the complexation of Cd(II) by the phytochelatin (gamma-Glu-Cys)(2)Gly assisted by multivariate curve resolution, J. Electroanal. Chem. 520 (1–2) (2002) 111–118.
[25] V. Dorcak, I. Sestakova, Electrochemical behavior of phytochelatins and related peptides at the hanging mercury drop electrode in the presence of cobalt(II) ions, Bioelectrochemistry 68 (1) (2006) 14–21.
[26] M. Fojta, M. Fojtova, L. Havran, H. Pivonkova, V. Dorcak, I. Sestakova, Electrochemical monitoring of phytochelatin accumulation in nicotiana tabacum cells exposed to sub-cytotoxic and cytotoxic levels of cadmium, Anal. Chim. Acta 558 (1–2) (2006) 171–178.
[27] T. Navratil, K. Novakova, B. Josypcuk, R. Sokolova, I. Sestakova, Voltammetric detection of phytochelatin transported across unmodified and protoplast modified model phospholipid membranes, Monatsh. Chem. 147 (1) (2016) 165–171.
[28] O. Zitka, H. Skutkova, O. Krystofova, P. Sobrova, V. Adam, J. Zehnalek, L. Havel, M. Beklova, J. Hubalek, I. Provaznik, R. Kizek, Rapid and ultrasensitive method for determination of phytochelatin(2) using high performance liquid chromatography with electrochemical detection, Int. J. Electrochem. Sci. 6 (5) (2011) 1367–1381.
[29] A. Janovjakova, M. Gal, J. Krahulec, R. Sokolova, M. Naumowicz, J. Hives, Native and denatured enzyme enterokinase determined by electrochemical methods, Monatsh. Chem. 148 (3) (2017) 549–553.
[30] T. Sotak, M. Hronec, M. Gal, E. Dobrocka, J. Skriniarova, Aqueous-phase oxidation of furfural to maleic acid catalyzed by copper phosphate catalysts, Catal. Lett. 147 (11) (2017) 2714–2723.
[31] M. Naumowicz, M.A. Kruszewski, M. Gal, Electrical properties of phosphatidylcholine bilayers containing canthaxanthin or beta-carotene, investigated by electrochemical impedance spectroscopy, J. Electroanal. Chem. 799 (2017) 563–569.
[32] I. Stanish, H.G. Monbouquette, Engineering a23187/edta-containing metal-sorbing vesicles for selective extraction of divalent heavy metal ions, J. Membr. Sci. 192 (1–2) (2001) 99–113.
[33] J.H. Vanzanten, H.G. Monbouquette, Biomimetic metal-sorbing vesicles - Cd^{2+} uptake by phosphatidylcholine vesicles doped with ionophore-A23187, Biotechnol. Prog. 8 (6) (1992) 546–552.
[34] M. Naumowicz, A.D. Petelska, Physicochemical modelling of the surface-active phospholipid bilayer relative to acid-base equilibria, J. Electroanal. Chem. 782 (2016) 233–240.
[35] F. Degryse, E. Smolders, R. Merckx, Labile Cd complexes increase Cd availability to plants, Environ. Sci. Technol. 40 (3) (2006) 830–836.
[36] C. Wang, L.Y. Wang, Q. Sun, Response of phytochelatins and their relationship with cadmium toxicity in a floating macrophyte pistia stratiotes l. At environmentally relevant concentrations, Water Environ. Res. 82 (2) (2010) 147–154.
[37] Z. Cadkova, J. Szakova, D. Miholova, B. Horakova, O. Kopecky, D. Krivska, I. Langrova, P. Tlustos, Bioaccessibility versus bioavailability of essential (Cu, Fe, Mn, and Zn) and toxic (Pb) elements from phyto hyperaccumulator pistia stratiotes: potential risk of dietary intake, J. Agric. Food Chem. 63 (8) (2015) 2344–2354.
[38] A. Alberich, C. Arino, J.M. Diaz-Cruz, M. Esteban, Soft modelling for the resolution of highly overlapped voltammetric peaks: application to some Pb-phytochelatin systems, Talanta 71 (1) (2007) 344–352.
[39] A. Walcarius, Analytical applications of silica-modified electrodes –a comprehensive review, Electroanalysis 10 (18) (1998) 1217–1235.
[40] I. Svancara, R. Metelka, K. Vytras, Piston-driven carbon paste electrode holders for electrochemical measurements, in: K. Vytras, K. Kalcher (Eds.), Sensing in Electroanalysis, University of Pardubice, Pardubice, 2005, pp. 7–18.
[41] I. Svancara, R. Metelka, K. Vytras, Casing for carbon paste for electrochemical measurements, Patent No. 301714, Czech Republic, 2010.
[42] K. Novakova, T. Navratil, I. Sestakova, M.P. Le, H. Vodickova, B. Zamecnikova, R. Sokolova, J. Bulickova, M. Gal, Characterization of cadmium ions transport across model and real biomembranes and indication of induced damage of plant tissues, Monatsh. Chem. 146 (5) (2015) 819–829.
[43] R.W. Taylor, D.R. Pfeiffer, C.J. Chapman, M.E. Craig, T.P. Thomas, Complexation chemistry of ionophores a23187 and ionomycin, Pure Appl. Chem. 65 (3) (1993) 579–584.
[44] M. Parisova, T. Navratil, I. Sestakova, J. Jaklova Dytrtova, V. Marecek, Influence of low molecular weight organic acids on transport of cadmium and copper ions across model phospholipid membranes, Int. J. Electrochem. Sci. 8 (2) (2013) 27–44.
[45] H.P. van Leeuwen, R.M. Town, Adsorptive stripping chronopotentiometry (adscp). Part 1: fundamental features, J. Electroanal. Chem. 610 (1) (2007) 9–16.
[46] N. Serrano, I. Sestakova, J.M. Diaz-Cruz, C. Arino, Adsorptive accumulation in constant current stripping chronopotentiometry as an alternative for the electrochemical study of metal complexation by thiol-containing peptides, J. Electroanal. Chem. 591 (1) (2006) 105–117.

9. Appendix III

Model Biological Membranes and Possibilities of Application of Electrochemical Impedance Spectroscopy for their Characterization

Skalová Štěpánka, Vyskočil Vlastimil, Barek Jiří, Navrátil Tomáš

Electroanalysis

Volume 30, Pages 207-219, Year 2018

Review

Wiley Online Library

ELECTROANALYSIS

DOI: 10.1002/elan.201700649

Model Biological Membranes and Possibilities of Application of Electrochemical Impedance Spectroscopy for their Characterization

Štěpánka Skalová,[a, b] Vlastimil Vyskočil,[b] Jiří Barek,[b] and Tomáš Navrátil*[a]

Abstract: Biological membranes are essential parts of living systems. They represent an interface between intracellular and extracellular space. Depending on their structure, they often perform very complex functions and play an important role in the transport of both charged and uncharged particles in any organism. Structure of the biological membranes, which play very important role in electrochemical processes inside living organisms, is very complicated and still not precisely defined and explained. Model lipid membranes are used to gain detail information about properties of real biological membranes and about associated electrochemical processes. Electrochemistry, especially electrochemical impedance spectroscopy (EIS), can play a useful role in the characterization of properties of model lipid membranes (planar and supported lipid bilayers, tethered lipid membranes, liposomes, etc.). This review is focused on model biological membranes and the possibilities and limitations of electrochemical methods and namely of EIS in this field.

Keywords: Model membrane · Phospholipid bilayer · Electrochemical impedance spectroscopy (EIS) · Planar lipid bilayer · Supported lipid bilayers · Tethered lipid bilayers · Liposomes

1 Introduction

Biological membranes play very important functions in living cells. The cell membrane separates the interior of all cells from the outside milieu. The basic function of the cell membrane is the cell protection from its surroundings without its isolation. The cell membrane is selectively permeable for ions and organic molecules and has an influence on movement of substances into and out of the cell [1].

Various techniques have been utilized for investigation of the formation of biological membranes, transporting processes across them, and functions and physical properties of these structures, e.g., fluorescence microscopy, fluorescence lifetime correlation spectroscopy combined with lifetime tuning, solvent relaxation technique, or confocal fluorescence correlation spectroscopy [2]. However, electrochemical methods can play very important role in this field. On the one hand, they have been employed in monitoring of elements, complexes or more complicated compounds, present on both sides of cell membranes (i.e., in intracellular and extracellular spaces), which are transported across them (e.g., Cd^{2+}, Pb^{2+}, Cu^{2+}) [3,4] or which affect the transporting processes across them (phytochelatins, low molecular weight organic acids (e.g., oxalic, citric, and malic) [3,5–9]). For these purposes, voltammetric techniques (e.g., cyclic voltammetry and differential pulse voltammetry) [4,10–12] and differential potentiometric stripping analysis (DPSA, chronopotentiometry) [7,8,13,14] have been utilized.

On the other hand, electrochemical techniques can be used in characterization of functions and physical properties of biological membranes. The most important electrochemical technique in this research seems to be electrochemical impedance spectroscopy (EIS) (e.g., [4,15–19]), which is discussed in this review.

2 Real Biological Membranes

Due to the invention of microscope, history of investigation of cell membrane structure started in the 17th century. Traube registered that outer layer must be semipermeable to allow transport of ions [20]. Quincke was the first who noticed the lipid nature of the cell membrane. He observed that a cell generally creates a spherical shape in water. In his time, oil was the only known material which exhibited this behavior [21]. He declared that the cell membrane consists of a fluid layer of fat [22,23]. Overton formed fundamental concepts of the structure and function of the cell membrane – the lipid theory of cell permeability and the lipid theory of narcosis [23]. He reached the conclusion that the cell membrane might be

[a] Š. Skalová, T. Navrátil
J. Heyrovský Institute of Physical Chemistry of the Czech Academy of Sciences, Dolejškova 3, 182 23 Prague 8, Czech Republic
E-mail: Tomas.Navratil@jh-inst.cas.cz
[b] Š. Skalová, V. Vyskočil, J. Barek
Charles University, Faculty of Science, Department of Analytical Chemistry, UNESCO Laboratory of Environmental Electrochemistry, Hlavova 2030/8, 128 43 Prague 2, Czech Republic

made of lecithin (phosphatidylcholine) and cholesterol [24,25].

At the beginning of the 20th century, the structure of the cell membrane started to be revealed. It was suggested that the cell membrane is a lipid bilayer [26]. However, it has been proved that it is incorrect. In the model of Davson and Danielli, the lipid bilayer is covered on one side with a globular protein layer which is not immersed to lipids [27]. The Robertson's model indicated that the cell membrane is created by "units" of lipids and proteins (but proteins were not an integral part) [28]. Models suggested by Davson and Danielli and by Robertson were thermodynamically unstable; hydrophobic areas of proteins were exposed to the aquatic environment. On the contrary, the model formulated by Benson and Green presumed that the inner mitochondrial membrane is formed by subunits of proteins, and lipids represent some kind of solvent only [29,30]. Results from these experiments were fundamental in the development of the "fluid mosaic" model [31–34]. This model, introduced by Singer and Nicolson [35], supposed that biological membranes consist mainly of lipid bilayer with proteins penetrating either half way or all the way through the membrane. The bilayer is completely liquid and the proteins are floating freely in the plane of the membrane. This model was the first which correctly incorporated fluidity, membrane channels, and multiple modes of protein/bilayer connected into one theory.

The cell membrane is composed of a thin layer of amphipathic phospholipids (class of lipids that is a major component of cell membranes). Phospholipids are spontaneously organized so that the hydrophobic "tail" regions are isolated from the surrounding polar fluid (regions are usually comprised of long fatty acid hydrocarbon chains – biological fatty acids usually include an even number of carbon atoms, with numbers of 16 and 18 being the most common). The hydrophilic "head" regions (which contain the negatively charged phosphate group and may include other polar groups) are kept in touch with the intracellular and extracellular faces of the resulting bilayer. Forces like Van der Walls, electrostatic, hydrogen bonds, and non-covalent interactions assist to the formation of the lipid bilayer. The major propelling force in the formation of bilayers is the hydrophobic interaction. Regulation of the movement of materials into and out of cells is one of the important functions of membranes. Organization of membrane forestalls diffusion of ions and polar molecules across the lipid bilayer, but enables passive diffusion of hydrophobic molecules. The plasma membrane also includes a large number of proteins, which contribute to

Štěpánka Skalová is a student of the PhD degree program of Analytical Chemistry at the Faculty of Science, Charles University, Prague, Czech Republic. She co-operates with the J. Heyrovský Institute of Physical Chemistry of the Czech Academy of Sciences, Prague, Czech Republic. Her research is focused on development of an electrochemical cell containing a biomembrane and a biosensor to investigate transport of biologically active substances across phospholipid membranes.

Vlastimil Vyskočil is an associate professor and the Head of the Group of Electrochemical Biosensors and Bioelectrochemistry in the UNESCO Laboratory of Environmental Electrochemistry at the Charles University (Prague, Czech Republic), Faculty of Science, Department of Analytical Chemistry. He received his M.Sc., Ph.D., RNDr. and Doc. degrees at the Charles University in Prague in 2005, 2010, 2010, and 2015, respectively. He published over 80 research papers (h-index of 18) and 11 book chapters in the area of novel electrochemical sensors and biosensors based on non-traditional electrode materials for investigation and determination of biologically active organic compounds.

Jiří Barek is a professor at the Charles University (Prague, Czech Republic), Faculty of Science, Department of Analytical Chemistry, and the Head of the UNESCO Laboratory of Environmental Electrochemistry. He published more than 500 papers (h-index of 35). His main research interest is the development of new voltammetric and amperometric methods for detection of trace amounts of biologically active organic compounds important from the point of view of the protection of the environment and human health.

Tomáš Navrátil is a research scientist at J. Heyrovský Institute of Physical Chemistry of the Czech Academy of Sciences, Department of Electrochemistry at the Nanoscale and an associate professor at the First Faculty of Medicine, Institute of Medical Biochemistry and Laboratory Diagnostics, Charles University, Prague, Czech Republic. Author/co-author of more than 190 of per reviewed research articles and reviews (H-index 32) and several book chapters. He graduated in analytical chemistry from Charles University, Prague (1996). He devotes himself to electrochemical methods (voltammetry, EIS), their combination with mathematical and statistical methods (elimination voltammetry, chemometry, biometry), to determination of trace amounts of biologically active organic substances of environmental importance, to development and testing of new electrochemical sensors and procedures.

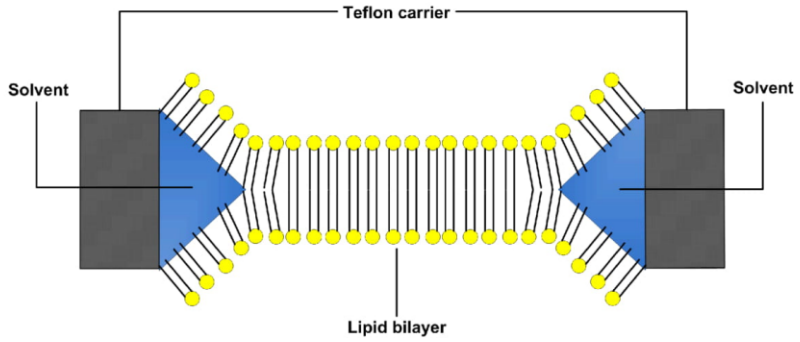

Fig. 1. Preparation of planar lipid bilayer according to Mueller (figure inspired by ref. [32]).

creation of further structures (transmembrane protein complexes – pores, channels, and gates).

One important function of the cell membrane is the transport of substances to and from the cells. The transfer of substances across the phospholipids bilayer can be passive (occurring without the input of cellular energy, movement of molecules along their concentration gradient), or active (requiring the cell to expend energy in transporting them), with help of transmembrane protein channels and transporters, endocytosis and exocytosis. Active transport of molecules from an area of low concentration to an area of high concentration demands energy, usually from ATP (adenosine triphosphate) (e.g., the sodium-potassium pump). Endocytosis and exocytosis are other energy-driven processes. When large molecules are transported into the cell, it is endocytosis and when molecules are excluded from the cell, it is exocytosis.

The permeability is due to passive diffusion of molecules (permeate molecules) across the membrane. The permeability is dependent principally on the electric charge and polarity of the molecule and, to a lesser degree, on the molar mass of the molecule. The cell membranes have hydrophobic nature. Therefore, small electrically neutral molecules (e.g., water) devolve over membrane easier than charged or hydrophobic molecules (e.g., oxygen) and nonpolar molecules (e.g., benzene). The small uncharged polar molecules usually diffuse via membrane channels. Large, uncharged, and polar molecules (e.g., glucose, sucrose) or ions do not pass through the bilayer easily. Hydrophilic molecules cannot pass the cell bilayer because of the difference in polarities, but they diffuse through the membrane due to membrane proteins (integral or peripheral). The membrane thus helps to keep the potential of the cell [36].

3 Models of Biological Membranes – Planar Lipid Bilayer

Model lipid bilayer is a structure, which is created *in vitro,* and it is a kind of imitation of bilayer of cell membranes *in vivo.* Only one pure synthetic lipid is included in the simplest model of the bilayer. Nevertheless, model bilayers, which have to approach to more physiologically relevant models, can be created by mixtures of several synthetic or natural lipids.

Planar lipid bilayer, also known as black lipid membrane (BLM), is the simplest model of these model biological membranes. The term "black" membrane indicates that it is dark in reflected light. The thickness of the membrane is just a few nanometers, which means that light reflected of the back face destructively interferes with the light reflected of the front face [37].

The model systems serve for understanding the properties and functioning of biological membranes (e.g., artificial liposomes or vesicles which imitate size and geometry of cell, but they miss ion channels and a number of other components commonly present in cells). The artificial BLM is used as a simplified model of biological membranes and is extensively utilized for electrical characterization of protein pores and ion channels. Protein pores are nonspecific channels, which transfer molecules through cell membranes [38–43].

For the formation of BLMs, there are two main methods. The first is the painting technique, which was introduced by Montal and Mueller (Figure 1) [32]. The BLM is formed by spreading a solution of lipids dissolved in an organic solvent. The chamber is divided in two compartments which are filled with salt solutions. A dispersion of lipids is led across the hole in the cell separating them with the use of a small paintbrush or a plastic rod. The cluster of lipids starts in the center of the hole to create a bilayer [32]. In the second method, the membrane bilayer is developed from the apposition of two lipid monolayers – a Langmuir-Blodgett technique

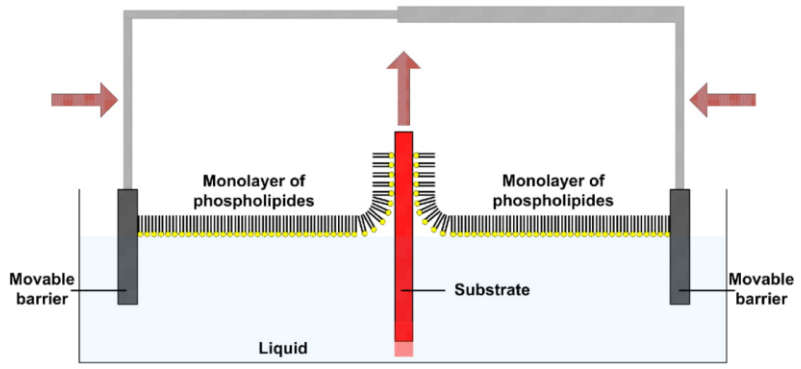

Fig. 2. Preparation of planar lipid bilayer according to Langmuir and Blodgett (figure inspired by ref. [45]).

(chapter 3.2 and Figure 2) [44,45]. A lipid is dissolved in a volatile solvent and this solution is applied on the water-air interface of each compartment. Monolayer is formed after evaporation of the solvent on the surface. The bilayer is developed after the formation of monolayers, when the amount of water in both compartments is increased above the hole.

Geometry of the BLM enables chemical and electrical access to both sides of the bilayer, so the physical attributes of this bimolecular film can be easily measured. Commonly, lipid bilayer is created from two lipid monolayers at an air-water interface by the apposition of their hydrocarbon chains, when a gap in Teflon (diameter of this gap is a few tens of micrometers) isolating two aqueous phases is lowered through the interface. Creation of the membrane is confirmed by an increase of the electrical capacity, as measured with a voltage clamp [44]. A planar lipid bilayer can be regarded as an imperfect capacitor from the electrical aspect. Two electrical properties are of especial interest: capacitance (C) and resistance (R).

The capacitance is the parameter which is regarded as the best tool for recording the stability and integrity of planar lipid bilayers. Three main methods for the determination of planar lipid bilayer capacitance are: i) a capacitance to period conversion method, ii) a discharge method, and iii) a capacitance to voltage conversion method. The measured capacitance must be standardized to the size of the lipid bilayer surface and the specific capacitance of the lipid bilayer for comparison between different studies. It is usually given as capacitance per unit area [15,46].

Resistance reaches value of the order of a few GΩ for planar lipid bilayer. The resistance is commonly calculated (measured) in accordance with Ohm's law as the ratio of voltage (applied to the planar lipid bilayer) and current (flowing through it) [46].

3.1 Effect of Cholesterol on Planar Lipid Bilayers

Cholesterol is a very important component of the cell membrane and does not form bilayers by itself, but it is dissolved in the bilayer [47]. It is nonhomogeneously distributed in biomembranes (high concentration is in the plasma membrane and low concentration in the membranes of intracellular organelles). In plasma membrane, it is present in the concentration range from 20 to 50 mol%. Cholesterol has a structural and a regulatory role in membranes (in maintaining proper fluidity and rigidity of the plasma membrane). The hydroxyl group on cholesterol reacts with the polar head groups of the membrane phospholipids and sphingolipids, while the bulky steroid and the hydrocarbon chain are inserted in the membrane together with the nonpolar fatty-acid chain of the other lipids. It is also believed that cholesterol asymmetry exists between the two leaflets of the bilayer [48,49].

The influence of cholesterol on the structure of the membrane has been investigated for several years using experimental [50–52] and computational techniques [53–55]. The influence of cholesterol on the partitioning of water or molecular oxygen into lipid membranes is well marked in membranes of saturated lipids as compared to membranes of unsaturated lipids [56,57]. It is not equally distributed in biomembranes with saturated and unsaturated phospholipids but instead accumulated in so-called lipid rafts [58–60]. Cholesterol improves the orientation and decrease of the fluidity of the bilayer lattice structure in the hydrated state up to 50 mol% in egg lecithin and up to 25 mol% in dipalmitoyllecithin. However, addition of 33–50 mol% of cholesterol to dipalmitoyllecithin increases the fluidity of the bilayer. This is attributed to a gel of liquid crystalline phase transition in dipalmitoyllecithin [61,62]. The influence of cholesterol on the structure of phosphatidylcholine bilayers was also studied. Cholesterol can either increase or decrease the width of the

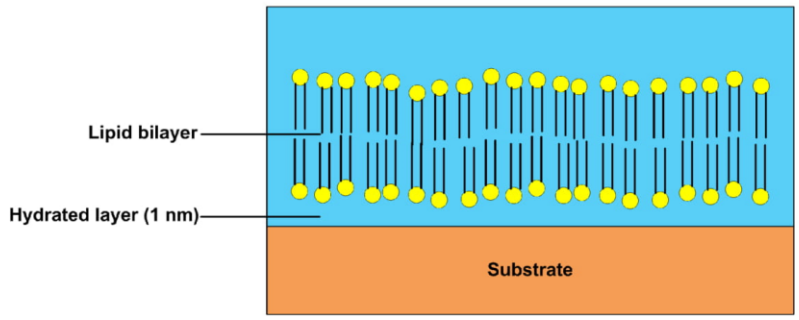

Fig. 3. Supported lipid bilayers (SLBs) (figure inspired by refs. [64,65]).

bilayer depending on the physical state and chain length of the phospholipids. Cholesterol increases the width of the membrane as it takes out the chain tilt from gel state lipids or increases the *trans* conformations of the chains for liquid crystalline lipids and saturated phosphatidylcholines. Nevertheless, cholesterol reduces the width of 18 carbon chain bilayers below the phase transition temperature as the long phospholipid chains must deform or twist to confirm the significantly shorter cholesterol molecule. However, the phosphatidylcholine head group conformation is not modified by the addition of cholesterol to the bilayer [12,63].

3.2 Supported Lipid Bilayers (SLBs)

Supported lipid bilayers (SLBs) are artificial lipid bilayer membranes commonly used as versatile biological membrane mimics and were reported firstly in the early 1980s by McConnell [64,65]. Planar structure of the membrane exists on a solid support (in same papers it is called substrate) and the upper face of the bilayer is exposed to free solution (solid-liquid interfaces) (Figure 3) [66]. The membrane from the solid surface is separated by an ultrathin water layer [67–71]. Mica, glass, and silicon oxide are the most commonly utilized supports for SLBs [67,72–75]. Even if the SLB is connected to a solid surface, the bilayer retains its fluidic properties [76,77]. It is used to study the fundamental physicochemical properties of lipid bilayers and to utilize them as cell membrane model systems *in vitro* (e.g., the research of lipid-lipid and cell-cell interactions, the functional role of membrane proteins [66,78–83], membrane-proteins interactions [81], as well as other biochemical processes such as molecular transport and signaling [66], for developing biosensors [84–87], for model systems for drug delivery [88,89] and for study of effect of surface charge of model biological membranes on their interactions with peptides) [90]. These bilayers are interesting systems for investigation of cell adhesion on an artificial support due to the structural similarity with the cell membrane using methods designed for surface analysis such as surface plasmon resonance (SPR), quartz crystal microbalance with dissipation monitoring (QCM-D), ellipsometry, total internal reflection fluorescence microscope (TIRF), and atomic force microscopy (AFM) [91].

There is a number of methods for the preparation of SLBs with different lipid mixtures (e.g., the Langmuir-Blodgett techniques (Figure 2), the Langmuir-Schaefer technique [65,92,93], the vesicle fusion technique [64], and a self-spreading technique, where lipid molecules are self-organized at a solid/liquid interface [94–97]). A substantial advantage consists in the fact that the different surface techniques of fabrication (e.g., photolithography, microcontact printing, etc.) influence and control properties of formed SLBs. However, it is necessary to take care about denaturation of biological molecules and artificial phenomena. One of the best advantages of the SLBs is their stability. SLBs remain undamaged although subject to high flow rates or vibrations. Another advantage of the SBLs is that their surface is accessible to a number of characterization tools which would be impossible or would provide lower resolution if performed on a freely floating sample. SBLs have also the ability to pattern the surface to create multiple isolated regions on the same support. Certain disadvantage of SBLs is the unwanted possibility of interactions with the support. The hydrophilicity of the support is one of the critical factors determining the SLB and support interaction because it influences the stability and the thickness of the water layer between the SLBs and supports. It is necessary to keep in mind that the lipid bilayer is a self-assembled structure because the hydrophilic-hydrophobic interaction surrounded by the water molecules bound to the head groups with hydrogen bonds. The direct visualization of the three-dimensional distribution of water layers above solid supports and lipid bilayers was obtained by AFM [98,99] and this information is essential to understand the water-mediated interaction between the SLBs and supports [100]. The properties and structures of SLBs are influenced by the chemical and physical properties of solid supports (substrates) because

the water layer between the SLBs and substrates keeps the fluidity and dynamics in SLBs. SLBs have unique substrate-induced phenomena, e.g., decoupling phase transition [101–103] and asymmetric molecular distribution between the upper and lower leaf of the SLB [40,104–110]. The space between the lower leaf of the bilayer and the solid support is insufficient to precede lipid-solid surface interactions and following spawning. This can cause a decrease in lipid mobility and denaturation of incorporated transmembrane proteins [78]. For this reason, SLBs do not fully comply with the natural fluidity of biological membranes. This problem can be solved by deposition of the lipid bilayer on a soft hydrated polymeric pad which functions as a lubricating layer (this system is called polymer-supported membrane) [76,111]. The polymer pad should be hydrophilic, soft, not too highly charged, and not extensively cross-linked [76], with a thickness less than 100 nm [75,78].

3.3 Tethered Bilayer Lipid Membranes (t-BLMs)

t-BLMs (Figure 4) belong to solid supported membranes and are based on the immobilization of a planar lipid bilayer on a solid support that enables characterization by a wide range of surface-sensitive analytical techniques [112]. They have the inner leaflet of a lipid bilayer covalently connected to a surface through a short spacer group [80,113,114]. This spacer group (in most cases a short oligomer and the anchor lipid which can bind to substrates (supports) by suitable chemistry) includes small surface roughness features and provides an ions and water reservoir underneath the membrane [84,115,116]. t-BLMs, which were inspired by planar lipid bilayers on solid supports, are utilized as sensing platforms for a broad spectrum of biophysical experiments such as peptide/membrane interactions, protein/membrane interactions, and reconstitution of pore-forming, lipid phase transitions, redox and receptor proteins, antigen/antibody binding, and photocurrent generation [117,118]. The great advantage is their long-term stability of the order of days, weeks or even months [119]. The Langmuir-Blodgett deposition technique for monolayer transfer was utilized at the beginning of production of these platforms [120]. At present, self-assembly methods are commonly applied for technical simplicity and high reproducibility. The first tethers for supporting planar lipid bilayers were derived from an alkanethiol tether that is covalently connected to thin films of metals, e.g., gold [121] or mercury [122], because sulfur atoms have strong affinity to metals [123,124]. The result is a self-assembled monolayer (SAM); the anchored lipid is self-assembled onto a substrate. If lipid vesicles are adsorbed onto the SAM, it creates a hybrid bilayer which is composed of a lower leaflet of alkanethiols and an upper leaflet of phospholipids [121,125]. The monolayer can also be incubated in an ethanol-lipid solution which is afterwards substituted by a buffer. This process leads then to the spontaneous creation of a bilayer [126]. The other approach is based upon the tethering of macromolecular spacers, e.g., polymer chains [78,127], polyelectrolyte layers [128], carbohydrates, or peptides [129–131], to the solid support. Subsequently, lipid vesicles are created at the planar lipid bilayer upon the layer of tethered macromolecules. There is some space (several nanometers) between the lipid bilayer and the solid support; this space is satisfactory to arrange transmembrane proteins and to support the ion transport across the membrane. For properties of the bilayer membrane, the spacer, its type, its length (tightly wracked and short spacer units give very high membrane resistance, but this can decrease incorporation of proteins), and its anchor type (e.g., anchor groups suitable for the connection of the membrane on noble metals [115,132] or on oxides of substrates [133,134]) are very important. Thiolipid-based tethered bilayers are a very interesting group of t-BLMs. In termed thiolipids, the central feature of these tethers is a hydrophilic spacer that is capped with a functional group for covalent immobilization and the other end of the spacer is connected to the hydrophilic head of a phospholipid [114,135,136]. This type of bilayers has excellent electrical sealing properties and long-term stability, which makes it a great platforms for studying ion channels, pore-forming toxins [137], and transmembrane proteins [138]. Metal thin films have advantageous properties for electrochemical and plasmonic optical applications. Thiolipid-based tethered bilayers on silicon oxide or silane for microelectronics are very interesting, too [112,133,139].

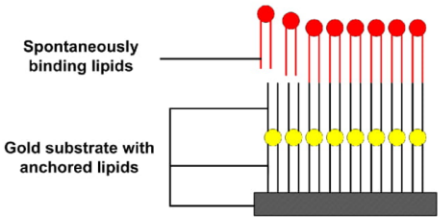

Fig. 4. Tethered bilayer lipid membranes (t-BLMs) (figure inspired by ref. [45]).

3.4 Liposomes

Liposomes are the artificially prepared vesicles composed of a lipid bilayer. They have numerous research and therapeutic applications. The building blocks of liposomes are amphiphilic lipids (often phospholipids) creating colloidal vesicles encapsulating a fraction of the aqueous phase in aqueous media via self-assembly. The bilayer is formed by hydrophobic chains of lipids and the polar head groups of the lipids are oriented towards the inner cavity and extravesicular solution [140,141]. Classification of liposomes is frequently done according to their size and lamellarity. Liposomes are classified into small unilamellar vesicles (SUV) (25–100 nm), large unilamellar vesicles

(LUV) (100-1000 nm), multilamellar vesicles (MUV) (normally above 100 nm in diameter), oligolamellar vesicles (OUV), and multivesicular vesicles (MVV) [142,143]. The characterization of liposome formulations and preparation is necessary in order to guarantee that liposomes encompass the required and expected properties for their specific application. Liposome size, surface charge, lamellarity, phase transition temperature, phospholipid composition and concentration, physical and chemical stability, entrapped volume, degree of drug encapsulation, and permeability are among the most relevant studied and investigated liposome characteristics. The important parameter is the surface charge of liposomes. This charge influences electrostatic interactions between liposomes and surrounding molecules, particles, and surfaces. It is governed by the structure of the lipid head group and composition of the aqueous buffer, including pH and ionic strength of the liposome dispersion. Water-soluble and water-insoluble agents can be encapsulated into the inner cavity or incorporated into the bilayer membrane of the liposome. The membrane of living cells is composed mostly of the phospholipids. Glycerophospholipids are the most commonly utilized naturally occurring phospholipids used in the preparation of liposomes; other major naturally occurring membrane-forming lipids involve sphingolipids, glycosphingolipids, and glycoglycerolipids. Additional major membrane compounds are proteins and cholesterol, which greatly reduce membrane permeability [144–147]. Liposomes are used as models of biological membranes, partitioning medium, and as drug carriers to deliver a broad range of drug types (e.g., anti-cancer, hormonal, enzymatic, and gene drugs), immunoactivators, etc. [142,143,148–151]. Liposomes can be applied as carriers for a wide spectrum of signaling molecules. Liposomes are also utilized as carriers for the delivery of dyes to textiles, pesticides to plants, enzymes and nutritional supplement to foods, and cosmetics to the skin [152,153]. Recently, we witness a tendency towards the analytical application of liposomes in biosensors and bioanalysis due to the possibility of encapsulation [154].

4 Electroporation

BLM is a relatively simple system that consists of planar dielectric sheets of phospholipid layers without protein channels, transporters of ions, etc., which are exposed to the electrolyte solution from both sides. It can be easily represented as a parallel-plate capacitor. Its typical resistance is very high (order of GΩ) and is called "gigaseal" (for the reason that hydrophobic part is impermeable for any charged particle). If some holes (nanometer-sized) are situated in the lipid bilayer, the resistance decreases considerably.

Application of a strong external electric field causes formation of pores. Such a phenomenon is called electroporation [155–157]. The electrical modulation of physical properties of biological membranes has increasing importance for manipulations in biological cells [158]. As it was mentioned above, external electric field can cause structural changes in biological membranes. This transformation can lead to rearrangement of phospholipid bilayers and to the development of pores. The membrane gets back to its normal state after removing of the electric field. Electroporation is reversible if the electric field does not exceed some critical limit and some critical time of its application. In case of an irreversible electroporation, the lipid bilayer does not close after the removing the applied electric field. The electroporation mechanisms of transporting processes and properties of membranes under influence of the electric field have been intensively studied. The measurement of current passing across the membrane and voltage between both sides of the phospholipid membrane can be realized by using electrodes placed in the aqueous compartment on both sides of the tested lipid bilayer. Two techniques are usually used to measure the properties of planar lipid bilayers: a voltage-clamp method (a voltage signal is applied on the planar lipid bilayer) and a current-clamp method (a current is applied on the planar lipid bilayer) [46]. Applications of these two methods are very useful, e.g., when electrically induced pores are studied in BLMs. The shape of pores is very unstable and their conductance is continuously changing during the experiment. A combination of the mentioned techniques with different kinds of high-frequency electromagnetic fields offers new additional possibilities of investigation of the structure-function relationships between the planar lipid bilayer and the membrane interacting peptides [46,159–161].

5 Electrochemical Impedance Spectroscopy as a Tool for Investigation of Functions and Physical and Mechanical Properties of Cell Membranes

EIS is an important tool and an alternating current (AC) method to study a planar lipid bilayer and to obtain a characterization of the electric properties of these membranes. EIS explores surface electrodynamics. The important physical information about the properties of the interface can be obtained due to electrochemical impedance spectra (differential capacitance, solution resistance, etc.) (see Figure 5), but for the detailed information, it is necessary to use modelling. The so-called equivalent electrical circuit (EEC) is a very usual way to model electrochemical impedance spectra. EEC models are created to reproduce the parameters of the EEC elements and the electrochemical spectral features. In the next step, these parameters are compared to the physical properties of the surface systems and processes [162–165].

5.1 Electrical Equivalent Circuits

Characterization of model membranes formed on polycarbonate carriers was tested by several EECs. Circuit consisting of one resistor (R_s) in serial combination with parallel combination of a resistor (R_p) and a capacitor

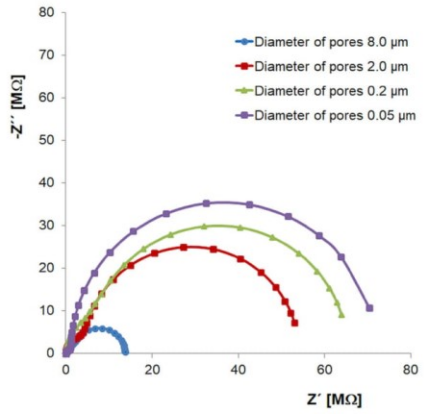

Fig. 5. Frequency characteristics (Nyquist plots) of membranes consisting of a mixture of lecithin and cholesterol (weight ratio 2:1) on polycarbonate carriers with different pores; frequency range 0.1 Hz–1 MHz; amplitude 0.005 V; inserted voltage −0.1 V (figure inspired by ref. [12]).

(C_p) is suitable for characterization of free polycarbonate membranes (Figure 6: A, B) [4,11] and of gel electrodes without covering by phospholipids [166].

Characterization of supported phospholipid bilayers formed in the pores of polycarbonate membranes, of metal electroplated surfaces, and of surfaces of polymer electrodes gave better results with two EECs (Figure 6: C, D) [4,167]. These two EECs differ from the simple circuit in Figure 6: A, B described above by the addition of a parallel combination of one capacitor and one resistor to the first capacitor (connected in series) [167].

The following EECs (Figure 6: E, F) have been used for the characterization of SLBs formed on the surface of polymer electrodes. These are composed of one resistor (R_s) in serial combination with two parallel combinations of resistors (R_{p1}, R_{p2}) and capacitors (C_{p1}, C_{p2}) [11]. According to ref. [166], the circuit Figure 6: F seems to be more suitable for the description of SLBs prepared on porous carriers.

The pairs of EECs in Figure 6: A and B, C and D, and E and F differ mutually by a capacitance (C_s) included serially to the first resistor. Each member (resistor, capacitor) of the circuits can be used for the characterization of the system. Serial resistors (R_s) correspond to the resistance of the electrolyte, connectors, etc. Similarly, the serial capacitances (C_s) (see Figure 6: B, D, F) represent the capacitances of these parts of the tested cells. However, importance of these capacitances for characterization of the formed SLBs proved to be negligible. Therefore, the EECs Figure 6B, D and F are not used [4,11,19].

Parallel capacitors of the circuits (denoted as C_p and C_{p1}) correspond to the parasitic capacitance of the supporting membrane; parallel resistors to its resistance (R_p and R_{p2}). The parallel combination of capacitors (denoted C_{p2}) and resistors (denoted R_{p2}) in the second pair of the circuits describe the electrical properties of the SLBs formed in the pores of the supporting membranes (including ionophores and transport of metal cations) [2,4,11,19,167,168].

Chemical stability, inertness, hydrophobicity/hydrophilicity, etc. belong to very important properties of sub-

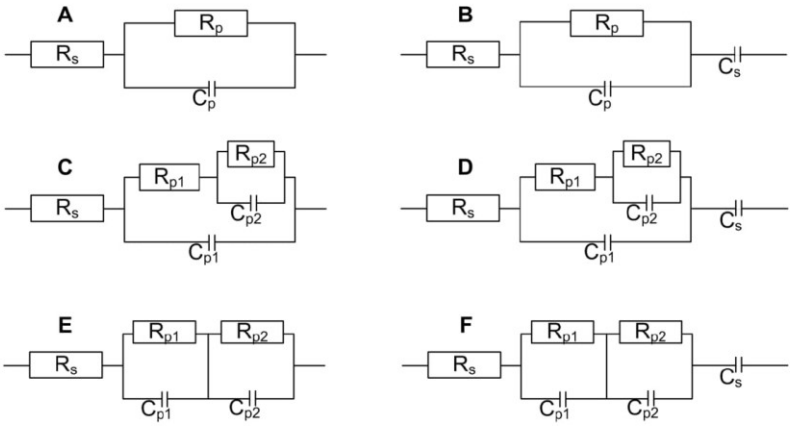

Fig. 6. Electrical equivalent circuits used for EIS characterization of SLBs formed on polymer surfaces (figure inspired by ref. [169]). (R_s = serial resistance, R_p = parallel resistance, C_s = serial capacitor, C_p = parallel capacitor).

strates (supports) [1]. However, there are some differences among used substrate types. For example, polyvinyl fluoride and polyacrylonitrile supports enable BLM formation of better quality (i.e., longer time stability, smaller diameters of pores. and better compatibility with formed BLMs) than polypropylene and polyethylene ones. For each experiment, there have to be optimized substrate parameters (pore diameters, pore shape, hydrophobicity / hydrophilicity) [1,37].

Used polycarbonate membrane can be characterized, e.g., by low affinity for stains providing higher optical contrast and making visibility under a microscope easy, by maximum transparentness, by negligible absorption and adsorption of filtrate, by nonhygroscopicity, by low tare weights, and by biological inertness [170,171].

5.2 Electrochemical Impedance Technique on SLBs

Solid SLBs in contrast to BLMs have the advantages of easy and reproducible preparation, long-term stability, and the possibility to use an electrically conductive support [172]. In this field, EIS is a very powerful method. It provides information about several relaxation regimes in one measurement, but data acquisition is rather slow and fitting procedures to quantify electrical parameters are often complicated. EIS has also been combined with current recordings at a constant voltage map of ion channel activity. Changes in impedance can be short-time resolved by measuring at one frequency during, e.g., bilayer formation, insertion of channel complexes [173], etc. The quality and properties of the membranes are evaluated by their capacitances which are connected with the bilayer thickness and the density of defects within the lipid membrane. Moreover, the kinetics of the bilayer formation and the stability of the lipid membrane are also studied by impedance analysis. Investigation of cell-penetrating peptides in SLBs by impedance spectroscopy is very important. This standard technique for characterization of the electrical properties of thin layers and interfaces is useful in investigation of SLBs interacting with peptides and protein molecules for the development of highly selective sensors based on ion transport through lipid membranes. Impedance spectroscopy enables to measure defect densities in the lipid membrane produced by such interactions with high sensitivity. Different regions of SLB system participate to different frequency domains of the impedance spectra. This method enables to differentiate among the changes occurring at the supporting semiconductor electrode and at the different interfaces lying between the support and the lipid membrane, and the changes in bulk membrane characteristics (such as conductivity and capacitance) [174,175]. Very important area of research on SLBs is impedance analysis of ion transport through channels from incorporated structures of synthetic or natural molecules in SLBs. In these studies, the selectivity between monovalent cations and its sequence of conductivity in lipid bilayers doped with gramicidin D (linear pentadecapeptide which produces a continuous channel through a lipid bilayer) can be investigated using EIS [163,164,176]. The conductance of the membranes demonstrates a linear dependence on the concentration of the cations in the bulk phase. This system can be studied for the development of biosensor devices based on ion transport through SLBs [163]. The design of biosensors based on SLBs on semiconductor devices and signal detection through current or capacitance measurement is an issue of interest [177]. For example, development of a biosensor for detection of cytochrome c with supported lipid films containing calixarenes by EIS was published by Mohsin et al in 2011 [86]. Other researches are interested in the partitioning of bioactive compounds in SLBs [178]. It was found that the positively charged drugs and peptides not only partition in the negatively charged membrane but also change its viscoelastic properties [179–182]. The advantages of EIS for kinetic and mechanism analysis involve the fact that it employs small signal analysis and that it is capable of probing relaxations over a wide frequency range using readily available instrumentation. A new approach to derive kinetic information relevant to mediated transport in SLBs was developed. Kinetic mechanism correctly describing ion transport assisted by ionophores of different nature (mobile carriers like valinomycin and channels like gramicidin) can thus be elucidated [176,183].

Another parameters, which have been frequently discussed in published papers, are mechanical properties of the lipids membranes, e.g., architecture of lipid tails their length, kinks, and asymmetry [184–186]. Wu et al. demonstrated in their study (realized by dissipative particle dynamics simulations) that a tail length of lipid is inversely proportional to diffusivity and mobility in SLBs and it is directly proportional to number of kinks. Diffusivity of lipids is increasing with temperature and asymmetry of tails, too [187]. Other parameters describing hydrophobic parts of lipid membranes are the elasticity modulus and the coefficient of dynamic viscosity. Monitoring these parameters can be used for observation of structural state and stability of lipid membranes [188,189].

5.3 Electrochemical Impedance Spectroscopy and t-BLMs

Various biological events can be monitored with electrochemical techniques on t-BLMs attached to a conducting surface. EIS is a suitable technique for characterization of solid supported membranes [190–192]. The t-BLMs can be presented as a relatively simple system consisting of a series of homogeneous conductor/dielectric layers. The geometry of t-BLMs is always asymmetric. The outer leaflet of the t-BLM is washed by an infinite reservoir of the solution, while the inner leaflet is in contact with the constrained volume of the electrolyte. Such heterogeneous and geometrically asymmetric systems should exhibit specific EIS features that reflect the nature and the extent of BLM heterogeneity. Different types of EECs were proposed for the experimental features of the electrochemical impedance spectra of the model membrane, but

the values of the EEC parameters are difficult to be connected with the physical properties of the system [193]. The fundamental parameter for a successful application of t-BLMs in a concept of biosensing is the incorporation of functional membrane proteins and the creation of pores (the ion-selective gramicidin channels [84,194], α-hemolysin [195,196], etc.). The pore can be used to detect polymers and proteins and can be modified as a receptor for divalent metal ions, organic compounds, etc. t-BLMs represent the stable biomimetic platform to host membrane proteins [192,197]. The effects of interactions between membrane and peptide can be detected by changes in the electrical properties of this system with the use of EIS. Bode plots (expressing impedance and phase angle as functions of the applied frequency) are very often used for presentation of EIS data [112,193].

5.4 Electrochemical Impedance Spectroscopy and Liposomes

Liposomes are applied and utilized in biomedical applications of Drug Delivery System (DDS) and the research is focused on drug encapsulation, targeting, and release control. The idea of releasing liposome contents as a bionsensor component is well known and fluorescent molecules or redox couples are often encapsulated by the liposomes [198–203]. An ELISA-inspired approach to biological detection consisting entirely of on-chip electrical impedance sensing and applied to HIV detection was reported [204]. At the core of this detection strategy is a micron-sized, antibody-functionalized liposome particle encapsulating concentrated phosphate buffered saline. These liposome tags can be quantified by impedance spectroscopy upon ion release in low conductivity media and are also shown to specifically bound surface-immobilized virus particles captured in a microfluidic channel.

It is known that the existence of free ions in the aqueous phase induces the conductivity of the solution. The electrical property of liposome suspension will be changed when the encapsulated ionic materials are released out of liposome population. By monitoring the impedance or conductivity changes of the solution, the release property of drugs might be evaluated [205]. EIS is based on the common conductive property of ionic substances and thus it has high potential to evaluate the release property of ionic-substances encapsulated in liposomes [206].

Novel means to quantify adsorption of liposomes with the use of EIS was described in [169]. This approach can be utilized to study the adsorption and adhesion of single giant liposomes when the electrode area is further reduced to the micrometer range. Moreover, the impedance approach provides a linear correlation between the surface coverage and the changes in the electrode capacitance recorded at AC frequency of 40 kHz [207]. The technique enables to distinguish between intact and disrupted liposomes with the prospect of forming surface-bound vesicle arrays on a micrometer scale well-suited to screen for membrane-active compounds. EIS measurements are also a powerful tool for investigation of the adsorption of giant vesicles on technical surfaces as well as for investigation of their thermal shape fluctuations.

6 Conclusions

This review deals with model systems of phospholipid biomembranes, which is a very important system in living cells. It summarizes the most frequently used model membranes and their connection with electrochemical phenomena, namely the application of electrochemical impedance spectroscopy as a useul tool for investigation and characterization of the properties of these membranes.

Highlights

1. Function and composition of different phospholipid membranes are reviewed with respect to possible electrochemical implications.
2. Characterization and formation of different model biological membranes are described including aspects relevant from electrochemical point of view.
3. Possibilities of application of electrochemical impedance spectroscopy for characterization of model phospholipid membranes are discussed.

Acknowledgments

Š.S. thanks the project Specific University Research (SVV 260440) and the project of the Czech Science Foundation (project GAČR No. 17-05387S). J.B., V.V., and T.N. thank the project of the Czech Science Foundation (project GAČR No. 17-03868S).

References

[1] K. Novakova, *Chem. Listy* **2015**, *109*, 166.
[2] T. Navratil, I. Sestakova, V. Marecek, K. Stulik, in *XXX Moderni Elektrochemicke Metody (Modern Electrochemical Methods XXX)* (Eds: J. Barek and T. Navratil), BEST Servis, Jetrichovice **2010**, pp. 119.
[3] J. Jaklova Dytrtova, M. Jakl, K. Novakova, T. Navratil, V. Sadek, *Monatsh. Chem.* **2015**, *146*, 831.
[4] T. Navratil, I. Sestakova, K. Stulik, V. Marecek, *Electroanalysis* **2010**, *22*, 2043.
[5] J. Jaklova Dytrtova, I. Sestakova, M. Jakl, T. Navratil, *Electroanalysis* **2009**, *21*, 573.
[6] J. Jaklova Dytrtova, M. Jakl, I. Sestakova, E. L. Zins, D. Schroder, T. Navratil, *Anal. Chim. Acta* **2011**, *693*, 100.
[7] J. Jaklova Dytrtova, M. Jakl, D. Schroder, T. Navratil, *Curr. Org. Chem.* **2011**, *15*, 2970.
[8] I. Sestakova, S. Skalova, T. Navratil, *J. Electroanal. Chem.* **2017**, doi:10.1016/j.jelechem.2017.11.052, In press.
[9] M. Casal, S. Paiva, O. Queiros, I. Soares-Silva, *FEMS Microbiol. Rev.* **2008**, *32*, 974.
[10] J. Jaklova Dytrtova, T. Navratil, V. Marecek, *Collect. Czech. Chem. Commun.* **2011**, *76*, 1917.

[11] T. Navratil, I. Sestakova, V. Marecek, *Int. J. Electrochem. Sci.* **2011**, *6*, 6032.
[12] K. Novakova, T. Navratil, I. Sestakova, V. Marecek, J. Chylkova, *Chem. Listy* **2014**, *108*, 219.
[13] M. Naumowicz, A. D. Petelska, *J. Electroanal. Chem.* **2016**, *782*, 233.
[14] I. Sestakova, K. Novakova, B. Josypcuk, T. Navratil, in *XXXIV Moderni Elektrochemicke Metody* (Modern Electrochemial Methods XXXIV) (Eds: T. Navratil and J. Barek), Best Servis, Jetrichovice **2014**, pp. 190.
[15] T. Navratil, K. Novakova, B. Josypcuk, R. Sokolova, I. Sestakova, *Monatsh. Chem.* **2016**, *147*, 165.
[16] M. Naumowicz, Z. Figaszewski, *Bioelectrochemistry* **2003**, *61*, 21.
[17] M. Naumowicz, Z. A. Figaszewski, *Biophys. J.* **2005**, *89*, 3174.
[18] J. Navarro-Laboulais, J. Trijueque, J. J. Garcia-Jareno, D. Benito, F. Vicente, *J. Electroanal. Chem.* **1998**, *444*, 173.
[19] M. Parisova, T. Navratil, I. Sestakova, J. Jaklova Dytrtova, V. Marecek, *Int. J. Electrochem. Sci.* **2013**, *8*, 27.
[20] M. Traube, *Arch. Anat. Physiol. Wiss. Med.* **1867**, *87*, 129.
[21] G. Quincke, *Über die Physikalischen Eigenschaften Dünner, Fester Lamellen*, Akademie der Wissenschaften, Berlin **1888**.
[22] O. Hertwig, M. Campbell, H. J. Campbell, *The Cell: Outlines of General Anatomy and Physiology*, Macmillan and Co., New York **1895**.
[23] A. Kleinzeller, *News Physiol. Sci.* **1997**, *12*, 49.
[24] C. E. Overton, *Studien der Narkose (Studies of Narcosis)*, Gustav Fischer, Jena, Germany **1901**.
[25] C. S. Helrich, *Aims Biophysics* **2017**, *4*, 415.
[26] E. Gorter, F. Grendel, *J. Exp. Med.* **1925**, *41*, 439.
[27] J. F. Danielli, H. Davson, *J. Cell. Comp. Physiol.* **1935**, *5*, 495.
[28] J. D. Robertson, *Prog. Biophys. Mol. Biol.* **1960**, *10*, 343.
[29] A. A. Benson, *Annu. Rev. Plant Physiol. Plant Mol. Biol.* **1964**, *15*, 1.
[30] D. E. Green, Tzagolof. A, *J. Lipid Res.* **1966**, *7*, 587.
[31] P. Mueller, D. O. Rudin, H. T. Tien, W. C. Wescott, *Nature* **1962**, *194*, 979.
[32] P. Mueller, D. O. Rudin, H. T. Tien, W. C. Wescott, *J. Phys. Chem.* **1963**, *67*, 534.
[33] H. T. Tien, S. Carbone, E. A. Dawidowi, *Nature* **1966**, *212*, 718.
[34] H. T. Tien, A. L. Diana, *Nature* **1967**, *215*, 1199.
[35] S. J. Singer, G. L. Nicolson, *Science* **1972**, *175*, 720.
[36] R. K. Murray, D. Bender, K. M. Botham, P. J. Kennelly, V. W. Rodwell, P. A. Weil, *Harper's Illustrated Biochemistry*, McGraw-Hill Lange, Columbus **2012**.
[37] Z. Aminipour, M. Khorshid, M. Bayoumi, P. Losada-Perez, R. Thoelen, S. Bonakdar, H. Keshvari, G. Maglia, P. Wagner, B. Van der Bruggen, *Phys. Status Solidi A* **2017**, *214*, 1700104.
[38] A. J. Heron, J. R. Thompson, A. E. Mason, M. I. Wallace, *J. Am. Chem. Soc.* **2007**, *129*, 16042.
[39] H. Bayley, O. Braha, L. Q. Gu, *Adv. Mater.* **2000**, *12*, 139.
[40] H. Bayley, P. S. Cremer, *Nature* **2001**, *413*, 226.
[41] J. J. Kasianowicz, E. Brandin, D. Branton, D. W. Deamer, *Proc. Natl. Acad. Sci. USA* **1996**, *93*, 13770.
[42] S. Howorka, S. Cheley, H. Bayley, *Nat. Biotechnol.* **2001**, *19*, 636.
[43] Y. Astier, O. Braha, H. Bayley, *J. Am. Chem. Soc.* **2006**, *128*, 1705.
[44] M. Montal, P. Mueller, *Proc. Natl. Acad. Sci. USA* **1972**, *69*, 3561.
[45] I. Prudovsky, T. K. S. Kumar, S. Sterling, D. Neivandt, *Int. J. Mol. Med. Sci.* **2013**, *14*, 3734.
[46] P. Kramar, D. Miklavcic, M. Kotulska, A. M. Lebar, in *Advances in Planar Lipid Bilayers Liposomes, Vol. 11*, (Ed: A. Iglic), Academic Press, Oxford **2010**, pp. 29.
[47] K. A. Melzak, S. A. Melzak, E. Gizeli, J. L. Toca-Herrera, *Materials* **2012**, *5*, 2306.
[48] D. Bach, E. Wachtel, *BBA-Biomembranes* **2003**, *1610*, 187.
[49] T. Rog, M. Pasenkiewicz-Gierula, I. Vattulainen, M. Karttunen, *BBA-Biomembranes* **2009**, *1788*, 97.
[50] P. L. Yeagle, *Biochim. Biophys. Acta* **1985**, *822*, 267.
[51] P. L. Yeagle, *Biochimie* **1991**, *73*, 1303.
[52] T. P. W. McMullen, R. N. McElhaney, *Curr. Opin. Colloid Interface Sci.* **1996**, *1*, 83.
[53] O. Edholm, A. M. Nyberg, *Biophys. J.* **1992**, *63*, 1081.
[54] S. W. Chiu, E. Jakobsson, R. J. Mashl, H. L. Scott, *Biophys. J.* **2002**, *83*, 1842.
[55] E. Falck, M. Patra, M. Karttunen, M. T. Hyvonen, I. Vattulainen, *J. Chem. Phys.* **2004**, *121*, 12676.
[56] W. K. Subczynski, J. S. Hyde, A. Kusumi, *Proc. Natl. Acad. Sci. USA* **1989**, *86*, 4474.
[57] W. K. Subczynski, A. Wisniewska, J. J. Yin, J. S. Hyde, A. Kusumi, *Biochemistry* **1994**, *33*, 7670.
[58] L. J. Pike, *J. Lipid Res.* **2003**, *44*, 655.
[59] H. J. Risselada, S. J. Marrink, *Proc. Natl. Acad. Sci. USA* **2008**, *105*, 17367.
[60] C. L. Wennberg, D. van der Spoel, J. S. Hub, *J. Am. Chem. Soc.* **2012**, *134*, 5351.
[61] J. M. Boggs, J. C. Hsia, *Biochim. Biophys. Acta* **1972**, *290*, 32.
[62] M. C. Blok, L. L. M. Vandeenen, J. Degier, *Biochim. Biophys. Acta* **1977**, *464*, 509.
[63] T. J. Mcintosh, *Biochim. Biophys. Acta* **1978**, *513*, 43.
[64] A. A. Brian, H. M. Mcconnell, *Proc. Natl. Acad. Sci. USA* **1984**, *81*, 6159.
[65] L. K. Tamm, H. M. Mcconnell, *Biophys. J.* **1985**, *47*, 105.
[66] V. Kiessling, M. K. Domanska, D. Murray, C. Wan, L. K. Tamm, in *Wiley Encyclopedia of Chemical Biology, Vol. 4*, (Ed: T. P. Begley), Wiley-InterScience, Hoboken, **2009**, pp. 411.
[67] E. T. Castellana, P. S. Cremer, *Surf. Sci. Rep.* **2006**, *61*, 429.
[68] S. J. Johnson, T. M. Bayerl, D. C. Mcdermott, G. W. Adam, A. R. Rennie, R. K. Thomas, E. Sackmann, *Biophys. J.* **1991**, *59*, 289.
[69] E. B. Watkins, C. E. Miller, D. J. Mulder, T. L. Kuhl, J. Majewski, *Phys. Rev. Lett.* **2009**, *102*, 238101.
[70] J. M. Crane, V. Kiessling, L. K. Tamm, *Langmuir* **2005**, *21*, 1377.
[71] J. Kim, G. Kim, P. S. Cremer, *Langmuir* **2001**, *17*, 7255.
[72] R. P. Richter, A. R. Brisson, *Biophys. J.* **2005**, *88*, 3422.
[73] H. Schonherr, J. M. Johnson, P. Lenz, C. W. Frank, S. G. Boxer, *Langmuir* **2004**, *20*, 11600.
[74] E. Reimhult, M. Zach, F. Hook, B. Kasemo, *Langmuir* **2006**, *22*, 3313.
[75] S. Nirasay, A. Badia, G. Leclair, J. P. Claverie, I. Marcotte, *Materials* **2012**, *5*, 2621.
[76] E. Sackmann, *Science* **1996**, *271*, 43.
[77] B. Kasemo, *Surf. Sci.* **2002**, *500*, 656.
[78] M. Tanaka, E. Sackmann, *Nature* **2005**, *437*, 656.
[79] E. K. Sinner, W. Knoll, *Curr. Opin. Chem. Biol.* **2001**, *5*, 705.
[80] I. Koper, *Mol. BioSyst.* **2007**, *3*, 651.
[81] R. Glazier, K. Salaita, *BBA-Biomembranes* **2017**, *1859*, 1465.
[82] Z. Zhang, M. Sohgawa, K. Yamashita, M. Noda, *Electroanalysis* **2016**, *28*, 620.

[83] H. Baghirov, S. Melikishvili, Y. Morch, E. Sulheim, A. K. O. Aslund, T. Hianik, C. D. Davies, *Colloids Surf. B* **2017**, *150*, 373.
[84] B. A. Cornell, V. L. B. Braach-Maksvytis, L. G. King, P. D. J. Osman, B. Raguse, L. Wieczorek, R. J. Pace, *Nature* **1997**, *387*, 580.
[85] O. Worsfold, N. H. Voelcker, T. Nishiya, *Langmuir* **2006**, *22*, 7078.
[86] M. A. Mohsin, F. G. Banica, T. Oshima, T. Hianik, *Electroanalysis* **2011**, *23*, 1229.
[87] G.-P. Nikoleli, D. P. Nikolelis, G. Evtugyn, T. Hianik, *TrAC Trends Anal. Chem.* **2016**, *79*, 210.
[88] J. W. Liu, A. Stace-Naughton, X. M. Jiang, C. J. Brinker, *J. Am. Chem. Soc.* **2009**, *131*, 1354.
[89] V. Cauda, H. Engelke, A. Sauer, D. Arcizet, C. Brauchle, J. Radler, T. Bein, *Nano Lett.* **2010**, *10*, 2484.
[90] M. Ionov, K. Ciepluch, Z. Garaiova, S. Melikishvili, S. Michlewska, L. Balcerzak, S. Glinska, K. Milowska, R. Gomez-Ramirez, F. J. de la Mata, D. Shcharbin, I. Waczulikova, M. Bryszewska, T. Hianik, *BBA-Biomembranes* **2015**, *1848*, 907.
[91] D. Afanasenkau, A. Offenhausser, *Langmuir* **2012**, *28*, 13387.
[92] C. W. Hollars, R. C. Dunn, *Biophys. J.* **1998**, *75*, 342.
[93] K. Morigaki, T. Baumgart, U. Jonas, A. Offenhausser, W. Knoll, *Langmuir* **2002**, *18*, 4082.
[94] J. Radler, H. Strey, E. Sackmann, *Langmuir* **1995**, *11*, 4539.
[95] K. Furukawa, H. Nakashima, Y. Kashimura, K. Torimitsu, *Lab Chip* **2006**, *6*, 1001.
[96] K. Furukawa, T. Aiba, *Langmuir* **2011**, *27*, 7341.
[97] K. Furukawa, H. Hibino, *Chem. Lett.* **2012**, *41*, 1259.
[98] D. Axelrod, *Traffic* **2001**, *2*, 764.
[99] T. Fukuma, M. J. Higgins, S. P. Jarvis, *Biophys. J.* **2007**, *92*, 3603.
[100] R. Tero, *Materials* **2012**, *5*, 2658.
[101] J. Yang, J. Appleyard, *J. Phys. Chem. B* **2000**, *104*, 8097.
[102] A. Charrier, F. Thibaudau, *Biophys. J.* **2005**, *89*, 1094.
[103] Z. V. Feng, T. A. Spurlin, A. A. Gewirth, *Biophys. J.* **2005**, *88*, 2154.
[104] S. Stanglmaier, S. Hertrich, K. Fritz, J. F. Moulin, M. Haese-Seiller, J. O. Radler, B. Nickel, *Langmuir* **2012**, *28*, 10818.
[105] A. P. Shreve, M. C. Howland, A. R. Sapuri-Butti, T. W. Allen, A. N. Parikh, *Langmuir* **2008**, *24*, 13250.
[106] F. F. Rossetti, M. Textor, I. Reviakine, *Langmuir* **2006**, *22*, 3467.
[107] J. T. Groves, N. Ulman, S. G. Boxer, *Science* **1997**, *275*, 651.
[108] M. C. Howland, A. R. Sapuri-Butti, S. S. Dixit, A. M. Dattelbaum, A. P. Shreve, A. N. Parikh, *J. Am. Chem. Soc.* **2005**, *127*, 6752.
[109] T. Okazaki, T. Inaba, Y. Tatsu, R. Tero, T. Urisu, K. Morigaki, *Langmuir* **2009**, *25*, 345.
[110] J. P. Overington, B. Al-Lazikani, A. L. Hopkins, *Nat. Rev. Drug Discov.* **2006**, *5*, 993.
[111] J. Y. Wong, C. K. Park, M. Seitz, J. Israelachvili, *Biophys. J.* **1999**, *77*, 1458.
[112] J. A. Jackman, W. Knoll, N. J. Cho, *Materials* **2012**, *5*, 2637.
[113] R. Naumann, S. M. Schiller, F. Giess, B. Grohe, K. B. Hartman, I. Karcher, I. Koper, J. Lubben, K. Vasilev, W. Knoll, *Langmuir* **2003**, *19*, 5435.
[114] B. Raguse, V. Braach-Maksvytis, B. A. Cornell, L. G. King, P. D. J. Osman, R. J. Pace, L. Wieczorek, *Langmuir* **1998**, *14*, 648.
[115] S. M. Schiller, R. Naumann, K. Lovejoy, H. Kunz, W. Knoll, *Angew. Chem. Int. Ed.* **2003**, *42*, 208.
[116] S. Terrettaz, M. Mayer, H. Vogel, *Langmuir* **2003**, *19*, 5567.
[117] M. Chadli, S. Rebaud, O. Maniti, B. Tillier, S. Cortes, A. Girard-Egrot, *Langmuir* **2017**, *33*, 10385.
[118] T. Ragaliauskas, M. Mickevicius, B. Rakovska, T. Penkauskas, D. J. Vanderah, F. Heinrich, G. Valincius, *BBA-Biomembranes* **2017**, *1859*, 669.
[119] H. Lang, C. Duschl, H. Vogel, *Langmuir* **1994**, *10*, 197.
[120] V. Vontscharner, H. M. McConnell, *Biophys. J.* **1981**, *36*, 421.
[121] A. L. Plant, *Langmuir* **1993**, *9*, 2764.
[122] R. Guidelli, L. Becucci, A. Dolfi, M. R. Moncelli, F. T. Buoninsegni, *Solid State Ionics* **2002**, *150*, 13.
[123] J. C. Love, L. A. Estroff, J. K. Kriebel, R. G. Nuzzo, G. M. Whitesides, *Chem. Rev.* **2005**, *105*, 1103.
[124] A. Demoz, D. J. Harrison, *Langmuir* **1993**, *9*, 1046.
[125] V. I. Silin, H. Wieder, J. T. Woodward, G. Valincius, A. Offenhausser, A. L. Plant, *J. Am. Chem. Soc.* **2002**, *124*, 14676.
[126] J. T. Buboltz, G. W. Feigenson, *BBA-Biomembranes* **1999**, *1417*, 232.
[127] C. A. Naumann, O. Prucker, T. Lehmann, J. Ruhe, W. Knoll, C. W. Frank, *Biomacromolecules* **2002**, *3*, 27.
[128] R. Kugler, W. Knoll, *Bioelectrochemistry* **2002**, *56*, 175.
[129] R. Naumann, E. K. Schmidt, A. Jonczyk, K. Fendler, B. Kadenbach, T. Liebermann, A. Offenhausser, W. Knoll, *Biosens. Bioelectron.* **1999**, *14*, 651.
[130] E. K. Schmidt, T. Liebermann, M. Kreiter, A. Jonczyk, R. Naumann, A. Offenhausser, E. Neumann, A. Kukol, A. Maelicke, W. Knoll, *Biosens. Bioelectron.* **1998**, *13*, 585.
[131] R. Naumann, T. Baumgart, P. Graber, A. Jonczyk, A. Offenhausser, W. Knoll, *Biosens. Bioelectron.* **2002**, *17*, 25.
[132] V. Atanasov, P. P. Atanasova, I. K. Vockenroth, N. Knorr, I. Koper, *Bioconjugate Chem.* **2006**, *17*, 631.
[133] I. Koeper, N. Knorr, V. Atanasov, J. R. Long, P. A. V. Anderson, R. Duran, W. Knoll, *Abstr. Pap. Am. Chem. Soc.* **2005**, *229*, U657.
[134] R. F. Roskamp, I. K. Vockenroth, N. Eisenmenger, J. Braunagel, I. Koper, *ChemPhysChem* **2008**, *9*, 1920.
[135] B. A. Cornell, G. Krishna, P. D. Osman, R. D. Pace, L. Wieczorek, *Biochem. Soc. Trans.* **2001**, *29*, 613.
[136] G. Krishna, J. Schulte, B. A. Cornell, R. Pace, L. Wieczorek, P. D. Osman, *Langmuir* **2001**, *17*, 4858.
[137] C. Soto, A. Del Valle, P. A. Valiente, U. Ros, M. E. Lanio, A. M. Hernandez, C. Alvarez, *Biochimie* **2017**, *138*, 20.
[138] L. Redondo-Morata, R. Lea Sanford, O. S. Andersen, S. Scheuring, *Biophys. J.* **2016**, *111*, 363.
[139] I. K. Vockenroth, C. Rossi, M. R. Shah, I. Koper, *Biointerphases* **2009**, *4*, 19.
[140] H. T. Tien, A. Ottova-Leitmannova, *Advances in Planar Lipid Bilayers Liposomes, Vol. 11*, (Ed: A. Iglic), Academic Press, Oxford **2010**, pp. 29.
[141] C. G. Siontorou, G. P. Nikoleli, D. P. Nikolelis, S. K. Karapetis, *Membranes* **2017**, *7*, 38.
[142] H. A. H. Rongen, A. Bult, W. P. van Bennekom, *J. Immunol. Methods* **1997**, *204*, 105.
[143] K. A. Edwards, A. J. Baeumner, *Talanta* **2006**, *68*, 1432.
[144] R. Bittman, L. Blau, *Biochemistry* **1972**, *11*, 4831.
[145] R. A. Demel, S. C. Kinsky, C. B. Kinsky, L. L. van Deene, *Biochim. Biophys. Acta* **1968**, *150*, 655.
[146] C. M. Bailey, A. Tripathi, A. Shukla, *Langmuir* **2017**, *33*, 11986.
[147] Z. Y. Zhang, Y. Murakami, T. Taniguchi, M. Sohgawa, K. Yamashita, M. Noda, *Electroanalysis* **2017**, *29*, 722.
[148] L. Zhang, F. X. Gu, J. M. Chan, A. Z. Wang, R. S. Langer, O. C. Farokhzad, *Clin. Pharmacol. Ther.* **2008**, *83*, 761.
[149] D. Peer, J. M. Karp, S. Hong, O. C. Farokhzad, R. Margalit, R. Langer, *Nat. Nanotechnol.* **2007**, *2*, 751.

[150] Gregoria. G, B. E. Ryman, *Biochem. J.* **1971**, *124*, P58.
[151] M. L. Immordino, F. Dosio, L. Cattel, *Int. J. Nanomed.* **2006**, *1*, 297.
[152] H. Barani, M. Montazer, *J. Liposome Res.* **2008**, *18*, 249.
[153] L. A. Meure, R. Knott, N. R. Foster, F. Dehghani, *Langmuir* **2009**, *25*, 326.
[154] K. Novakova, T. Navratil, I. Sestakova, M. P. Le, H. Vodickova, B. Zamecnikova, R. Sokolova, J. Bulickova, M. Gal, *Monatsh. Chem.* **2015**, *146*, 819.
[155] M. Kanduser, M. Sentjurc, D. Miklavcic, *Eur. Biophys. J.* **2006**, *35*, 196.
[156] G. C. Troiano, L. Tung, V. Sharma, K. J. Stebe, *Biophys. J.* **1998**, *75*, 880.
[157] J. Kolek, K. Sedlar, I. Provaznik, P. Patakova, *Biotechnol. Biofuels* **2016**, *9*, 14.
[158] T. Kotnik, D. Miklavcic, *Biophys. J.* **2006**, *90*, 480.
[159] Y. Hanyu, T. Yamada, G. Matsumoto, *Biochemistry* **1998**, *37*, 15376.
[160] H. Yamaguchi, H. Nakanishi, *BBA-Biomembranes* **1993**, *1148*, 179.
[161] T. F. Eibert, M. Alaydrus, F. Wilczewski, V. W. Hansen, *IEEE Trans. Biomed. Eng.* **1999**, *46*, 1013.
[162] J. R. Macdonald, W. B. Johnson, *Impedance Spectroscopy: Theory, Experiment, and Applications, 2nd Editionk* (Eds. E. Barsukov and J. R. Macdonald), Wiley-InterScience, Hoboken, **2006**, pp. 1.
[163] C. Steinem, A. Janshoff, H. J. Galla, M. Sieber, *Bioelectrochem. Bioenerg.* **1997**, *42*, 213.
[164] A. E. Vallejo, C. A. Gervasi, *Bioelectrochemistry* **2002**, *57*, 1.
[165] L. J. C. Jeuken, S. A. Weiss, P. J. F. Henderson, S. D. Evans, R. J. Bushby, *Anal. Chem.* **2008**, *80*, 9084.
[166] G. Laputkova, M. Legin, J. Sabo, *Chem. Listy* **2010**, *104*, 353.
[167] T. Navratil, I. Sestakova, J. Jaklova Dytrtova, M. Jakl, V. Marecek, *WSEAS Trans. Environ. Dev.* **2010**, *6*, 208.
[168] T. Navratil, I. Sestakova, V. Marecek, in *XXXI Moderni Elektrochemicke Metody (Modern Electrochemical Methods XXXI)* (Eds: T. Navratil and J. Barek), BEST Servis, Jetrichovice **2011**, pp. 91.
[169] T. Navratil, I. Sestakova, V. Marecek, *Int. J. Energy Environ.* **2011**, *5*, 337.
[170] K. Novakova, T. Navratil, I. Sestakova, J. Langmaier, M. Heyrovsky, B. Zamecnikova, H. Vodickova, in *XXXIV Moderni Elektrochemicke Metody (Modern Electrochemical Methods XXXIV)* (Eds: T. Navratil, M. Fojta, and K. Peckova), Best Servis, Jetrichovice **2014**, pp. 114.
[171] K. Novakova, T. Navratil, I. Sestakova, V. Marecek, J. Chylkova, in *XXXIII Moderni Elektrochemicke Metody (Modern Electrochemical Methods XXXIII)* (Eds: T. Navratil, M. Fojta, and K. Peckova), Best Servis, Jetrichovice **2013**, pp. 128.
[172] C. Steinem, A. Janshoff, W. P. Ulrich, M. Sieber, H. J. Galla, *BBA-Biomembranes* **1996**, *1279*, 169.
[173] A. Lundgren, J. Hedlund, O. Andersson, M. Branden, A. Kunze, H. Elwing, F. Hook, *Anal. Chem.* **2011**, *83*, 7800.
[174] Z. Salamon, G. Lindblom, G. Tollin, *Biophys. J.* **2003**, *84*, 1796.
[175] P. Diao, D. L. Jiang, X. L. Cui, D. P. Gu, R. T. Tong, B. Zhong, *Bioelectrochem. Bioenerg.* **1999**, *48*, 469.
[176] P. E. Alvarez, C. A. Gervasi, A. E. Vallejo, *J. Biol. Phys.* **2007**, *33*, 421.
[177] S. Gritsch, P. Nollert, F. Jahnig, E. Sackmann, *Langmuir* **1998**, *14*, 3118.
[178] T. N. Tun, P. J. Cameron, A. T. A. Jenkins, *Biosens. Bioelectron.* **2011**, *28*, 227.
[179] K. Kannisto, L. Murtomaki, T. Viitala, *Colloids Surf. B* **2011**, *86*, 298.
[180] S. Jaksch, O. Holderer, M. Gvaramia, M. Ohl, M. Monkenbusch, H. Frielinghaus, *Sci. Rep.* **2017**, *7*, 4417.
[181] C. Satriano, G. Lupo, C. Motta, C. D. Anfuso, P. Di Pietro, B. Kasemo, *Colloids Surf. B* **2017**, *149*, 48.
[182] G. B. Soriano, R. da Silva Oliveira, F. F. Camilo, L. Caseli, *J. Colloid Interface Sci.* **2017**, *496*, 111.
[183] F. Berthier, J. P. Diard, L. Pronzato, E. Walter, *Automatica* **1996**, *32*, 973.
[184] D. M. Miller, H. E. Findlay, O. Ces, R. H. Templer, P. J. Booth, *Nanotechnology* **2016**, *27*, 494004.
[185] M. Przybylo, D. Drabik, K. Szostak, T. Borowik, B. Klosgen, J. Dobrucki, A. F. Sikorski, M. Langner, *Biochim. Biophys Acta* **2017**, *1859*, 1301.
[186] M. M. Nerurkar, N. F. H. Ho, P. S. Burton, T. J. Vidmar, R. T. Borchardt, *J. Pharm. Sci.* **1997**, *86*, 813.
[187] H. L. Wu, H. K. Tsao, Y. J. Sheng, *J. Chem. Phys.* **2016**, *144*, 154904.
[188] T. Hianik, *J. Biotechnol.* **2000**, *74*, 189.
[189] T. Hianik, in *Bioelectrochemistry. Fundamentals, Experimental Techniques and Applications* (Ed: P. E. Bartlett), Wiley, Chichester, **2008**, pp. 87.
[190] A. Janshoff, C. Steinem, *Anal. Bioanal. Chem.* **2006**, *385*, 433.
[191] S. Terrettaz, H. Vogel, *MRS Bull.* **2005**, *30*, 207.
[192] I. K. Vockenroth, D. Fine, A. Dodobalapur, A. T. A. Jenkins, I. Koper, *Electrochem. Commun.* **2008**, *10*, 323.
[193] G. Valincius, T. Meskauskas, F. Ivanauskas, *Langmuir* **2012**, *28*, 977.
[194] K. Lum, H. I. Ingolfsson, R. E. Koeppe, 2nd, O. S. Andersen, *Biophys. J.* **2017**, *113*, 1757.
[195] L. Q. Gu, S. Cheley, H. Bayley, *J. Gen. Physiol.* **2001**, *118*, 481.
[196] S. Cheley, M. S. Malghani, L. Z. Song, M. Hobaugh, J. E. Gouaux, J. Yang, H. Bayley, *Protein Eng.* **1997**, *10*, 1433.
[197] I. Sestakova, T. Navratil, B. Josypcuk, *Electroanalysis* **2016**, *28*, 2754.
[198] J. T. Connelly, S. Kondapalli, M. Skoupi, J. S. L. Parker, B. J. Kirby, A. J. Baeumner, *Anal. Bioanal. Chem.* **2012**, *402*, 315.
[199] K. A. Edwards, O. R. Bolduc, A. J. Baeumner, *Curr. Opin. Chem. Biol.* **2012**, *16*, 444.
[200] S. R. Nugen, P. J. Asiello, J. T. Connelly, A. J. Baeumner, *Biosens. Bioelectron.* **2009**, *24*, 2428.
[201] M. C. Sandstrom, L. M. Ickenstein, L. D. Mayer, K. Edwards, *J. Control. Release* **2005**, *107*, 131.
[202] D. Volodkin, H. Mohwald, J. C. Voegel, V. Ball, *J. Controlled Release* **2007**, *117*, 111.
[203] X. M. Liu, B. Yang, Y. L. Wang, J. Y. Wang, *BBA-Biomembranes* **2005**, *1720*, 28.
[204] G. L. Damhorst, C. E. Smith, E. M. Salm, M. M. Sobieraj, H. K. Ni, H. Kong, R. Bashir, *Biomed. Microdevices* **2013**, *15*, 895.
[205] F. Bordi, C. Cametti, S. Sennato, D. Viscomi, *J. Colloid Interface Sci.* **2006**, *304*, 512.
[206] G. M. Chen, Z. W. Jiang, M. Yoshimoto, Y. L. Wei, *Colloids Surf. B* **2009**, *74*, 32.
[207] J. Wegener, C. R. Keese, I. Giaever, *Exp. Cell Res.* **2000**, *259*, 158.

Received: October 18, 2017
Accepted: November 28, 2017
Published online on December 21, 2017

10. Appendix IV

Miniaturized Voltammetric Cell for Cathodic Voltammetry Making Use of an Agar Membrane

Skalová Štěpánka, Gonçalves Luís Moreira, Navrátil Tomáš, Barek Jiří, Rodrigues José António, Vyskočil Vlastimil

Journal of Electroanalytical Chemistry

Volume 821, Pages 47-52, Year 2018

Journal of Electroanalytical Chemistry 821 (2018) 47–52

Contents lists available at ScienceDirect

Journal of Electroanalytical Chemistry

journal homepage: www.elsevier.com/locate/jelechem

Miniaturized voltammetric cell for cathodic voltammetry making use of an agar membrane

Štěpánka Skalová[a,b], Luís Moreira Gonçalves[c,d], Tomáš Navrátil[b,*], Jiří Barek[a], José António Rodrigues[c], Vlastimil Vyskočil[a]

[a] Charles University, Faculty of Science, Department of Analytical Chemistry, UNESCO Laboratory of Environmental Electrochemistry, Albertov 6, 128 43 Prague 2, Czech Republic
[b] J. Heyrovský Institute of Physical Chemistry of the Czech Academy of Sciences, Dolejškova 3, 182 23 Prague 8, Czech Republic
[c] REQUIMTE/LAQV, Departamento de Química e Bioquímica, Faculdade de Ciências, Universidade do Porto, Rua do Campo Alegre, s/n, 4169-007 Porto, Portugal
[d] Departamento de Química Fundamental, Instituto de Química, Universidade de São Paulo (USP), Av. Prof. Lineu Prestes 748, 05508-000 São Paulo, SP, Brazil

ARTICLE INFO

Keywords:
Voltammetry
Solid amalgam electrode
Urine analysis
Water analysis
Anticancer drugs

ABSTRACT

Analysis of samples available in small volumes is an important challenge in analytical chemistry. Therefore, we have dealt with the development of a new miniaturized micro-volume voltammetric cell (MVVC) for the determination of reducible organic compounds in micro-volumes (20–50 μL). The MVVC is composed of two compartments, a micro-volume compartment, where the analyte is present along with the working electrode, separated by means of an agar membrane (about 2 mm) from a large-volume compartment containing the supporting electrolyte and the counter and reference electrodes. This MVVC was tested by the determination of sodium anthraquione-2-sulfonate as a model substance for structurally similar anthraquinone-based anti-cancer drugs. Using differential pulse voltammetry at a polished silver solid amalgam electrode, the following analytical parameters were obtained: linear dynamic range from 1 μmol L^{-1} to 1 mmol L^{-1}, repeatability of 0.7% (on the concentration level 0.1 mmol L^{-1}), and limit of detection of 0.15 μmol L^{-1}.

1. Introduction

Pharmacotherapy has unquestionable importance in our society; for many patients it represents the last chance to treat a life-threatening illness. To optimize the applied individual dosage of drugs, it may be necessary to monitor their therapeutic levels in different human fluids (blood, saliva, urine, etc.). This procedure improves safety and efficiency of the applied remedies; individualized pharmacotherapy is acquiring huge relevance in medicine [1]. However, therapeutic drug monitoring can be quite complicated, since it may be rather specific for each particular drug or group of drugs [2–6]. Therapeutic drug monitoring has particular relevance when side-effects are common, like in chemotherapy [7]. Anthraquinones are among frequently used antitumor drugs [8]. They have four mechanisms of action [9–15]: a) inhibition of DNA and RNA synthesis by intercalating between base pairs of the DNA/RNA strand; b) inhibition of topoisomerase II enzyme, preventing the relaxing of supercoiled DNA and thus blocking DNA transcription and replication; c) generation of free radicals of oxygen, which can damage DNA chains; d) induction of histone eviction from chromatin that deregulates DNA damage response, epigenome and transcriptome. The basic molecular structure, which is characteristic for all anthracycline derivatives, is the anthraquinone skeleton. The quinone–hydroquinone redox system is the electrochemically active part of anthraquinones. This system is important part of living systems as an electron–proton carrier in the respiratory chain [16].

Various analytical techniques for the determination of anthracycline derivatives can be found in literature, e.g., HPLC with fluorescence detection [17,18], capillary electrophoresis (CE) coupled with in-column double optical-fiber light-emitting diode (LED) induced fluorescence detection [19,20], and fluorescence techniques [21,22]. Electroanalytical techniques seem to be suitable for analysis and monitoring of various drugs due to their simplicity, high sensitivity, swiftness, portability, low acquisition and operating costs, versatility and easy adaptation to several sample preparation techniques [23–25]. A few voltammetric methods for the determination of anthraquinone-based compounds, making use of different types of working electrodes, can be found in literature, examples include glassy carbon electrode [26], meniscus modified silver solid amalgam electrode [27], hanging mercury drop electrode [28], and carbon paste electrode [29]. The determination of drugs in practical clinical analysis is complicated by the

* Corresponding author.
E-mail address: navratil@jh-inst.cas.cz (T. Navrátil).

https://doi.org/10.1016/j.jelechem.2017.12.073
Received 29 November 2017; Received in revised form 21 December 2017; Accepted 29 December 2017
Available online 03 January 2018
1572-6657/

availability of only small volumes (microliters) of body fluids to be analyzed. Therefore, miniaturized electrochemical systems for measurements in micro-volumes may be required for the analysis of biological samples [30,31]. Therefore, this paper is focused on the development of a miniaturized micro-volume voltammetric cell (MVVC) compatible with the use of a silver solid amalgam electrode (AgSAE) introduced to maintain the advantages of mercury electrodes without their toxicity [32,33]. They can frequently substitute liquid mercury electrodes due to a broad potential window, mechanical stability, easy manipulation, and high hydrogen overvoltage [34–39], and they have been proven as suitable working electrodes for drug determination [40–45]. Sodium anthraquinone-2-sulfonate (AQ), from which a number of antineoplastic drugs are derived, was used as the model substance [46].

2. Material and methods

2.1. Reagents and samples

All reagents (except agar) were dissolved in ultra-pure water (conductivity < 0.05 μS cm^{-1}) from a Millipore Direct-Q 3 UV water purification system (Merck, Czech Republic). A stock solution of 0.01 mol L^{-1} AQ was prepared by dissolving appropriate amount of AQ (Merck, Czech Republic) in ultra-pure water. It was stored in the dark at 5 °C. AQ samples of required concentration were prepared by dilution of the stock solution by ultra-pure water and addition of Britton-Robinson buffer (BRB) (its concentration amounted to 10%). The thus prepared sample was inserted into the micro-volume compartment. Agar (p.a.) was purchased from Fluka BioChemika, Czech Republic. Sodium sulfite (Na_2SO_3, p.a.), sodium chloride (NaCl, p.a.), and potassium chloride (KCl, p.a.) were purchased from Penta Švec, Czech Republic. The BRB was prepared by mixing 0.04 mol L^{-1} of boric acid (H_3BO_3, p.a., Sigma-Aldrich, Czech Republic), acetic acid (CH_3COOH), phosphoric acid (H_3PO_4) and 0.2 mol L^{-1} of sodium hydroxide (NaOH) (all p.a., Merck, Czech Republic).

Tap water (sampled in J. Heyrovský Institute of Physical Chemistry of the Czech Academy of Sciences, Czech Republic) and human urine, obtained from a healthy 26-year-old female volunteer, were used as model matrices.

2.2. Voltammetric measurements

Voltammetric measurements were carried out with a PalmSense potentiostat/galvanostat (Electrochemical Sensor Interface, Palm Instruments, The Netherlands) equipped with a PSTrace software (version 4.2.2). A three-electrode arrangement was used: Ag|AgCl (3 mol L^{-1} KCl) (Monokrystaly, Czech Republic) as a reference electrode, a platinum wire (diameter of 1 mm, Monokrystaly, Czech Republic) as an auxiliary electrode, and a polished silver solid amalgam electrode (p-AgSAE) and a mercury meniscus modified silver solid amalgam electrode (m-AgSAE) (both disc diameter of 0.5 mm, lab-made in the J. Heyrovský Institute of Physical Chemistry of the Czech Academy of Sciences, Czech Republic [27]) as working electrodes were used. The p-AgSAE was mechanically renewed by polishing on fine task wipes (Kimtech Science Delicate Task Wipes, Kimberly-Clark, France) before each measurement. After each polishing, mercury meniscus creation, or any pause longer than one hour, the electrodes were activated by insertion of cleaning potential of − 2200 mV for 300 s in 0.2 mol L^{-1} KCl. Before each record, both electrodes were electrochemically regenerated by insertion of regeneration potentials $E_{reg,1}$ of − 1050 mV and $E_{reg,2}$ of + 80 mV, each for 0.1 s imposed 200 times for the p-AgSAE and 400 times for the m-AgSAE.

Oxygen was removed by nitrogen bubbling or by addition of solid sodium sulfite. All measurements were carried out at laboratory temperature (25 ± 2 °C). All solutions were stored in glass bottles protected from light at laboratory temperature.

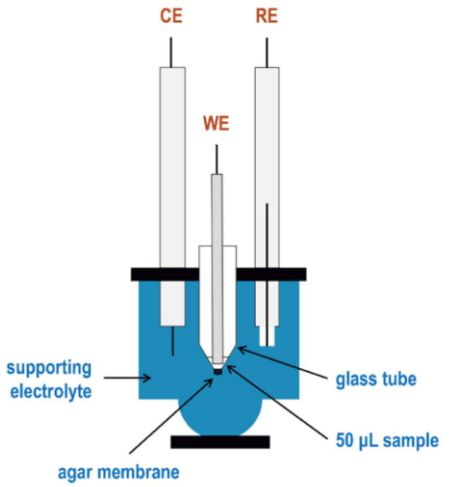

Fig. 1. Scheme of the micro-volume voltammetric cell. WE – working electrode, CE – counter electrode, RE – reference electrode.

The AQ samples were analyzed using differential pulse voltammetry (DPV). The influence of pH on the voltammetric behavior of AQ and the optimization of the DPV parameters in a large-volume voltammetric cell (LVVC) can be found in literature [27]. The optimized parameter of DPV measurements were: scan rate (ν) of 25 mV s^{-1}, pulse height (E_{pulse}) of − 50 mV, pulse width (t_{pulse}) of 100 ms, step potential (E_{step}) of 5 mV, and sweep potential range (E_{range}) from initial potential (E_{in}) of − 300 mV to final potential (E_{fin}) of − 900 mV.

Human urine was diluted 1:1 by deionized water to reduce undesirable effects of interfering compounds. 50 μL of model urine samples spiked with AQ (resulting concentrations 1, 10, and 100 μmol L^{-1}) containing 10% of BRB (of pH 9 for the p-AgSAE and of pH 10 for the m-AgSAE) were transferred into the micro-volume compartment of the MVVC.

2.3. Micro-volume voltammetric cell and preparation of the agar membrane

The MVVC consists of two separated compartments (Fig. 1). The micro-volume compartment is a glass tube with an agar membrane at the bottom. Micro-volume of sample (20–50 μL) was transferred into this compartment, and a working electrode was inserted into this tube. The different glass tubes were used: a) tube with a 2.0 mm diameter and an agar membrane thickness of 2.5 mm (GT1); b) tube with a 2.5 mm diameter and an agar membrane thickness of 2.1 mm (GT2). The large-volume compartment is formed by a 20 mL voltammetric vessel filled with the supporting electrolyte solution (BRB, pH 9 for the p-AgSAE and pH 10 for the m-AgSAE) in which the reference and auxiliary electrodes are immersed.

An agar membrane was used as a conductive junction between the two compartments. An agar solution was prepared using 10 mL of 0.1 mol L^{-1} sodium chloride and 0.3 g of agar. The solution was heated on a water bath until the agar dissolution. 1 mL of thus prepared solution was transferred into a beaker, and the glass tube was immersed into the agar solution for 10 min. During this time, a solid membrane at the bottom of the tube was formed. Then, the glass tube was removed and rinsed with deionized water. Similarly, after each measurement, agar membrane was rinsed with deionized water, too. It was confirmed that simple, nevertheless thorough, rinsing with deionized water is

sufficient to prevent any cross-contamination of the agar membrane.

The glass tubes with the agar membrane were stored in a humidity chamber in the dark at 5 °C. The agar solution could be stored under such conditions for two weeks. The repeatability of the preparation of agar membrane was verified by repeating the DPV determination of 0.1 mmol L^{-1} AQ.

3. Results and discussion

3.1. Optimization of agar membrane preparation

Firstly, the most suitable solvent of agar was searched for using NaCl, KCl, and BRB solutions. Hardening of the agar solution with BRB took too long. In the case of KCl or NaCl, gelatinization was shortened to about 10 min. The ratio of agar and salt in the tested solution was 30 g L^{-1} to 0.1 mol L^{-1} KCl/NaCl. The DP voltammograms of AQ (50 μL, concentration of 0.1 mmol L^{-1}) recorded in the MVVC using the p-AgASE, with the membrane prepared from the agar solution with NaCl, exhibited better repeatability and were more symmetrical than those recorded using the agar solution with KCl. Increasing concentration of agar positively influences the gelatinization process, but to some limiting concentration level only. Moreover, the formed membrane is more compact, AQ transport across such membrane is facilitated, and agar adhesion to glass is increasing with the increasing agar concentration. In the case of membrane prepared from the agar solution with NaCl, the registered voltammetric peaks exhibited better repeatability and were more symmetrical than those recorded using the agar solution with KCl. Therefore, the 0.1 mol L^{-1} NaCl solution was chosen as solvent of agar.

The thickness of the prepared agar membrane in the GTs was dependent on the amount of the agar solutions, more precisely on solution heights (h_{ag}) in used beakers. Different volumes of agar (corresponding h_{ag} of 4.0, 3.4, 2.8, 2.3, 1.7, and 1.0 mm) were transferred into the beaker. Using the above-described procedure, the agar membrane of different thickness was prepared at the bottom of a glass tube. It was concluded that using the h_{ag} about 2.3 mm, the agar membrane of optimum properties can be prepared (time stability, repeatability of membrane preparation, repeatability of recorded current signals, best developed AQ current signals, minimum difference between AQ peak potential in comparison with signals measured in the LVVC, etc.). Finally, using this membrane, DPV peaks of 0.1 mmol L^{-1}AQ were recorded (with RSD of 1.6% for GT1 and 1.3% for GT2, respectively).

Finally, the concentration of agar solution was optimized. The concentrations were tested from 0.01 g mL^{-1} to 0.05 g mL^{-1}. When the agar solution concentration was lower than 0.015 g mL^{-1}, hardening took more than 30 min. It could be concluded that 0.03 g of agar in 1 mL of solvent yielded the best results (RSD of 0.8% in the case of GT1 and 0.7% in the case of GT2). The DPV peak currents of AQ increased with the increasing agar concentration, and from 0.03 g mL^{-1} to 0.05 g mL^{-1}, they were almost constant and, simultaneously, the highest peaks were recorded.

3.2. Storage of micro-volume compartment with formed agar membrane and removal of oxygen

Optimum conditions for storing of the micro-volume compartment containing an agar membrane were tested by DPV determination of AQ. 50 μL of solution of AQ (c_{AQ} = 0.1 mmol L^{-1}) were placed on the agar membrane in the micro-volume compartment. 20 mL of BRB (pH 9) were placed in the voltammetric vessel as the supporting electrolyte in the large-volume compartment. The p-AgSAE was used as the working electrode. The agar membrane was prepared using the optimized parameters described above.

First, glass tubes were stored in the solution of 0.1 mol L^{-1} NaCl at 5 °C. Fixation of the agar membrane to the glass wall of the tube was not perfect after a 7-day storage, and a sample could partly flow through it. Therefore, storage in a humidity chamber saturated with deionized water vapors at 5 °C was tested. The humidity chamber was realized by a Petri dish in which the stored glass tube was inserted and in which a vessel with deionized water was placed. Substantial changes of the agar membrane quality were not observed within 7 days of storage (RSD from 0.5% to 1.1%, average DPV peak currents of AQ were almost constant from the 2nd till the 7th day (from − 0.101 μA to − 0.104 μA)). Therefore, glass tubes with the agar membrane were stored in this humidity chamber for other experiments.

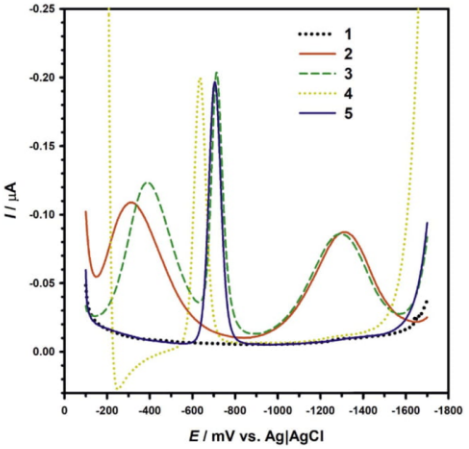

Fig. 2. DPV at the p-AgSAE in the MVVC in BRB (pH 9), with agar membrane height of 4.0 mm. 1) supporting electrolyte without AQ after removing oxygen by bubbling with nitrogen; 2) non-deaerated supporting electrolyte without AQ; 3) non-deaerated supporting electrolyte containing AQ (0.1 mmol L^{-1}); 4) supporting electrolyte containing AQ (0.1 mmol L^{-1}) after oxygen removal by addition of 20 mg of solid sodium sulfite; 5) supporting electrolyte containing AQ (0.1 mmol L^{-1}) after oxygen removal by bubbling with nitrogen. E_{in} = − 100 mV; E_{fin} = − 1700 mV; E_{step} = 5 mV; E_{pulse} = − 50 mV; t_{pulse} = 100 ms.

It was found in pilot experiments that air oxygen present in the sample disturbs the AQ determination (baseline overlaps the AQ reduction signal and it is not possible to reach limit of detection (*LOD*) below 10 μmol L^{-1}). Therefore, two ways of oxygen removing were tested: 1) by the addition of 20 mg of solid sodium sulfite to 50 μL of the sample in the micro-volume compartment, and 2) by the inlet of nitrogen (for ca 1 min) above the sample placed in the micro-volume compartment (Fig. 2). Due to simple and fast application, the addition of solid sodium sulfite was first tested for oxygen removal with positive outcome. However, solid sodium sulfite can be used only in neutral and alkaline solutions. This limitation did not represent any problem in the particular case of AQ, since BRB at pH 9 was used as the supporting electrolyte with the p-AgSAE and BRB at pH 10 with the m-AgSAE. Nevertheless, more generally applicable removal of oxygen via nitrogen was tested as well. No significant difference between both ways of oxygen removal (Fig. 2) was observed. These experiments were realized as pilot experiments, i.e., before optimization of the agar membrane thickness, and the thickness used here was about two times higher (4.0 mm) than the finally optimized one. Consequently, the peaks recorded using this thick membrane were broader and peak potentials were shifted to more negative potentials.

Narrower potential window and peak potential shift to more positive potentials in the case of curve 4, Fig. 2, was caused by the sodium sulfite addition, i.e., by a small pH decrease (this trend was described more in detail in [27]). The presence of a valley on the curve 4, Fig. 2, before the AQ peak has not been reliably explained up to now.

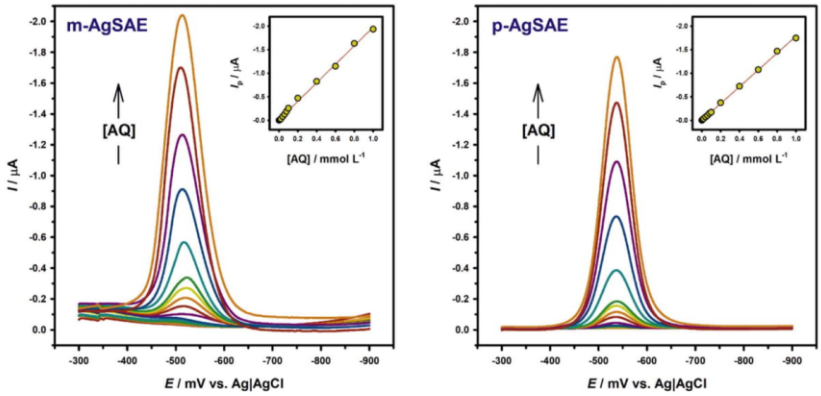

Fig. 3. DPV voltammograms of AQ (4 μmol L^{-1}–1 mmol L^{-1}) at the m-AgSAE in BRB (pH 10) in the presence of oxygen in the MVVC (left side) and of AQ (1 μmol L^{-1}–1 mmol L^{-1}) at the p-AgSAE in BRB (pH 9) after oxygen removal by addition of 20 mg of solid sodium sulfite in the MVVC (right side). GT1 (agar membrane thickness of 2.5 mm, diameter of 2.0 mm); E_{in} = − 300 mV; E_{fin} = − 900 mV; E_{step} = 5 mV; E_{pulse} = − 50 mV; t_{pulse} = 100 ms. Corresponding concentration dependences are in inset.

Possible evaporation of the sample caused by the nitrogen inlet was tested using a Cd^{2+} reduction peak. Since the peak current of the DPV reduction peaks of a 1 μmol L^{-1} Cd^{2+} solution were not changed during repeated measurements in 10 min, it could be concluded that the volume of the sample in this compartment was not changed due to the nitrogen inlet.

3.3. Determination of AQ in the MVVC

The concentration dependences of AQ were measured in both voltammetric cells, i.e. in the MVVC (sample volume of 50 μL) and in the LVVC (sample volume of 10 mL). Voltammograms on the p-AgSAE in the MVVC (Fig. 3, right side) and in the LVVC (data not shown) were recorded both before (data not shown) and after the removal of oxygen (Fig. 3, right side). Voltammograms on the m-AgSAE in the MVVC (Fig. 3, left side) were recorded in the presence of oxygen only, because handling with the solid amalgam surface modified by mercury meniscus proved to be more complicated. It has been more difficult to immerse mercury meniscus in such a small volume of sample without touching the surface of the agar membrane.

Oxygen was removed by bubbling with nitrogen in the LVVC. Agar membrane was prepared according to optimized parameters (see Chapter 3.1). The *LOD* was calculated according IUPAC using the direct signal method [47].

The results are summarized in Table 1. The difference between the *LOD* of AQ in the LVVC and in the MVVC under the same conditions is not significant: the *LODs* were 0.12 μmol L^{-1} (in the LVVC), 0.22 μmol L^{-1} (in the MVVC with GT1), and 0.15 μmol L^{-1} (in MVVC with GT2), respectively. Therefore, it is clear that the proposed MVVC is a reliable tool for voltammetric determination in micro-volumes. The *LODs* in the MVVC at the p-AgSAE obtained in the presence of oxygen (4.0 μmol L^{-1} using GT1 and 4.6 μmol L^{-1} using GT2, respectively) are somewhat higher in comparison with those achieved after oxygen removal (0.22 μmol L^{-1} using GT1 and 0.15 μmol L^{-1} using GT2). Similarly, it is possible to conclude that the differences between the *LODs* obtained at GT1 and GT2 (i.e., using a different agar membrane area and agar membrane height) are not significant. Therefore, the proposed arrangement is suitable for micro-volume voltammetry and its performance is not influenced by small deviations in its fabrication. The obtained concentration dependences were linear over the measured concentration ranges and their parameters are summarized in Table 1.

3.4. Voltammetric determination of AQ in tap water and human urine

Determination of AQ in model samples of tap water and human urine in the MVVC was used to test the practical applicability of this

Table 1
Parameters of AQ concentration dependences measured by DPV. Confidence intervals were calculated on the level of significance α = 0.05. Supporting electrolyte: BRB (pH 9) at the p-AgSAE and BRB (pH 10) at the m-AgSAE. Oxygen was removed by addition of 20 mg of sodium sulfite (GT – glass tube, r – correlation coefficient).

Tested system	GT	Linear dynamic range/mol L^{-1}	Slope[d]/mA mol^{-1} L	r	*LOD*/μmol L^{-1}
p-AgSAE in LVVC (without oxygen[a])	–	2×10^{-7}–1×10^{-3}	− 0.509 ± 0.062	− 0.991	0.12
m-AgSAE in LVVC (without oxygen[a])	–	4×10^{-7}–1×10^{-3}	− 2.484 ± 0.087	− 0.998	0.24
p-AgSAE in MVVC	1	6×10^{-6}–1×10^{-3}	− 1.073 ± 0.029	− 0.999	4.0
(with oxygen[b])	2	6×10^{-6}–1×10^{-3}	− 1.084 ± 0.019	− 0.999	4.6
m-AgSAE in MVVC	1	4×10^{-6}–1×10^{-3}	− 1.966 ± 0.055	− 0.998	3.9
(with oxygen[b])[c]	2	6×10^{-6}–1×10^{-3}	− 1.367 ± 0.061	− 0.997	4.1
p-AgSAE in MVVC	1	6×10^{-7}–1×10^{-3}	− 1.783 ± 0.025	− 0.999	0.22
(without oxygen[b])	2	6×10^{-7}–1×10^{-3}	− 1.831 ± 0.016	− 0.999	0.15

[a] LVVC – sample volume of AQ with BRB buffer of 10 mL.
[b] MVVC – sample volume of AQ with BRB buffer of 50 μL.
[c] Experiments with the m-AgSAE in the MVVC were realized in the presence of oxygen only.
[d] All intercepts were not significantly different from zero (α = 0.05).

Table 2
Determination of AQ by DPV at the p-AgSAE in spiked model sample solutions (tap water and urine) in the MVVC. Confidence intervals were calculated on the level of significance $\alpha = 0.05$. Oxygen was removed by addition of 20 mg of sodium sulfite (GT - glass tube).

	AQ added/ mol L^{-1}	AQ found/mol L^{-1}	Recovery/%	RSD/%
Tap water				
1st day				
GT1	1×10^{-6}	$(1.010 \pm 0.057) \times 10^{-6}$	101.0 ± 5.7	1.9
	1×10^{-5}	$(0.999 \pm 0.063) \times 10^{-5}$	100.0 ± 6.3	1.0
	1×10^{-4}	$(1.013 \pm 0.021) \times 10^{-4}$	101.3 ± 2.1	2.3
GT2	1×10^{-6}	$(0.998 \pm 0.017) \times 10^{-6}$	99.3 ± 4.4	0.32
	1×10^{-5}	$(1.011 \pm 0.012) \times 10^{-5}$	101.1 ± 1.1	2.1
	1×10^{-4}	$(0.975 \pm 0.061) \times 10^{-4}$	97.5 ± 6.1	1.5
7th day				
GT1	1×10^{-6}	$(0.998 \pm 0.017) \times 10^{-6}$	99.8 ± 1.7	0.82
	1×10^{-5}	$(1.003 \pm 0.011) \times 10^{-5}$	100.3 ± 1.1	1.3
	1×10^{-4}	$(1.022 \pm 0.031) \times 10^{-4}$	102.2 ± 3.1	3.2
GT2	1×10^{-6}	$(0.980 \pm 0.021) \times 10^{-6}$	98.0 ± 2.1	0.81
	1×10^{-5}	$(0.989 \pm 0.021) \times 10^{-5}$	98.9 ± 2.1	0.14
	1×10^{-4}	$(1.002 \pm 0.012) \times 10^{-4}$	100.2 ± 1.2	1.3
Urine				
1st day				
GT1	2×10^{-6}	$(1.97 \pm 0.12) \times 10^{-6}$	98.3 ± 6.1	1.5
	2×10^{-5}	$(2.02 \pm 0.11) \times 10^{-5}$	101.1 ± 5.5	2.1
	2×10^{-4}	$(2.024 \pm 0.057) \times 10^{-4}$	101.2 ± 2.9	2.2
GT2	2×10^{-6}	$(1.96 \pm 0.26) \times 10^{-6}$	98 ± 13	0.83
	2×10^{-5}	$(2.00 \pm 0.10) \times 10^{-5}$	100.2 ± 5.2	1.2
	2×10^{-4}	$(1.94 \pm 0.12) \times 10^{-4}$	97.1 ± 6.1	1.9
7th day				
GT1	2×10^{-6}	$(1.96 \pm 0.18) \times 10^{-6}$	98.1 ± 9.2	0.81
	2×10^{-5}	$(2.00 \pm 0.22) \times 10^{-5}$	100 ± 11	2.1
	2×10^{-4}	$(1.99 \pm 0.14) \times 10^{-4}$	99.3 ± 7.0	0.64
GT2	2×10^{-6}	$(1.94 \pm 0.26) \times 10^{-6}$	97 ± 13	2.9
	2×10^{-5}	$(2.05 \pm 0.11) \times 10^{-5}$	102.6 ± 5.4	2.6
	2×10^{-4}	$(1.98 \pm 0.23) \times 10^{-4}$	99 ± 11	0.82

cell. The above found optimized parameters of the agar membrane preparation and of DPV were used for these determinations. The determinations were repeated five times on the same day, and they were repeated after 7 days again in the same glass tubes with the same agar membranes to verify the stability of the agar membrane. The standard additions were prepared in an Eppendorf tube and then pipetted to GTs. The results are summarized in Table 2. There were no interfering substances present in non-spiked tap water or human urine. The results after 7 days did not differ significantly, thus confirming sufficient stability of the membrane used.

4. Conclusions

A new micro-volume voltammetric cell has been developed based on a commercially available large-volume voltammetric cell with an inserted micro-volume cell for the sample with a miniaturized working electrode connected via a conductive agar membrane to the large-volume cell with a classical reference and auxiliary electrode. This arrangement was successfully tested for voltammetric determination of AQ at the m-AgSAE and p-AgSAE in 50 µL of model sample. The concentration calibration curve of AQ in BRB (pH 9) at the p-AgSAE was linear in the concentration range from 1 µmol L^{-1} up to 1 mmol L^{-1}, with *LOD* about 0.2 µmol L^{-1}. The agar membrane thickness and its area did not influence the results significantly. The results of the determination of AQ in model samples of tap water and urine confirmed the practical applicability of the developed cell for sensitive determination of electrochemically reducible organic compounds in micro-volumes.

Acknowledgements

Š.S. thanks the ERASMUS exchange project, the project Specific University Research (SVV 260440), and the project of the Czech Science Foundation (project GAČR No. 17-05387S). J.B. and T.N. thank the project of the Czech Science Foundation (project GAČR No. 17-03868S). L.M.G. wishes to acknowledge Fundação para a Ciência e a Tecnologia (SFRH/BPD/76544/2011).

References

[1] W.P. Norbert, F. Heiner, Why should we bother? Ethical and social issues in individualized medicine, Curr. Drug Targets 7 (12) (2006) 1721–1727.
[2] T. Buclin, V. Gotta, A. Fuchs, N. Widmer, J. Aronson, Monitoring drug therapy, Br. J. Clin. Pharmacol. 73 (6) (2012) 917–923.
[3] J.S. Kang, M.H. Lee, Overview of therapeutic drug monitoring, Korean J. Intern. Med. 24 (1) (2009) 1–10.
[4] G. Schutze, M.J. Schwarz, Therapeutic drug monitoring for individualised risk reduction in psychopharmacotherapy, Trac-Trends Anal. Chem. 84 (2016) 14–22.
[5] M. Gal, M. Hromadova, L. Pospisil, J. Hives, R. Sokolova, V. Kolivoska, J. Bulickova, Voltammetry of hypoxic cells radiosensitizer etanidazole radical anion in water, Bioelectrochemistry 78 (2) (2010) 118–123.
[6] T. Mackulak, M. Vojs, R. Grabic, O. Golovko, A.V. Stanova, L. Birosova, A. Medvedova, J. Hives, M. Gal, A. Kromka, A. Hanusova, Occurrence of pharmaceuticals, illicit drugs, and resistant types of bacteria in hospital effluent and their effective degradation by boron-doped diamond electrodes, Monatsh. Chem. 147 (1) (2016) 97–103.
[7] G. McMahon, R. O'Connor, Therapeutic drug monitoring in oncology: does it have a future? Bioanalysis 1 (3) (2009) 507–511.
[8] G. Cassinelli, The roots of modern oncology: from discovery of new antitumor anthracyclines to their clinical use, Tumori 102 (3) (2016) 226–235.
[9] G. Scambia, P.B. Panici, G. Contu, R. Devincenzo, G. Ferrandina, G. Isola, A. Maccio, S. Mancuso, Mechanisms and modulation of resistance to anthracyclines, Int. J. Oncol. 4 (4) (1994) 951–959.
[10] Z.A. Zhang, Y.K. Gong, Q. Zhou, Y. Hu, H.M. Ma, Y.S. Chen, Y. Igarashi, L.F. Pan, G.L. Tang, Hydroxyl regioisomerization of anthracycline catalyzed by a four-enzyme cascade, Proc. Natl. Acad. Sci. U. S. A. 114 (7) (2017) 1554–1559.
[11] B.X. Pang, X.H. Qiao, L. Janssen, A. Velds, T. Groothuis, R. Kerkhoven, M. Nieuwland, H. Ovaa, S. Rottenberg, O. van Tellingen, J. Janssen, P. Huijgens, W. Zwart, J. Neefjes, Drug-induced histone eviction from open chromatin contributes to the chemotherapeutic effects of doxorubicin, Nat. Commun. 4 (2013) 1–13.
[12] J.A. Ribeiro, C.M. Pereira, F. Silva, Electrochemistry of the interaction between bioactive drugs daunorubicin and dopamine and DNA at a water/oil interface, Electrochim. Acta 180 (2015) 687–694.
[13] G. Golunski, A. Borowik, A. Lipinska, M. Romanik, N. Derewonko, A. Woziwodzka, J. Piosik, Pentoxifylline affects idarubicin binding to DNA, Bioorg. Chem. 65 (2016) 118–125.
[14] L. Scaglioni, R. Mondelli, R. Artali, F.R. Sirtori, S. Mazzini, Nemorubicin and doxorubicin bind the G-quadruplex sequences of the human telomeres and of the c-MYC promoter element Pu22, Biochim. Biophys. Acta Gen. Subj. 1860 (6) (2016) 1129–1138.
[15] R. Sokolova, J.E. Nycz, S. Ramesova, J. Fiedler, I. Degano, M. Szala, V. Kolivoska, M. Gal, Electrochemistry and spectroelectrochemistry of bioactive hydroxyquinolines: a mechanistic study, J. Phys. Chem. B 119 (20) (2015) 6074–6080.
[16] P.S. Guin, S. Das, P.C. Mandal, Electrochemical reduction of quinones in different media: a review, Int. J. Electrochem. 2011 (22) (2011).
[17] J. Han, J. Zhang, H.Y. Zhao, Y. Li, Z.L. Chen, Simultaneous determination of doxorubicin and its dipeptide prodrug in mice plasma by HPLC with fluorescence detection, Chin. J. Pharm. Anal. 6 (3) (2016) 199–202.
[18] C.B.P. da Silva, I.P. Julio, G.E. Donadel, I. Martins, UPLC-MS/MS method for simultaneous determination of cyclophosphamide, docetaxel, doxorubicin and 5-fluorouracil in surface samples, J. Pharmacol. Toxicol. Methods 82 (2016) 68–73.
[19] X.P. Yang, F. Qian, L.X. Xie, X.C. Yang, X.M. Cheng, M.M.F. Choi, Determination of doxorubicin in plasma by using ce coupled with in-column tapered optic-fiber light-emitting diode induced fluorescence detection, Electrophoresis 35 (5) (2014) 762–769.
[20] X.P. Yang, H.H. Gao, F. Qian, C. Zhao, X.J. Liao, Internal standard method for the measurement of doxorubicin and daunorubicin by capillary electrophoresis with in-column double optical-fiber led-induced fluorescence detection, J. Pharm. Biomed. Anal. 117 (2016) 118–124.
[21] X.F. Wei, X.D. Huang, Y. Fang, Q.K. Zhang, Determination of idarubicin using CdTe quantum dots as fluorescence probes, J. Nanosci. Nanotechnol. 16 (7) (2016) 6992–6997.
[22] M.R. Alcaraz, A.V. Schenone, M.J. Culzoni, H.C. Goicoechea, Modeling of second-order spectrophotometric data generated by a pH-gradient flow injection technique for the determination of doxorubicin in human plasma, Microchem. J. 112 (2014) 25–33.
[23] B. Yosypchuk, T. Navratil, A.N. Lukina, K. Peckova, J. Barek, Solid amalgam composite electrode as a new sensor for the determination of biologically active compounds, Chem. Anal. 52 (6) (2007) 897–910.
[24] L.M. Goncalves, I.M. Valente, J.A. Rodrigues, Recent advances in membrane-aided extraction and separation for analytical purposes, Sep. Purif. Rev. 46 (3) (2017) 179–194.
[25] R.M. Ramos, L.M. Goncalves, V. Vyskocil, J.A. Rodrigues, Free sulphite determination in wine using screen-printed carbon electrodes with prior gas-diffusion

microextraction, Electrochem. Commun. 63 (2016) 52–55.
[26] S. Kurbanoglu, B. Bozal-Palabiyik, M. Gumustas, B. Uslu, S.A. Ozkan, Investigation of voltammetric behavior and electroanalytical determination of anticancer epirubicin via glassy carbon electrode using differential pulse and square wave voltammetry techniques, Rev. Roum. Chim. 60 (5–6) (2015) 491–499.
[27] S. Skalova, T. Navratil, J. Barek, V. Vyskocil, Voltammetric determination of sodium anthraquinone-2-sulfonate using silver solid amalgam electrodes, Monatsh. Chem. 148 (3) (2017) 577–583.
[28] Y.H. Hahn, H.Y. Lee, Electrochemical behavior and square wave voltammetric determination of doxorubicin hydrochloride, Arch. Pharm. Res. 27 (1) (2004) 31–34.
[29] S.H. Zhang, K.B. Wu, S.S. Hu, Carbon paste electrode based on surface activation for trace adriamycin determination by a preconcentration and voltammetric method, Anal. Sci. 18 (10) (2002) 1089–1092.
[30] X.L. Xu, S. Zhang, H. Chen, J.L. Kong, Integration of electrochemistry in micro-total analysis systems for biochemical assays: recent developments, Talanta 80 (1) (2009) 8–18.
[31] A. Hajkova, V. Vyskocil, B. Josypcuk, J. Barek, A miniaturized electrode system for voltammetric determination of electrochemically reducible environmental pollutants, Sensors Actuators B Chem. 227 (2016) 263–270.
[32] L. Novotny, B. Yosypchuk, Solid silver amalgam electrodes, Chem. Listy 94 (12) (2000) 1118–1120.
[33] O. Mikkelsen, K. Schroder, Dental amalgam in voltammetry some preliminary results, Anal. Lett. 33 (15) (2000) 3253–3269.
[34] B. Yosypchuk, L. Novotny, Nontoxic electrodes of solid amalgams, Crit. Rev. Anal. Chem. 32 (2) (2002) 141–151.
[35] T. Navratil, B. Yosypchuk, J. Barek, A multisensor for electrochemical sequential autonomous automatic measurements, Chem. Anal. 54 (1) (2009) 3–17.
[36] J. Barek, J. Fischer, T. Navratil, K. Peckova, B. Yosypchuk, J. Zima, Nontraditional electrode materials in environmental analysis of biologically active organic compounds, Electroanalysis 19 (19–20) (2007) 2003–2014.
[37] R. Fadrna, B. Yosypchuk, M. Fojta, T. Navratil, L. Novotny, Voltammetric determination of adenine, guanine, and DNA using liquid mercury free polished silver solid amalgam electrode, Anal. Lett. 37 (3) (2004) 399–413.
[38] J. Fischer, L. Vanourkova, A. Danhel, V. Vyskocil, K. Cizek, J. Barek, K. Peckova, B. Yosypchuk, T. Navratil, Voltammetric determination of nitrophenols at a silver solid amalgam electrode, Int. J. Electrochem. Sci. 2 (3) (2007) 226–234.
[39] J. Barek, E. Dodova, T. Navratil, B. Yosypchuk, L. Novotny, J. Zima, Voltammetric determination of N,N-dimethyl-4-amine-carboxyazobenzene at a silver solid amalgam electrode, Electroanalysis 15 (22) (2003) 1778–1781.
[40] R. Selesovska, L. Bandzuchova, T. Navratil, J. Chylkova, Voltammetric determination of leucovorin using silver solid amalgam electrode, Electrochim. Acta 60 (2012) 375–383.
[41] L. Bandzuchova, R. Selesovska, T. Navratil, J. Chylkova, L. Novotny, Voltammetric monitoring of electrochemical reduction of riboflavin using silver solid amalgam electrodes, Electrochim. Acta 75 (2012) 316–324.
[42] K. Peckova, T. Navratil, B. Yosypchuk, J.C. Moreira, K.C. Leandro, J. Barek, Voltammetric determination of azidothymidine using silver solid amalgam electrodes, Electroanalysis 21 (15) (2009) 1750–1757.
[43] R. Selesovska, L. Bandzuchova, T. Navratil, Voltammetric behavior of methotrexate using mercury meniscus modified silver solid amalgam electrode, Electroanalysis 23 (1) (2011) 177–187.
[44] J. Barek, J. Fischer, T. Navratil, K. Peckova, B. Yosypchuk, Silver solid amalgam electrodes as sensors for chemical carcinogens, Remote Sensors 6 (4) (2006) 445–452.
[45] L. Bandzuchova, R. Selesovska, T. Navratil, J. Chylkova, Electrochemical behavior of folic acid on mercury meniscus modified silver solid amalgam electrode, Electrochim. Acta 56 (5) (2011) 2411–2419.
[46] E. Laborda, A. Molina, Q. Li, C. Batchelor-McAuley, R.G. Compton, Square wave voltammetry at disc microelectrodes for characterization of two electron redox processes, Phys. Chem. Chem. Phys. 14 (23) (2012) 8319–8327.
[47] J.N. Miller, J.C. Miller, Statistics and chemometrics for analytical chemistry, 2nd ed., Pearson Education, Harlow, 2005.

11. **Appendix V**

Comparison of Doxorubicin Determination Using Two Voltammetric Techniques

Skalová Štěpánka, Langmaier Jan, Barek Jiří, Vyskočil Vlastimil, Navrátil Tomáš

submitted to Electrochimica Acta **(2019)**

Doxorubicin determination using two voltammetric techniques - a comparative study

Štěpánka Skalová[1,2], Jan Langmaier[1], Jiří Barek[2], Vlastimil Vyskočil[2], Tomáš Navrátil[1]*

[a] J. Heyrovský Institute of Physical Chemistry of the Czech Academy of Sciences, Dolejškova 3, 182 23 Prague 8, Czech Republic

[b] Charles University, Faculty of Science, Department of Analytical Chemistry, UNESCO Laboratory of Environmental Electrochemistry, Albertov 6, 128 43 Prague 2, Czech Republic

* e-mail: Tomas.Navratil@jh-inst.cas.cz

A B S T R A C T

Doxorubicin (DOX) represents an anthracycline-based antibiotic drug. DOX determination in body fluids is relevant for treatment, monitoring and individual dosage optimization. Two novel methods of DOX determination have been compared in this manuscript: i) Differential pulse cathodic stripping voltammetry (DPCSV) on a polished silver solid amalgam electrode (p-AgSAE) in a specially designed micro-volume voltammetric cell (MVVC) and ii) Differential pulse voltammetry (DPV) on polarized liquid/liquid interface represented by a supported membrane prepared by impregnating a polyvinylidenfluoride microporous filter with a room-temperature ionic liquid (RTIL) tridodecylmethylammonium tetrakis[3,5-bis(trifluoro-methyl)phenyl]borate (TDMA-TFPB). Moreover, elimination voltammetry with linear scan (EVLS) has been applied for elucidation of controlling reaction processes observed at p-AgSAE.

DPCSV method on p-AgSAE is applicable for the determination of DOX in linear dynamic range (*LDR*) from 0.6 to 10 μmol L^{-1} with limit of detection (*LOD*) 0.44 μmol L^{-1}. Applicability of this method was verified on analysis of spiked human urine samples with recovery of 100.7 ± 6.6 % (c_{DOX} = 1.0 μmol L^{-1}) and relative standard deviation (RSD) 4.3%.

Using the above-mentioned liquid/liquid interface method, similar results have been achieved (*LOD* 0.84 μmol L^{-1}, *LDR* from 1 to 40 μmol L^{-1}). Nevertheless, due to the presence of some interfering compounds and of charged lipophilic compounds, this method must be preceded by a separation step in the case of body fluids analysis.

Keywords: (maximum 5)

Doxorubicin

Body fluids
Micro-Volume voltammetric cell
Amalgam
Room-temperature ionic liquid

Article history:
Received
Received in revised form
Accepted
Available online

1. Introduction

Doxorubicin (DOX, Fig. 1) is an antineoplastic antibiotic, which has been widely used for the treatment of various cancerous diseases such as sarcoma, several forms of lymphoma, and leukemia [1-3]. Its mechanism of action consists of more than 4 different path ways, e.g., a) inhibition of DNA synthesis in tumor cell, b) creation of free radicals, which can destroy DNA, c) induction of DNA damage due to interference of DOX with topoisomerase II and d) induction of apoptosis [4].

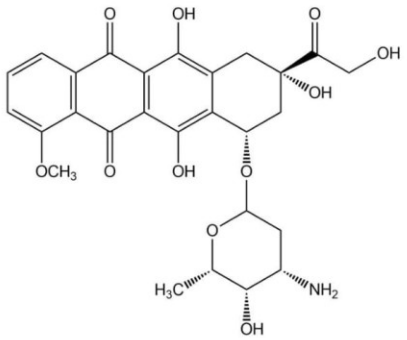

Fig. 1. Structural formula of doxorubicin.

Determination of DOX levels in body fluids presents a new opportunity for more accurate and more correct individualization of drug dosage in order to increase the effectiveness of

treatment [5] and to reduce side effects connected with its overdose, which is in the case of DOX dangerous especially for its cardiotoxicity [6].

A specific method of determination has to be developed for each individual drug [7]. A few analytical techniques applicable for DOX and other anthracycline drugs determination have been developed, e.g., high performance liquid chromatography with fluorescence detector (HPLC-FLD) for determination in tumor samples, in cell culture, and placental perfusion media [8, 9], dispersive liquid-liquid microextraction (HLLME) HPLC-FLD in hospital effluent [10], capillary electrophoresis (CE) with laser-induced fluorescence detection in cell lysate [11], CE with in-column double optical-fiber LED-induced fluorescence detection in rabbit plasma [12], and *ex vivo* solid-phase microextraction coupled to liquid chromatography-tandem mass spectrometry in lung tissue [13].

The most important for utilization of electrochemical methods for anthraquinone drugs is the presence of electrochemically active chinon-hydrochinon redox system, which can be used for their voltammetric determination [14]. Various voltammetric methods have been reported, using different types of electrode materials, e.g., silver solid amalgam electrodes [15], a glassy carbon electrode modified with polyaniline [16], electrospun carbon nanofiber and TiO_2 nanoparticles modified electrodes [17], and a hanging mercury drop electrode [18]. Among advantages of these methods belong their high sensitivity, simple electrode preparation, high accuracy, precision and versatility and significantly lower operating costs compared to modern instrumental separation methods [19-23]. Therefore, the electrochemical methods present a viable alternative, especially in high-throughput applications.

Because in many cases, only a relatively small amount of the analyzed body fluid is available, a miniaturized micro-volume voltammetric cell (MVVC) was recently developed by our research group which is can be used for volumes as low as 20-50 μL and which was successfully tested by the determination of sodium anthraquione-2-sulfonate [24].

Transfer processes of ionized DOX across a polarized liquid/liquid interfaces using the voltammetric techniques have been recently investigated [25]. The authors studied basic thermodynamic properties such as the formal transfer potential, partition coefficient and Gibbs energy of DOX^+ transfer processes at the water/1,2-DCE (1,2-dichloroethane) interface. Analytical part of the article is based on DC and differential pulse stripping voltammetry at water/PVC-NPOE (2-nitrophenyl octyl ether) interface. The study presents important dependence of standard Gibbs energy ($\Delta_w{}^oG_{DOX}{}^0$) of DOX^+ transfer on pH from which may be concluded that the protonated form of DOX^+ is dominant at pH values lower pH < 8. Since the correlation of the ion transfer standard Gibbs energies across the

water/TDMA-TFPB and water/1,2-DCE interface is close to 1:1 [26], the experimental value of pH ~ 3 employed for the aqueous electrolyte (1 mmol L^{-1} HCl) in this study makes sure that the DOX is in aqueous solution present exclusively in its protonated form.

In this article, we have used DOX as a representative of anthracycline anticancer drugs. We have developed and compared two methods for its determination: a) differential pulse cathodic stripping voltammetry (DPCSV) on polished silver solid amalgam electrode (p-AgSAE) in the above mentioned MVVC [24] and differential pulse voltammetry (DPV) on polarized liquid/liquid interface represented by a supported membrane prepared by impregnating a polyvinylidenfluoride microporous filter with a room-temperature ionic liquid (RTIL) tridodecylmethylammonium tetrakis[3,5-bis(trifluoro-methyl)phenyl]borate (TDMA-TFPB).

2. Experimental Part

2.1. Reagents and Samples

All used reagents were dissolved in redistilled water (conductivity < 0.05 μS cm^{-1}) from the purification system Millipore Direct-Q 3 UV water (Merck, Czech Republic).

The Britton - Robinson buffer (BRB) was prepared by mixing an appropriate amount of 0.04 mol L^{-1} of boric acid (H_3BO_3, p.a., Sigma-Aldrich, Czech Republic), 0.04 mol L^{-1} acetic acid (CH_3COOH), 0.04 mol L^{-1} phosphoric acid (H_3PO_4) and 0.2 mol L^{-1} of sodium hydroxide (NaOH) (all p.a., Merck, Czech Republic).

A stock solution of 1×10^{-3} mol L^{-1} DOX was prepared by dissolving an appropriate amount of DOX (99.7 %, Alfa Aesar, USA) in redistilled water and stored in the dark at 5 °C. The analyzed DOX samples of different concentrations were prepared by dilution of the stock solution by the ultra-pure redistilled water and addition of BRB ($V_{\text{DOX solution}}/V_{\text{BRB}}$ was 9:1). Agar (p.a.) was purchased from Fluka BioChemika, Czech Republic. Sodium sulfite (Na_2SO_3, p.a.), sodium chloride (NaCl, p.a.), and potassium chloride (KCl, p.a.) were purchased from Penta Švec, Czech Republic.

Analyzed model samples of human urine were obtained from a healthy 27-year-old female volunteer. Tap water was obtained at J. Heyrovský Institute of Physical Chemistry of the Czech Academy of Sciences.

Doxorubicin hydrochloride and sodium tetrakis[3,5-bis(trifluoromethyl)phenyl]borate dihydrate (NaTFPB) were obtained from Alfa Aesar and Dojindo Laboratories, respectively. Tetraethylammonium chloride (TEACl), tridodecylmethylammonium chloride (TDMACl)

and LiCl were purchased as analytical grade chemicals from Fluka. All substances were used as received without any other purification. Room-temperature ionic liquid (RTIL) TDMA-TFPB was prepared by metathesis from the corresponding salts in acetone. The resulting solution was filtered and purified using a column filled with aluminum oxide (Fluka, for chromatography). After evaporation of acetone the obtained RTIL was several times washed with deionized water and dried out in a laboratory oven at a temperature not exceeding 75 °C.

2.2. Instrumentation

2.2.1. Voltammetry in micro-volume voltammetric cell

Electrochemical measuring system was analogous to that described in ref. [24].

Voltammetric measurements in MVVC were carried out using an Eco-Tribo-Polarograph (ETP) (Polaro-Sensors, Czech Republic) controlled by MultiElchem (version 3.1) software. Following three-electrode arrangement was used: the reference electrode - Ag|AgCl (3 mol L^{-1} KCl) (Monokrystaly, Czech Republic), the auxiliary electrode - platinum wire (∅ 1 mm, Monokrystaly, Czech Republic), and the working electrode p-AgSAE inserted in the MVVC (∅ 0.5 mm, lab-made in the J. Heyrovský Institute of Physical Chemistry of the Czech Academy of Sciences, Czech Republic) [15].

The separating agar membrane of MVVC was prepared by adding of 0.2 g agar powder to 10 mL of 0.1 mol L^{-1} NaCl. Then the solution was heated up on a water bath until complete agar powder dissolving. The agar membrane was formed on the bottom of the micro-volume sample compartment of the used MVVC [24].

The p-AgSAE had to be mechanically renewed by polishing on fine task wipes (Kimtech Science Delicate Task Wipes, Kimberly-Clark, France) before each set of measurements. Thereafter, its surface was activated by insertion of the cleaning potential of –2200 mV for 300 s in 0.2 mol L^{-1} KCl. Before each recording of voltammetric curve, p-AgSAE was electrochemically regenerated by potentials pulses $E_{reg,1}$ of -1050 mV and $E_{reg,2}$ of +80 mV, each for 0.1 s and applied 200 times.

Oxygen was removed by nitrogen passing through and over the cell. All measurements were carried out at laboratory temperature (25 ± 2 °C).

DOX samples were analyzed using DPCSV applying following parameters: scan rate (v) of 20 mV s^{-1}, pulse height (E_{pulse}) of –50 mV, pulse width (t_{pulse}) of 100 ms, sweep potential

range (E_{range}) from initial potential (E_{in}) of –200 mV to final potential (E_{fin}) of –800 mV, accumulation potential (E_{acc}) of –300 mV, and accumulation time (t_{acc}) of 120 s.

50 µL of tap water or of model human urine (human urine was initially diluted 1:1 by deionized water) were spiked with DOX solution containing 10% v/v of BRB ($V_{DOX\ solution}/V_{BRB}$ was 9:1). Resulting concentrations of DOX in analyzed samples amounted to 1 and 10 µmol L^{-1}, respectively. Solutions with standard additions were prepared in Eppendorf tubes and afterwards they were transferred to the glass tube with the agar membrane surface on the bottom. Finally, the working electrode was immersed into MVVC for the DPCSV experiment. All statistical parameters (e.g., limits of detections (*LODs*), limits of quantifications (*LOQs*), slopes, confidence intervals were calculated were calculated as described in [27]. The direct signal method according to IUPAC has been used for *LODs* and *LOQs* calculations [27].

2.2.2. Voltammetry on polarized liquid/liquid interface

The most important part of the electrochemical cell used for voltammetric experiments performed on polarized liquid/liquid interfaces is the supported membrane which has been prepared by impregnating a polyvinylidenfluoride microporous filter (Millipore, type GVHP 1300, pore size of 0.22 µm, thickness of ~112 µm) with TDMA-TFPB [28]. The membrane disk (∅ 0.9 cm) was cut off from the impregnated filter and mounted in a home-made four-electrode cell [29]. The area of the membrane exposed to the aqueous electrolyte solution was 0.0707 cm^2. All voltammetric experiments were performed at the ambient temperature of 25±2 °C using the cell with the TDMA-TFPB membrane, which can be described by the following Scheme 1,

Ag′|AgCl|1mM HCl (w′) ‖TDMA-TFPB (o)‖1mM HCl, x µmol L^{-1} R^+ (w) |AgCl|Ag (Scheme 1)

where 1 mmol L^{-1} HCl serves as an acidic electrolyte (pH ~ 3), x = 1 – 40, R^+ represents chloride salts of the internal standard cation TEA^+ or the investigated protonated doxorubicin (DOX^+) and (o) denotes the RTIL organic phase. Both reference Ag|AgCl electrodes were connected to the aqueous phases (w) and (w') through the Luggin capillary the tip of which was filled with the aqueous agar gel containing 100 mmol L^{-1} LiCl. The cell potential *E* (Eq. 1),

$$E = \varphi^{Ag} - \varphi^{Ag'} = \Delta_o^w\varphi - \Delta_o^{w'}\varphi - E_{ref} \quad (1)$$

was controlled by the CHI potentiostat (Model 920C, CH Instruments, USA) equipped with the automatic compensation of the ohmic potential (IR) drop. The instrument was also used to measure the complex impedance of the cell enabling to estimate the solution resistance (typically 60 – 110 kΩ) for the adjustment of the ohmic potential drop compensation.

The cyclic voltammograms (CV) of the univalent ion transfer were characterized using the midpoint potential which is defined as $E_m = (E_{p+} + E_{p-}) / 2$, where E_{p+} and E_{p-} are the positive and negative voltammetric peak potentials, respectively, and by the positive peak current I_p^+. The transfer of the single charged ion or mono-protonated DOX is generally controlled by the linear diffusion. The peak current I_p^+ (in A) is then described by the equation (Eq. 2) [30],

$$I_{p+} = (2.31 \times 10^5)\, A\, (D_i^w\, v)^{1/2}\, c_i^{o,w} \quad (2)$$

where D_i^w is the ion diffusion coefficient in the aqueous phase in $cm^2\ s^{-1}$, A is the interfacial area in cm^2, v is the sweep rate in $V\ s^{-1}$, and $c_i^{o,w}$ is the bulk ion concentration in $mol\ cm^{-3}$.

DPV experiments were carried out using the cell characterized by the Scheme 1 as well. Experimental parameters were set as follows: Amplitude of 50 mV, potential increment of 4 mV, potential pulse width of 0.2 s, sampling time 0.02 s, pulse period of 0.5 s (corresponds to scan rate 8 mVs^{-1}) and 30 s of preconditioning. DPV curves were background corrected.

3. Results and Discussions

3.1. Determination of doxorubicin in the micro-volume voltammetric cell

Firstly, the influence of pH on DPV behavior of DOX (Fig. 2) was investigated (sample volume of 50 µL) on p-AgSAE. Under alkaline conditions of pH 8 and higher, DOX degrades to several different products [31]. pH 6 was chosen, as it provided well developed peak with highest I_p (Fig. 3). Cyclic voltammetry and elimination voltammetry were also

used for study of the DOX voltammetric behavior. CV showed one cathodic and one anodic peak (Fig. 2, inset). The CV peaks correspond to a quasireversible process. The inset in Fig. 2 exhibits relatively broad cathodic peak. The elimination voltammetry with linear scan (EVLS) [32-34] separated this signal into two peaks (at −500 mV and −650 mV at pH 6). This method confirmed that both cathodic processes are diffusion controlled at lower scan rate set (10, 20 40, and 80 mV s^{-1}) as well as at higher scan rate set (80, 160, 320, and 640 mV s^{-1}). On the other hand, the elimination anodic signal remained unseparated as one peak. In the case of the anodic as well as both cathodic peaks, the influence of adsorption was confirmed using EVLS. More precisely, it was revealed that all processes occur in weakly-adsorbed state. Due to the fact that the ratios of elimination peak heights vs. elimination counter-peak heights did not correspond to the theoretical value 3:4, we can conclude that adsorption is relatively weak in the case of the anodic signal and very weak in the case of the cathodic signal [35].

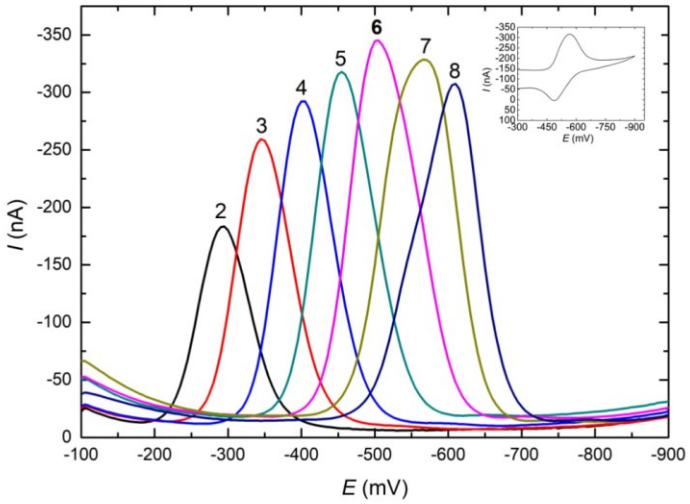

Fig. 2. DP voltammograms of 1×10^{-4} mol L^{-1} DOX on the p-AgSAE in BRB pH 2 - 8 (values given above the curve) after bubbling with nitrogen. Scan rate (v) of 20 mV s^{-1}, pulse height (E_{pulse}) of –50 mV, pulse width (t_{pulse}) of 100 ms, potential range (E_{range}) = −100 to −900 mV.

Presence of air oxygen has led to background rise and subsequent decrease of DOX peak current. Two ways of oxygen removal were therefore tested: a) addition of 20 mg of Na_2SO_3; b) bubbling of the analyzed solution with N_2 (Fig. 3). The use of solid sodium sulfite in acidic solutions is not appropriate due to its decomposition under such conditions [36], oxygen removal by Na_2SO_3 was hence tested at pH 6 and pH 7. At both tested pH values, i.e., at pH 6 (Fig. 3.A) and at pH 7 (Fig. 3.B), addition of Na_2SO_3 has led to decrease of DOX peak current, presumably corresponding to undesirable reduction of DOX by the Na_2SO_3. Nitrogen bubbling was therefore chosen as the optimum procedure and used for all further measurements.

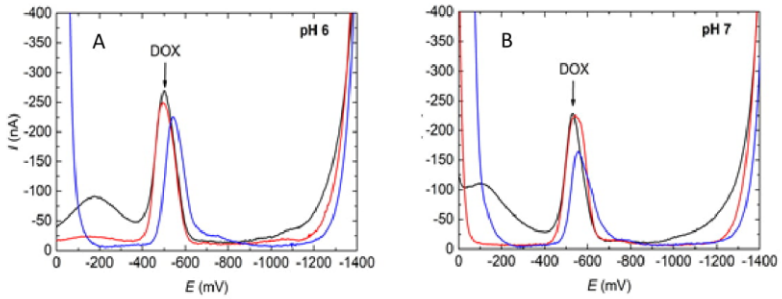

Fig. 3. DPCS voltammograms of DOX (c_{DOX} = 1×10^{-4} mol L^{-1}) on the p-AgSAE in the MVVC in BRB (**A:** pH 6 and **B:** pH 7). Curves: *Black*: before oxygen removing, *Blue:* with Na_2SO_3; *Red*: after bubbling with nitrogen. Parameters: v of 20 mV s^{-1}, E_{pulse} of –50 mV, t_{pulse} of 100 ms, E_{range} = 0 to −1700 mV, accumulation potential (E_{acc}) of –300 mV, and accumulation time (t_{acc}) of 120 s.

Then, influence of the used E_{acc} and t_{acc} on signal height and signal repeatability was optimized (Fig. 4). E_{acc} was optimized in the potential range from 200 mV to –300 mV (at –400 mV DOX reduction starts at p-AgSAE). The highest and sufficiently reproducible peak was observed at the accumulation potential of –300 mV, difference between peak currents at 200 mV and –300 mV was more than 50 %. After that, t_{acc} was investigated in the range from 0 s to 180 s (Fig. 4.B). The peak current increased with increasing accumulation time, the difference between peaks at t_{acc} = 120 s and t_{acc} = 180 s was, however, not too significant (about 14 % only). Moreover, the repeatability of the experiments gradually

decreased with increasing t_{acc}. Therefore, for further measurements t_{acc} =120 s was chosen as optimum accumulation time.

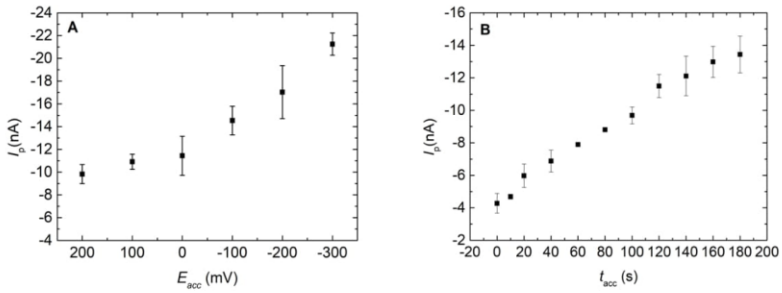

Fig. 4. The dependence of peak current of DPCSV of DOX model sample (c_{DOX} = 1×10^{-6} mol L^{-1}) on the p-AgSAE in the MVVC in BRB (pH 6) after bubbling with nitrogen on E_{acc} (**A**) and t_{acc} (**B**). (v = 20 mV s^{-1}; E_{pulse} = –50 mV; t_{pulse} = 80 ms; E_{range} = 0 to −1700 mV. **A:** t_{acc} = 30 s; E_{acc} = 200, 100, 0, –100, –200 and –300 mV; **B:** E_{acc} = –300 mV; t_{acc} = 0, 10, 30, 60, 90, 120, 150 and 180 s). The error-bars correspond to the calculated confidence intervals on the level of significance α = 0.05.

Afterwards, the concentration dependence of peak current on DOX concentration was investigated in two concentration ranges: from 0.6 µmol L^{-1} to 100 µmol L^{-1} (Fig. 5) and from 0.6 µmol L^{-1} to 6 µmol L^{-1} (Fig. 6) using DPCSV on p-AgSAE under the above-mentioned optimized conditions. In the whole investigated concentration interval, the dependence could be approximated by an adsorption isotherm (Fig. 5). This confirms the above-mentioned conclusion of EVLS about the influence of week absorption on the recorded processes. The recorded DOX concentration dependence was linear in the range from 0.6 µmol L^{-1} to 10 µmol L^{-1} (Fig. 6).

The achieved chemometric parameters have been summarized in Table 1. The repeatability of measurement was 3.7% on the concentration level of 0.6 µmol L^{-1} and 3.2% on the concentration level of 100 µmol L^{-1} (for 10 measurements).

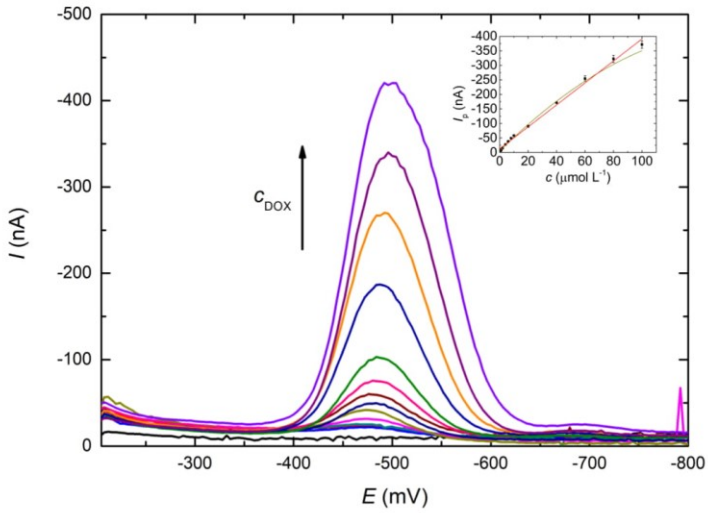

Fig. 5. DPCS voltammograms of DOX model sample (c = 0.6 µmol L^{-1} - 100 µmol L^{-1}) on p-AgSAE in BRB (pH 6) after oxygen removal by bubbling with N_2. (v = 20 mV s^{-1}; E_{pulse} = –50 mV; t_{pulse} = 80 ms; E_{range} = –200 - −800 mV, E_{acc} = –300 mV, t_{acc} = 120 s). Baseline is depicted in black. *Inset*: Corresponding concentration curves with linear (red) and polynomial (green) approximations. The error-bars correspond to the calculated confidence intervals on the level of significance α = 0.05.

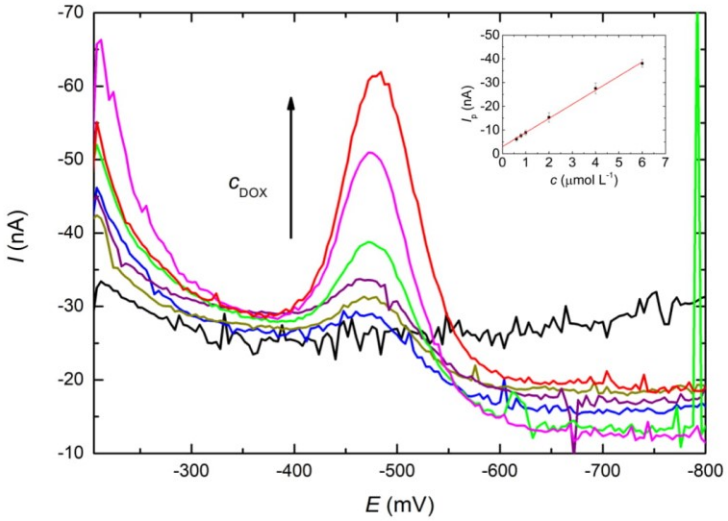

Fig. 6. DPCS voltammograms of DOX model sample (c = 0.6 μmol L^{-1} - 6 μmol L^{-1}) on p-AgSAE in BRB (pH 6) after oxygen removal by bubbling with N_2. (v = 20 mV s^{-1}; E_{pulse} = –50 mV; t_{pulse} = 80 ms; E_{range} = −200 to −800 mV, E_{acc} = –300 mV, t_{acc} = 120 s). Baseline is depicted in black. Inset: Corresponding concentration curve with linear approximation. The error-bars correspond to the calculated confidence intervals on the level of significance α = 0.05.

Table 1

Parameters of DOX concentration dependences measured by DPCSV on p-AgSAE in BRB (pH 6) after oxygen removal by bubbling with N_2. Confidence intervals were calculated on the level of significance α = 0.05; r - correlation coefficient.

Concentration range	Slope	Intercept	r	*LOD*
μmol L^{-1}	nA L μmol^{-1}	nA		μmol L^{-1}
0.6 - 10	–5.61 ± 0.26	–3.7 ±1.4	–0.999	0.44
0.6 - 100	–3.78 ± 0.18	–12.6 ± 7.5	–0.997	5.49

3.1.1. Model samples of doxorubicin - spiked tap water and human urine

The applicability of the developed DPCSV method on the p-AgSAE for DOX determination in real samples was tested using spiked tap water and human urine samples. Each measurement was repeated five times and statistically evaluated. The results are summarized in Table 2. It could be concluded that no any interfering substances present in spiked tap water and human urine have been found.

Table 2

Determination of DOX by DPCSV on the p-AgSAE in spiked model sample solutions (tap water and human urine) in the MVVC. Oxygen was removed by bubbling with nitrogen. Confidence intervals were calculated on the level of significance α = 0.05.

Tap water				Urine			
Added	Found	Recovery	RSD	Added	Found	Recovery	RSD
μmol L^{-1}	μmol L^{-1}	%	%	μmol L^{-1}	μmol L^{-1}	%	%
1.0	1.072±0.070	100.6±6.6	5.9	1.0	1.010±0.061	100.7±6.6	4.3
10	1.059±0.090	105.1±9.0	5.6	10	1.050±0.072	105.1±6.3	5.0

3.2 Cyclic and differential pulse voltammetry on polarized liquid/liquid interfaces

3.2.1. Cyclic voltammetry on polarized liquid/liquid interface

Fig. 7 shows several voltammograms of DOX cation overlapped by two ones of the TEA^+ cation, which is used as the internal reference ion for voltammetry on polarized liquid/liquid interfaces. The positive peak currents I_p^+ for both transferred ions are proportional to their concentration in compliance with Eq. 2, see the inset in Fig. 7, and derived ion diffusion coefficients for TEA^+ and DOX^+ equal to $D_{TEA}^{w} = 1.8\text{x}10^{-5}$ cm^2 s^{-1} and $D_{DOX}^{w} = 6.9\text{x}10^{-6}$ cm^2 s^{-1}, respectively. E_m represents a reasonable estimate of the reversible half-wave potential $E_{1/2}^{rev}$ and may be considered as a measure of the standard Gibbs energy of the ion transfer from the aqueous phase (w) to the TDMA-TFPB phase (o), $\Delta_w^o G^o$. This parameter is believed to reflect a degree of the ion lipophilicity, which plays the key role in transport processes in the liquid membrane systems. The rigorous procedure for the evaluation of $\Delta_w^o G^o$ for the DOX^+ cation is based on the determination of midpoint potential E_m for the DOX^+ cation and

TEA^+ transfers [28, 37]. Using the simplified procedure based on the known value of $\Delta_w^o G_{TEA}^o$, i.e. −3.3 kJ mol^{-1}, for the TEA^+ ion transfer across the water/TDMA-TFPB interface [37], and considering the direct proportionality (Eq. 3),

$$\Delta_w^o G^0 = -3.3x10^3 + F\Delta E_m \quad (3)$$

where ΔE_m is the difference between the midpoint potentials for the DOX^+ cation and TEA^+, then the standard Gibbs energy of the DOX^+ transfer equals to $\Delta_w^o G_{DOX}^o$ = 27.9 kJ mol^{-1}, the value of which points to a quite low lipophilicity.

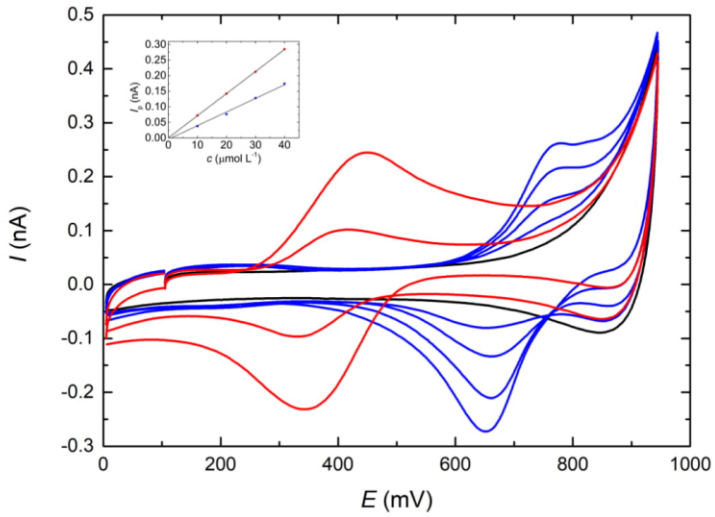

Fig. 7. Cyclic voltammograms (v = 10 mV s^{-1}) measured using the TDMA-TFPB membrane cell (Scheme 1) in the absence (black line) and in the presence of 10 and 30 µmol L^{-1} TEA^+ (red lines) and 10, 20, 30, and 40 µmol L^{-1} DOX^+ (blue lines) in the aqueous phase (pH~3). Inset: Dependence of the forward peak currents I_p^+ on the TEA^+ (red points) and DOX^+ (blue points) concentrations.

3.2.2. Differential pulse voltammetry on polarized liquid/liquid interface

Illustrative DPV voltammograms of DOX^+ measured in the concentration range from 1 to 10 µmol L^{-1} are depicted in Fig. 8. The dependence of the positive DPV peak current on the DOX^+ concentration is linear in the whole tested concentration range and may be presumably

extended to higher concentrations (till about 40 μmol L^{-1}). Compare to the differential pulse stripping voltammetry (DPSV) of DOX^+ on water/PVC-NPOE interface described at [25], the DPV *LOD* for DOX^+ estimated in this study is at least one order of magnitude lower (*LOD* = 0.84 μmo.L^{-1}), most likely thanks to much better temperature and chemical stability of the water/TDMA-TFPB interface. Sensitivity of the DPV peak current vs. DOX^+ concentration dependence (see the inset in Fig. 8) has the potential to reach significantly lower detection limit for its determination. However, DOX molecule tends to adsorb on voltammetric cell walls (on both glass and Plexiglas®) and therefore its concentrations well below 1 μmol L^{-1} are difficult to detect.

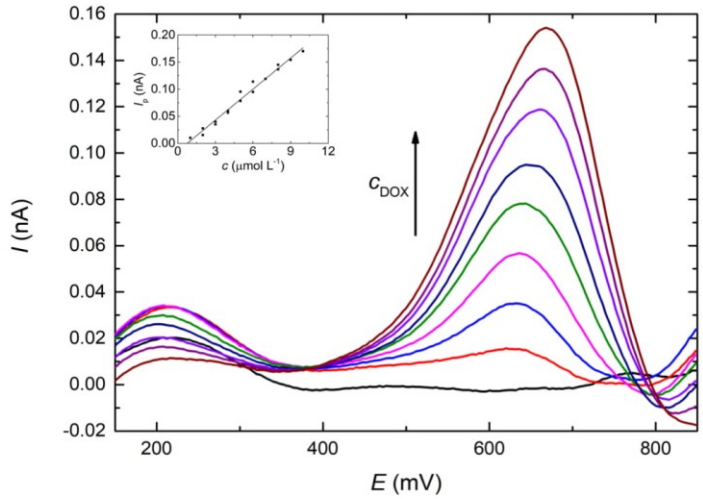

Fig. 8. Background corrected DP voltammograms of 0, 2, 3, 4, 5, 6, 7, 8, and 9 μmol L^{-1} DOX^+ transfers from the aqueous phase (pH~3) measured using the TDMA-TFPB membrane cell (Scheme 1). Inset: Dependence of the forward peak current I_p^+ on the DOX^+ concentration *c* (1 - 10 μmol L^{-1} with 1 μmol L^{-1} increment).

However, DOX determination in body fluids is considerably troublesome since those fluids contain high concentration of electrolytes (NaCl, etc.) which narrow the potential window and DOX^+ transfer is close to its edge. Moreover, presence of significant amount of charged lipophilic compounds (amines, amino acids, etc.) blocks the water/TDMA-TFPB

interface. From this point of view, coupling of separation and voltammetric techniques seems to be necessary.

4. Conclusions

A rapid, simple, and sensitive DPCSV method for the determination of DOX on p-AgSAE using MVVC in aquatic and body fluids samples was developed. The calibration curve in BRB (pH = 6) was linear in the concentration range from 0.6 to 10 μmol L^{-1}, with the *LOD* 0.44 μmol L^{-1}. The repeatability of measurement was 3.7% for concentration of 0.6 μmol L^{-1} and 3.2% for concentration of 0.1 mmol L^{-1}. Applicability of the method was tested on spiked samples of tap water (recovery 100.6±6.6%, RSD 5.9%, on the DOX level 1 μmol L^{-1}) and urine (recovery 100.7±6.6%, RSD 4.3%, on the DOX level of 1 μmol L^{-1}). Those results demonstrate the practical applicability of the developed DPCSV method on p-AgSAE for sensitive determination of anti-cancer drugs in small volumes (50 μL) using the MVVC.

Similar results with *LOD* (0.84 μmol L^{-1}) and *LDR* (from 1 to 40 μmol L^{-1}), have been achieved using DPV on polarized liquid/liquid interface represented by a supported membrane prepared by impregnating a polyvinylidenfluoride microporous filter with a room-temperature ionic liquid (RTIL) tridodecylmethylammonium tetrakis[3,5-bis(trifluoro-methyl)phenyl]borate (TDMA-TFPB). However, comparison to the DPCSV method, this liquid/liquid method does not seem applicable for DOX determination in body fluids in concentration order of μmol L^{-1} due to the presence of interfering compounds (e.g., chlorides) and of charged lipophilic compounds (amines, amino acids, etc.). Therefore, a separation step must be inserted before polarized liquid/liquid interface voltammetric step.

Acknowledgements

This research was carried out within the framework of Specific University Research (SVV 260440). Š.S. thanks the GAUK (No. 243-250753), J.L. and Š.S. thank the Czech Science Foundation (GA CR project No. 17-05387S), J.B. and T.N. thank the Czech Science Foundation (GA CR project No. 17-03868S).

References

[1] B. Chen, X.Y. Peng, L. Pentassuglia, C.C. Lim, D.B. Sawyer, Molecular and cellular mechanisms of anthracycline cardiotoxicity, Cardiovascular Toxicology 7 (2007) 114.

[2] T. Simunek, M. Sterba, O. Popelova, M. Adamcova, R. Hrdina, V. Gersl, Anthracycline-induced cardiotoxicity: Overview of studies examining the roles of oxidative stress and free cellular iron, Pharmacological Reports 61 (2009) 154.

[3] G. Cassinelli, The roots of modern oncology: from discovery of new antitumor anthracyclines to their clinical use, Tumori 2016 (2016) 226.

[4] D.A. Gewirtz, A critical evaluation of the mechanisms of action proposed for the antitumor effects of the anthracycline antibiotics Adriamycin and daunorubicin, Biochemical Pharmacology 57 (1999) 727.

[5] N.W. Paul, H. Fangerau, Why should we bother? Ethical and social issues in individualized medicine, Current Drug Targets 7 (2006) 1721.

[6] G. McMahon, R. O'Connor, Therapeutic drug monitoring in oncology: does it have a future?, Bioanalysis 1 (2009) 507.

[7] T. Buclin, V. Gotta, A. Fuchs, N. Widmer, J. Aronson, Monitoring drug therapy, British Journal of Clinical Pharmacology 73 (2012) 917.

[8] A.T. Lucas, S.K. O'Neal, C.M. Santos, T.F. White, W.C. Zamboni, A sensitive high performance liquid chromatography assay for the quantification of doxorubicin associated with DNA in tumor and tissues, Journal of Pharmaceutical and Biomedical Analysis 119 (2016) 122.

[9] M. Shah, L. Bourner, S. Ali, S. Al-Enazy, M.M. Youssef, M. Fisler, E. Rytting, HPLC method development for quantification of doxorubicin in cell culture and placental perfusion media, Separations 5 (2018).

[10] D.M. Souza, J.F. Reichert, A.F. Martins, A simultaneous determination of anti-cancer drugs in hospital effluent by DLLME HPLC-FLD, together with a risk assessment, Chemosphere 201 (2018) 178.

[11] J. Mbuna, T. Kaneta, Capillary electrophoresis with laser-induced fluorescence detection for application in intracellular investigation of anthracyclines and multidrug resistance proteins, Analytical Sciences 31 (2015) 1121.

[12] X.P. Yang, H.H. Gao, F. Qian, C. Zhao, X.J. Liao, Internal standard method for the measurement of doxorubicin and daunorubicin by capillary electrophoresis with in-column double optical-fiber LED-induced fluorescence detection, Journal of Pharmaceutical and Biomedical Analysis 117 (2016) 118.

[13] A. Roszkowska, M. Tascon, B. Bojko, K. Gorynski, P.R. Dos Santos, M. Cypel, J. Pawliszyn, Equilibrium ex vivo calibration of homogenized tissue for in vivo SPME quantitation of doxorubicin in lung tissue, Talanta 183 (2018) 304.

[14] P.S. Guin, S. Das, P.C. Mandal, Electrochemical reduction of quinones in different media: A review, International Journal of Electrochemistry 2011 (2011) 22.

[15] S. Skalova, T. Navratil, J. Barek, V. Vyskocil, Voltammetric determination of sodium anthraquinone-2-sulfonate using silver solid amalgam electrodes, Monatshefte fur Chemie 148 (2017) 577.

[16] R. Shamagsumova, A. Porfireva, V. Stepanova, Y. Osin, G. Evtugyn, T. Hianik, Polyaniline–DNA based sensor for the detection of anthracycline drugs, Sensors and Actuators B: Chemical 220 (2015) 573.

[17] E. Arkan, G. Paimard, K. Moradi, A novel electrochemical sensor based on electrospun TiO2 nanoparticles/carbon nanofibers for determination of Idarubicin in biological samples, Journal of Electroanalytical Chemistry 801 (2017) 480.

[18] Y. Hahn, H.Y. Lee, Electrochemical behavior and square wave voltammetric determination of doxorubicin hydrochloride, Archives of Pharmacal Research 27 (2004) 31.

[19] J. Barek, J. Fischer, T. Navratil, K. Peckova, B. Yosypchuk, J. Zima, Nontraditional electrode materials in environmental analysis of biologically active organic compounds, Electroanalysis 19 (2007) 2003.

[20] P. Cizkova, T. Navratil, I. Sestakova, B. Yosypchuk, Verification of applicability of mercury meniscus modified silver solid amalgam electrode for determination of heavy metals in plant matrices, Electroanalysis 19 (2007) 161.

[21] J. Fischer, L. Vanourkova, A. Danhel, V. Vyskocil, K. Cizek, J. Barek, K. Peckova, B. Yosypchuk, T. Navratil, Voltammetric determination of nitrophenols at a silver solid amalgam electrode, International Journal of Electrochemical Science 2 (2007) 226.

[22] J. Barek, J. Fischer, T. Navratil, K. Peckova, B. Yosypchuk, Silver solid amalgam electrodes as sensors for chemical carcinogens, Sensors 6 (2006) 445.

[23] R. Fadrna, B. Yosypchuk, M. Fojta, T. Navratil, L. Novotny, Voltammetric determination of adenine, guanine, and DNA using liquid mercury free polished silver solid amalgam electrode, Analytical Letters 37 (2004) 399.

[24] S. Skalova, C. Goncalves, T. Navratil, J. Barek, J.A. Rodrigues, V. Vyskocil, Miniaturized voltammetric cell for cathodic voltammetry making use of an agar membrane, Journal of Electroanalytical Chemistry 821 (2018) 47.

[25] S. Jeshycka, H.Y. Han, H.J. Lee, Voltammetric understanding of ionizable doxorubicin transfer reactions across liquid/liquid interfaces and sensor development, Electrochimica Acta 245 (2017) 203.

[26] J. Langmaier, S. Zalis, Z. Samec, V. Bovtun, M. Kempa, Origin of the correlation between the standard Gibbs energies of ion transfer from water to a hydrophobic ionic liquid and to a molecular solvent, Electrochimica Acta 87 (2013) 591.

[27] J.N. Miller, J.C. Miller, Statistics and chemometrics for analytical chemistry, 2nd ed., Pearson Education, Harlow, 2005.

[28] J. Langmaier, Z. Samec, Cyclic voltammetry of ion transfer across a room temperature ionic liquid membrane supported by a microporous filter, Electrochemistry Communications 9 (2007) 2633.

[29] Z. Samec, A. Trojanek, E. Samcova, Ion and pore fluid transport-properties of a nafion(R) membrane separating 2 electrolyte-solutions .1. Kinetics of the proton and alkali-metal cation-transport, Journal of Electroanalytical Chemistry 389 (1995) 1.

[30] J. Langmaier, Z. Samec, Voltammetry of ion transfer across a polarized room-temperature ionic liquid membrane facilitated by valinomycin: theoretical aspects and application, Analytical Chemistry 81 (2009) 6382.

[31] D. Kaushik, G. Bansal, Four new degradation products of doxorubicin: An application of forced degradation study and hyphenated chromatographic techniques, Journal of Pharmaceutical Analysis 5 (2015) 285.

[32] L. Bandzuchova, R. Selesovska, T. Navratil, J. Chylkova, L. Novotny, Voltammetric monitoring of electrochemical reduction of riboflavin using silver solid amalgam electrodes, Electrochimica Acta 75 (2012) 316.

[33] S. Sebkova, T. Navratil, M. Kopanica, Comparison of different types of silver composite electrodes to varied amount of silver on example of determination of 2-nitronaphtalene, Analytical Letters 36 (2003) 2767.

[34] J. Skopalova, T. Navratil, Application of elimination voltammetry to the study of electrochemical reduction and determination of the herbicide metribuzin, Chemia Analityczna (Warsaw) 52 (2007) 961.

[35] L. Trnkova, R. Kizek, O. Dracka, Application of elimination voltammetry to adsorptive stripping of DNA, Electroanalysis 12 (2000) 905.

[36] S. Kikuchi, K. Honda, S. Kim, Removal of dissolved oxygen by sodium sulfite. Application to the polarographic study Bulletin of the Chemical Society of Japan 27 (1953) 65.

[37] J. Langmaier, S. Zalis, Z. Samec, Lipophilicity of acetylcholine and related ions examined by ion transfer voltammetry at a polarized room-temperature ionic liquid membrane, Journal of Electroanalytical Chemistry 815 (2018) 183.

Tables

Table 1

Parameters of DOX concentration dependences measured by DPCSV on p-AgSAE in BRB (pH 6) after oxygen removal by bubbling with N_2. Confidence intervals were calculated on the level of significance $\alpha = 0.05$; *r* - correlation coefficient.

Concentration range	Slope	Intercept	*r*	*LOD*
µmol L^{-1}	nA L μmol^{-1}	nA		µmol L^{-1}
0.6 - 10	–5.61 ± 0.26	–3.7 ±1.4	–0.999	0.44
0.6 - 100	–3.78 ± 0.18	–12.6 ± 7.5	–0.997	5.49

Table 2

Determination of DOX by DPCSV on the p-AgSAE in spiked model sample solutions (tap water and human urine) in the MVVC. Oxygen was removed by bubbling with nitrogen. Confidence intervals were calculated on the level of significance $\alpha = 0.05$.

Tap water				Urine			
Added	Found	Recovery	RSD	Added	Found	Recovery	RSD
µmol L^{-1}	µmol L^{-1}	%	%	µmol L^{-1}	µmol L^{-1}	%	%
1.0	1.072±0.070	100.6±6.6	5.9	1.0	1.010±0.061	100.7±6.6	4.3
10	1.059±0.090	105.1±9.0	5.6	10	1.050±0.072	105.1±6.3	5.0

Legend for Figures

Fig. 1. Structural formula of doxorubicin.

Fig. 2. DP voltammograms of 1×10^{-4} mol L^{-1} DOX on the p-AgSAE in BRB pH 2 - 8 (values given above the curve) after bubbling with nitrogen. Scan rate (v) of 20 mV s^{-1}, pulse height (E_{pulse}) of –50 mV, pulse width (t_{pulse}) of 100 ms, potential range (E_{range}) = −100 to −900 mV.

Fig. 3. DPCS voltammograms of DOX (c_{DOX} = 1×10^{-4} mol L^{-1}) on the p-AgSAE in the MVVC in BRB (**A:** pH 6 and **B:** pH 7). Curves: *Black*: before oxygen removing, *Blue:* with Na_2SO_3; *Red*: after bubbling with nitrogen. Parameters: v of 20 mV s^{-1}, E_{pulse} of –50 mV, t_{pulse} of 100 ms, E_{range} = 0 to −1700 mV, accumulation potential (E_{acc}) of –300 mV, and accumulation time (t_{acc}) of 120 s.

Fig. 4. The dependence of peak current of DPCSV of DOX model sample (c_{DOX} = 1×10^{-6} mol L^{-1}) on the p-AgSAE in the MVVC in BRB (pH 6) after bubbling with nitrogen on E_{acc} (**A**) and t_{acc} (**B**). (v = 20 mV s^{-1}; E_{pulse} = –50 mV; t_{pulse} = 80 ms; E_{range} = 0 to −1700 mV. **A:** t_{acc} = 30 s; E_{acc} = 200, 100, 0, –100, –200 and –300 mV; **B:** E_{acc} = –300 mV; t_{acc} = 0, 10, 30, 60, 90, 120, 150 and 180 s). The error-bars correspond to the calculated confidence intervals on the level of significance α = 0.05.

Fig. 5. DPCS voltammograms of DOX model sample (c = 0.6 μmol L^{-1} - 100 μmol L^{-1}) on p-AgSAE in BRB (pH 6) after oxygen removal by bubbling with N_2. (v = 20 mV s^{-1}; E_{pulse} = –50 mV; t_{pulse} = 80 ms; E_{range} = –200 - −800 mV, E_{acc} = –300 mV, t_{acc} = 120 s). Baseline is depicted in black. *Inset*: Corresponding concentration curves with linear (red) and polynomial (green) approximations. The error-bars correspond to the calculated confidence intervals on the level of significance α = 0.05.

Fig. 6. DPCS voltammograms of DOX model sample (c = 0.6 μmol L^{-1} - 6 μmol L^{-1}) on p-AgSAE in BRB (pH 6) after oxygen removal by bubbling with N_2. (v = 20 mV s^{-1}; E_{pulse} = –50 mV; t_{pulse} = 80 ms; E_{range} = −200 to −800 mV, E_{acc} = –300 mV, t_{acc} = 120 s). Baseline is depicted in black. Inset: Corresponding concentration curve with linear approximation. The

error-bars correspond to the calculated confidence intervals on the level of significance $\alpha = 0.05$.

Fig. 7. Cyclic voltammograms (v = 10 mV s^{-1}) measured using the TDMA-TFPB membrane cell (Scheme 1) in the absence (black line) and in the presence of TEA^+ 10 and 30 µmol L^{-1} (red lines) and DOX^+ 10, 20, 30, and 40 µmol L^{-1} (blue lines) in the aqueous phase (pH~3). Inset: Dependence of the forward peak currents I_p^+ on the TEA^+ (red points) and DOX^+ (blue points) concentrations.

Fig. 8. Background corrected DP voltammograms of 0, 2, 3, 4, 5, 6, 7, 8, and 9 µmol L^{-1} DOX^+ transfers from the aqueous phase (pH~3) measured using the TDMA-TFPB membrane cell (Scheme 1). Inset: Dependence of the forward peak current I_p^+ on the DOX^+ concentration c (1 - 10 µmol L^{-1} with 1 µmol L^{-1} increment).

Figures

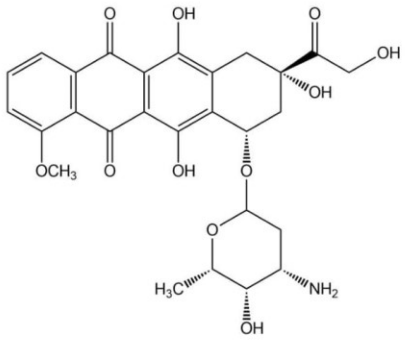

Fig. 1. Structural formula of doxorubicin.

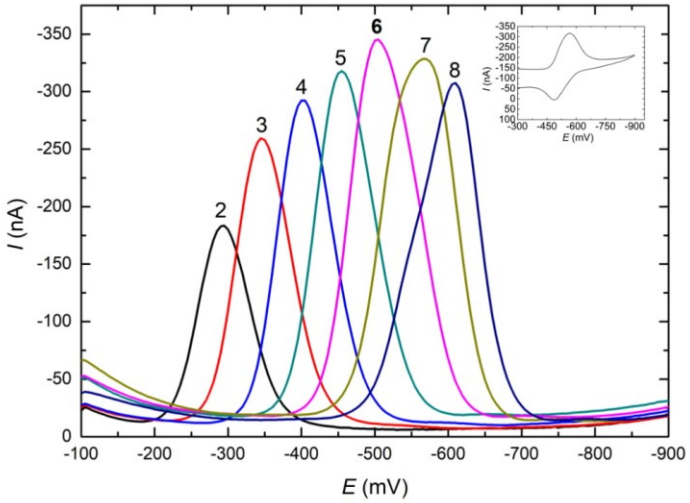

Fig. 2. DP voltammograms of 1×10^{-4} mol L^{-1} DOX on the p-AgSAE in BRB pH 2 - 8 (values given above the curve) after bubbling with nitrogen. Scan rate (v) of 20 mV s^{-1}, pulse height (E_{pulse}) of –50 mV, pulse width (t_{pulse}) of 100 ms, potential range (E_{range}) = −100 to −900 mV.

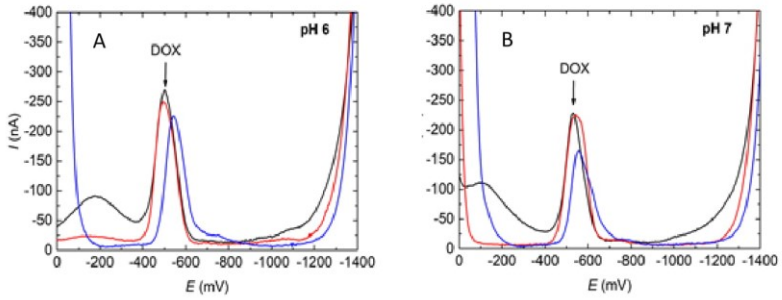

Fig. 3. DPCS voltammograms of DOX (c_{DOX} = 1×10^{-4} mol L^{-1}) on the p-AgSAE in the MVVC in BRB (**A:** pH 6 and **B:** pH 7). Curves: *Black*: before oxygen removing, *Blue:* with Na_2SO_3; *Red*: after bubbling with nitrogen. Parameters: v of 20 mV s^{-1}, E_{pulse} of –50 mV, t_{pulse} of 100 ms, E_{range} = 0 to −1700 mV, accumulation potential (E_{acc}) of –300 mV, and accumulation time (t_{acc}) of 120 s.

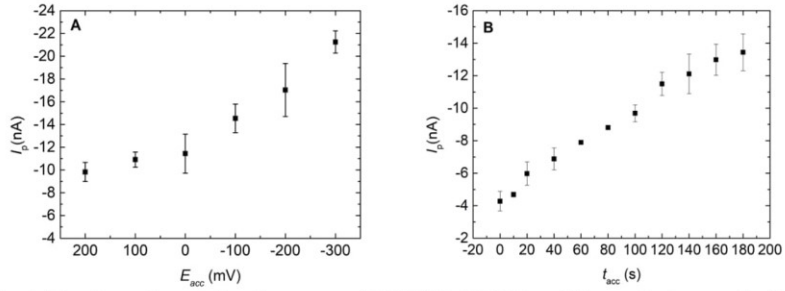

Fig. 4. The dependence of peak current of DPCSV of DOX model sample (c_{DOX} = 1×10^{-6} mol L^{-1}) on the p-AgSAE in the MVVC in BRB (pH 6) after bubbling with nitrogen on E_{acc} (**A**) and t_{acc} (**B**). (v = 20 mV s^{-1}; E_{pulse} = –50 mV; t_{pulse} = 80 ms; E_{range} = 0 to −1700 mV. **A:** t_{acc} = 30 s; E_{acc} = 200, 100, 0, –100, –200 and –300 mV; **B:** E_{acc} = –300 mV; t_{acc} = 0, 10, 30, 60, 90, 120, 150 and 180 s). The error-bars correspond to the calculated confidence intervals on the level of significance α = 0.05.

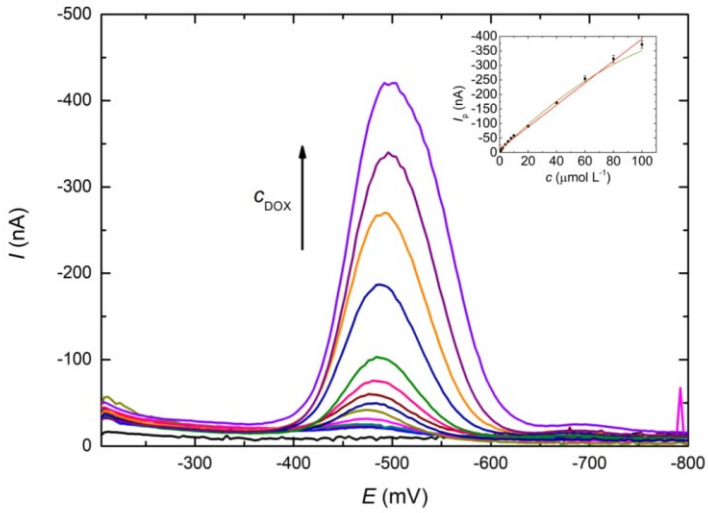

Fig. 5. DPCS voltammograms of DOX model sample (c = 0.6 µmol L^{-1} - 100 µmol L^{-1}) on p-AgSAE in BRB (pH 6) after oxygen removal by bubbling with N_2. (v = 20 mV s^{-1}; E_{pulse} = –50 mV; t_{pulse} = 80 ms; E_{range} = –200 - −800 mV, E_{acc} = –300 mV, t_{acc} = 120 s). Baseline is depicted in black. *Inset*: Corresponding concentration curves with linear (red) and polynomial (green) approximations. The error-bars correspond to the calculated confidence intervals on the level of significance α = 0.05

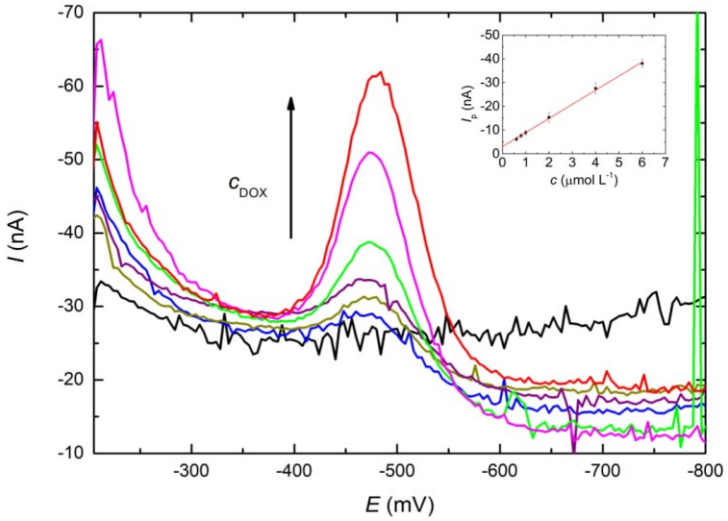

Fig. 6. DPCS voltammograms of DOX model sample (c = 0.6 µmol L^{-1} - 6 µmol L^{-1}) on p-AgSAE in BRB (pH 6) after oxygen removal by bubbling with N_2. (v = 20 mV s^{-1}; E_{pulse} = –50 mV; t_{pulse} = 80 ms; E_{range} = −200 to −800 mV, E_{acc} = –300 mV, t_{acc} = 120 s). Baseline is depicted in black. Inset: Corresponding concentration curve with linear approximation. The error-bars correspond to the calculated confidence intervals on the level of significance α = 0.05.

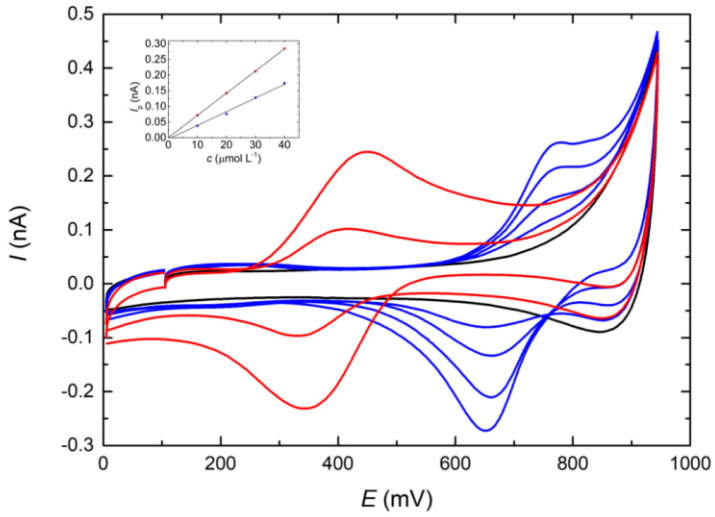

Fig. 7. Cyclic voltammograms (v = 10 mV s^{-1}) measured using the TDMA-TFPB membrane cell (Scheme 1) in the absence (black line) and in the presence of TEA^+ 10 and 30 µmol L^{-1} (red lines) and DOX^+ 10, 20, 30, and 40 µmol L^{-1} (blue lines) in the aqueous phase (pH~3). Inset: Dependence of the forward peak currents I_p^+ on the TEA^+ (red points) and DOX^+ (blue points) concentrations.

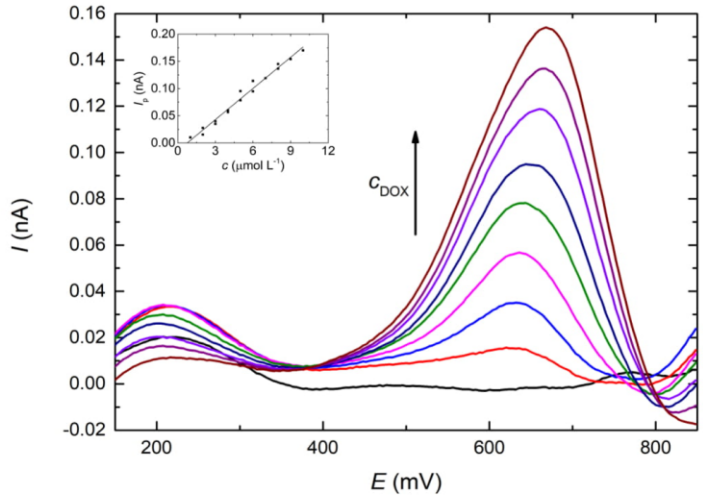

Fig. 8. Background corrected DP voltammograms of 0, 2, 3, 4, 5, 6, 7, 8, and 9 μmol L^{-1} DOX^+ transfers from the aqueous phase (pH~3) measured using the TDMA-TFPB membrane cell (Scheme 1). Inset: Dependence of the forward peak current I_p^+ on the DOX^+ concentration c (1 - 10 μmol L^{-1} with 1 μmol L^{-1} increment).

12. Confirmation of Participation

1. **Skalova S**, Navratil T, Barek J, Vyskocil V: Voltammetric Determination of Sodium Anthraquinone-2-Sulfonate Using Silver Solid Amalgam Electrodes, *Monatshefte für Chemie – Chemical Monthly 148(3)*, 577-583 (**2017**)
   Impact factor: 1.282; Percentage of participation of Mgr. Štěpánka Skalová ~ **65 %.**

2. Sestakova I, **Skalova S**, Navratil T: Labile Lead Phytochelatin Complex Could Enhance Transport of Lead Ions across Biological Membrane, *Journal of Electroanalytical Chemistry 821*, 92-96 (**2018**)
   Impact factor: 3.012; Percentage of participation of Mgr. Štěpánka Skalová ~ **40 %**.

3. **Skalova S**, Vyskocil V, Barek J, Navratil T: Model Biological Membranes and Possibilities of Application of Electrochemical Impedance Spectroscopy for their Characterization, *Electroanalysis 30*, 207-219 (**2018**)
   Impact factor: 2.471; Percentage of participation of Mgr. Štěpánka Skalová ~ **65 %**.

4. **Skalova S**, Gonçalves LM, Navratil T, Barek J, Rodrigues JA, Vyskocil V: Miniaturized Voltammetric Cell for Cathodic Voltammetry Making Use of an Agar Membrane, *Journal of Electroanalytical Chemistry 821*, 47-52 (**2018**)
   Impact factor: 3.012; Percentage of participation of Mgr. Štěpánka Skalová ~ **45%**

5. **Skalova S**, Langmaier J, Barek J, Vyskocil V, Navratil T: Comparison of Doxorubicin Determination Using Two Voltammetric Techniques, ***submitted to Electrochimica Acta*** (**2019**)
   Impact factor: 5.16; Percentage of participation of Mgr. Štěpánka Skalová ~ **35 %**

I declare that the percentage of participation of Mgr. Štěpánka Skalová at the above given papers corresponds to above given numbers.

Prague, 28.7.2019 prof. RNDr. Jiří Barek, CSc.

13. List of Publications

1. **Skalova S**, Svadlakova T, Shaikh Qureshi WM, Dev K, Mokry J: Induced Pluripotent Stem Cells and their Use in Cardiac and Neural Regenerative Medicine, *International Journal of Molecular Sciences 16(2)*, 4043-4067 (**2015**)

2. **Skalova S**, Stavkova K, Hajkova A, Barek J, Fischer J, Wang J, Vyskocil V: Interaction of Genotoxic 2-Nitrofluorene and its Metabolites with DNA *in vivo* and its Monitoring Using Electrochemical DNA Biosensors *in vitro*, *Chemické Listy 111*, 178-185 (**2017**)

3. **Skalova S**, Navratil T, Barek J, Vyskocil V: Voltammetric Determination of Sodium Anthraquinone-2-Sulfonate Using Silver Solid Amalgam Electrodes, *Monatshefte für Chemie – Chemical Monthly 148(3)*, 577-583 (**2017**)

4. Sestakova I, **Skalova S**, Navratil T: Labile Lead Phytochelatin Complex Could Enhance Transport of Lead Ions Across Biological Membrane, *Journal of Electroanalytical Chemistry 821*, 92-96 (**2018**)

5. **Skalova S**, Vyskocil V, Barek J, Navratil T: Model Biological Membranes and Possibilities of Application of Electrochemical Impedance Spectroscopy for their Characterization, *Electroanalysis 30*, 207-219 (**2018**)

6. **Skalova S**, Gonçalves LM, Navratil T, Barek J, Rodrigues JA, Vyskocil V: Miniaturized Voltammetric Cell for Cathodic Voltammetry Making Use of an Agar Membrane, *Journal of Electroanalytical Chemistry 821*, 47-52 (**2018**)

7. **Skalova S**, Langmaier J, Barek J, Vyskocil V, Navratil T: Comparison of Doxorubicin Determination Using Two Voltammetric Techniques, ***submitted to Electrochimica Acta*** (**2019**)

14. Oral Presentations

1. **Skalova S**, Stavkova K, Vyskocil V, Barek J: Study of 2-Nitrofluorene Interaction with DNA at a Glassy Carbon Electrode, *XXXVI. Moderní Elektrochemické Metody* – Jetřichovice, Czech Republic (23. 05. 2016 – 27. 05. 2016)

2. **Skalova S**, Navratil N, Vyskocil V: Development of DNA Biosensor to Study Interactions of 2-Nitrofluorene with DNA, *The Student Seminar of JHI 2016* – Liblice, Czech Republic (10. 05. 2016 – 11. 05. 2016)

3. **Skalova S**, Stavkova K, Barek J, Vyskocil V: Electrochemical Determination of 2-Nitrofluorene, *12th International Students Conference Modern Analytical Chemistry* – Prague, Czech Republic (22. 09. 2016 – 23. 09. 2016)

4. **Skalova S**, Barek J, Rodrigues JA, Gonçalves LM, Navratil T, Vyskocil V: Pilot Experiments with a Micro-Volume Voltammetric Cell for the Determination of Electrochemically Reducible Organic Compounds, *13th International Students Conference Modern Analytical Chemistry* – Prague, Czech Republic (21. 09. 2017 – 22. 09. 2017)

5. **Skalova S**, Navratil T, Barek J, Vyskocil V: Determination of Doxorubicin Hydrochloride Using a Miniaturized Voltammetric Cell, *1st Cross-border Seminar on Electroanalytical Chemistry*, Furth im Wald, Germany (04. 04. 2018 – 06. 04. 2018)

6. **Skalova S**, Navratil T, Barek J, Vyskocil V: Application of a Micro-Volume Voltammetric Cell for Determination of Doxorubicin Hydrochloride, *XXXVIII.*

Moderní elektrochemické metody – Jetřichovice, Czech Republic (21. 05. 2018 – 25. 05. 2018)

7. **Skalova S**, Fischer J, Navratil T, Barek J, Vyskocil V: Amperometric Detection of Anthraquinone-2-Sulfonate at a Dual Glassy Carbon Electrode, *2nd Cross-Border Seminar on Electroanalytical Chemistry* – České Budějovice, Czech Republic (10. 04. 2019 – 12. 04. 2019)

8. **Skalova S**, Fischer J, Barek J, Vyskocil V, Navratil T, Kucera J: Voltammetric Determination of Anthraquinone-2-Sulphonate in Physiological Saline Solution on Various Electrode Surfaces, *52nd Heyrovský Discussion* – Liblice, Czech Republic (16. 06. – 20. 06. 2019)

15. Poster Presentation

1. **Skalova S**, Stavkova K, Vyskocil V: Voltammetric Determination of Genotoxic 2-Nitrofluorene at a Glassy Carbon Electrode, *16th International Conference on Electroanalysis ESEAC* – Bath, United Kingdom (12. 06. 2016 – 16. 06. 2016)

2. **Skalova S**, Navratil T, Barek J, Vyskocil V, Gonçalves LM, Rodrigues JA: Miniaturized Voltammetric Cell for the Determination of Anthraquinone-Based Anti-Cancer Drugs, *XIX Euroanalysis 2017*, Stockholm, Sweden (28. 08. 2017 – 01. 09. 2017)

3. **Skalova S**, Navratil T, Barek J, Vyskocil V: Monitoring of Concentration of Doxorubicine Hydrochloride Using Miniaturized Voltammetric Cell, *17th International Conference on Electroanalysis IMA* – Rhodos, Greece (03. 06. 2018 – 06. 06. 2018)

4. **Skalova S**, Fischer J, Barek J, Vyskocil V, Navratil T, Krejci J: Voltammetric Detection of Anthraquinone-2-Sulfonate After Its Separation by Means of a Microdialysis Catheter, *XXV International Symposium on Bioelectrochemistry and Bioenergetics* – Limerick, Ireland (26. 05. 2019 – 30. 05. 2019)

16. Internship

Long-term foreign internship in laboratory of prof. José António Rodrigues, Department of Chemistry and Biochemistry, Faculty of Science University of Porto, Portugal (01. 02. 2017 – 30. 06. 2017)

17. Grants

Principal Investigatior

Electrochemical Analysis of Anti-Cancer Drugs in a Micro-Volume Voltammetric Cell. Grant Agency of Charles University. Project 243-259753, 2018-2019.

Team member

New Approaches for Monitoring of Transport of Selected Xenobiotics across Biomimetic Membranes. Czech Science Foundation. Project No. 17-05387S, 2017-2019.